

University of Nottingham

UK | CHINA | MALAYSIA

Optimal Deployment of Negative Emissions Technologies for Sustainable Energy Planning with Process Integration Techniques

Purusothmn Nair S Bhasker Nair

20258078

Supervised by Professor Dr Ir Dominic C. Y. Foo

Department of Chemical and Environmental Engineering

University of Nottingham Malaysia

A thesis submitted in partial fulfilment of the requirements for the degree of Doctor of Philosophy in Chemical Engineering

Table of Contents

ABSTRACT i

ACKNOWLEDGEMENTS iii

DECLARATIONS iv

LIST OF TABLES v

LIST OF FIGURES vii

ABBREVIATIONS x

NOMENCLATURE xi

Chapter 1: INTRODUCTION 1

1.1 Research Motivation 1

1.2 Research Scope 9

1.3 Research Aims and Objectives 10

1.4 Problem Statement 10

Chapter 2: LITERATURE SURVEY 12

2.1 Pinch Analysis 12

2.2 Carbon Emissions Pinch Analysis (CEPA) 12

2.3 Planning of CO_2 Capture and Storage in CEPA 13

2.4 Mathematical Optimisation Approaches in CO_2 Emissions Reduction 16

2.5 Applications of CEPA 17

2.6 Negative Emissions Technologies 20

2.7 Research Gap 25

Chapter 3: GRAPHICAL TARGETING TECHNIQUE FOR THE DEPLOYMENT OF ENERGY-PRODUCING NEGATIVE EMISSIONS TECHNOLOGIES 28

3.1 Targeting Technique without the Deployment of CO_2 Capture and Storage 28

3.1.1 Example 1 30

3.2 Targeting Technique with the Deployment of CO_2 Capture and Storage 32

3.2.1 Example 1 (Revisited) 41

3.2.2 Example 2 47

3.3 Chapter Summary 51

Chapter 4: GRAPHICAL TARGETING TECHNIQUE FOR THE DEPLOYMENT OF ENERGY-CONSUMING NEGATIVE EMISSIONS TECHNOLOGIES 53

4.1 Targeting Technique of Energy-Consuming Negative Emissions Technologies without the Deployment of CO_2 Capture and Storage 53

4.1.1 Case Study 56

4.2 Targeting Technique of Energy-Consuming Negative Emissions Technologies with the Deployment of CO_2 Capture and Storage 59

4.2.1 Case Study (Revisited) 62

4.3 Targeting Technique of Energy-Consuming and Energy-Producing Negative Emissions Technologies without the Deployment of CO_2 Capture and Storage 66

4.3.1 Case Study (Revisited) 68

4.4 Targeting Technique of Energy-Consuming and Energy-Producing Negative Emissions Technologies with the Deployment of CO_2 Capture and Storage 71

4.4.1 Case Study (Revisited) 72

4.5 Chapter Summary 74

Chapter 5: ALGEBRAIC TARGETING TECHNIQUE FOR THE DEPLOYMENT OF NEGATIVE EMISSIONS TECHNOLOGIES 76

5.1 Targeting Technique of Energy-Producing Negative Emissions Technologies without the Deployment of CO_2 Capture and Storage 76

5.1.1 Example 1 80

5.2 Targeting Technique for Deployment of CO_2 Capture and Storage and Renewable Energy Sources 83

5.2.1 Example 1 (Revisited) 86

5.3 Targeting Technique of Energy-Producing Negative Emissions Technologies with the Deployment of CO_2 Capture and Storage 91

5.3.1 Example 1 (Revisited) 92

5.4 Targeting Technique of Energy-Consuming Negative Emissions Technologies with and without the Deployment of CO_2 Capture and Storage 94

5.4.1 Example 1 (Revisited) 96

5.5 Chapter Summary 101

Chapter 6: MULTIPERIOD ENERGY PLANNING MODEL FOR CO_2-INTENSIVE INDUSTRIES 102

6.1 Methodology of Hybrid Approach in Multiperiod Energy Planning 103

6.2 Case Study 110

6.3 Scenario 1 (without CO_2 load transfer) 115

6.4 Scenario 2 (With CO_2 Load Transfer) 121

6.5 Chapter Summary 126

Chapter 7: CONCLUSIONS AND FUTURE WORK 127

7.1 Conclusion 127

7.2 Future Work 128

Appendix A 130

Appendix B 132

Appendix C 135

REFERENCES 152

ABSTRACT

It is critical to limit global warming to within 1.5 °C by year 2100 to minimise catastrophic impacts. The increased deployment of renewable energy sources, alongside *CO_2 capture and storage* (CCS) in energy planning, remains a key mitigation technique in minimising climate change impacts. Although the generation of renewable energy sources approaches the state of a carbon-neutral system, other processes such as fossil fuel-based generation, manufacturing, and transportation are net-carbon positive. Additionally, renewable energy sources pose challenges such as their sensitivity to environmental conditions, geographical locations, and seasonal changes. On the other hand, CCS systems entail a high capital expenditure, as well as additional operating costs due to parasitic power losses. Therefore, the deployment of *negative emissions technologies* (NETs) as a carbon management option is imperative. The generation of electricity from power plants with the installation of NETs can offset positive emissions from elsewhere in a system. Despite the lack of technological maturity of NETs, their full-scale deployment is expected to take place within the next few decades. Potential interactions with energy infrastructures need to be considered during scale-up. Therefore, this research focuses on the optimal deployment of NETs alongside renewable energy sources and CCS in efforts to mitigate climate change impacts. In this thesis, several techniques based on *Carbon Emissions Pinch Analysis* (CEPA) are developed for *carbon-constrained energy planning* (CCEP). Initially, an extended graphical targeting technique is developed for the deployment of energy-producing NETs (EP-NETs) during energy planning. The graphical targeting technique that was originally developed for the planning of CCS deployment in power plants is now extended to determine the minimum deployment of EP-NETs during energy planning. Next, a graphical targeting technique is developed for the deployment of energy-consuming NETs (EC-NETs) for sustainable energy planning. This graphical targeting technique demonstrates the usefulness of EC-NETs for an effective carbon management strategy. However, the energy demand of EC-NETs requires compensation from additional renewable energy sources. This compensation can be reduced with the deployment of CCS. On the other hand, the deployment of EC-NETs coupled with EP-NETs eliminates the need for renewable energy sources as compensatory power, as the latter is supplied by EP-NETs. Besides, a generic algebraic targeting technique is developed for the deployment of renewable energy sources, CCS and NETs, to eliminate the iterative procedure

of the graphical targeting technique. Lastly, a multiperiod energy planning model making use of the combined automated targeting model (ATM) and superstructural models is developed to determine the optimum deployment of energy sources for CO_2-intensive industries other than the power generation sector. This research demonstrated the importance of NETs, CCS, and renewable energy sources in mitigating climate change impacts. The systematic methodology developed in this research can assist the future decarbonisation of various CO_2-intensive processes.

ACKNOWLEDGEMENTS

I would like to take this opportunity to offer my sincerest gratitude to all my PhD supervisors specifically Professor Dr Dominic Foo and Professor Dr Raymond Tan. Throughout this research journey, I have gained plenty of experience by exchanging research ideas with these two individuals. I was often encouraged to think critically and analytically during problem-solving. My collaboration with these two individually changed my working style, as well as my approach to solving complex problems. These skills would be particularly beneficial in my career development, as well as my personal life. I would like to thank Dr Nishanth Chemmangattuvalappil for his guidance regarding fuzzy optimisation and disjunctive programming. A special mention to Dr Michael Short from the University of Surrey for his guidance throughout my programming journey. I first interacted with Dr Michael Short in March 2021 after receiving the news that we successfully secured funding from the British Council as part of the COP26 Trilateral Research Initiative. As a lead developer for this project, I was required to learn Python since I had no prior experience in programming. Dr Michael supplied me with valuable materials to learn Pyomo and within three months, I successfully created my first ever multiperiod energy planning model. During my research attachment to the University of Surrey, I worked alongside Dr Michael Short to further develop the mathematical model. Most recently, I also re-formulated the mathematical formulations in Chapter 6 in Python. This would not have been possible without the guidance from Dr Michael Short during the early phase of learning. Finally, I would like to thank my wife, Hemavathi Rajarajan and my family for their constant support throughout this challenging period. My wife was particularly critical in ensuring that I am always on the right track in terms of research motivation. She was the only person outside my academic circle with whom I keep bouncing off ideas as well as sharing the challenges and bottlenecks that arose during my PhD. She would also limit my working hours to ensure I am not burning out throughout this marathon. I would not have completed my PhD without her constant support. A special mention to the British Council for funding the development of an optimal decarbonisation software framework as part of the COP26 Trilateral Research Initiative.

DECLARATIONS

I hereby declare that this thesis is all my work unless stated otherwise and has not been submitted for a degree at any other university.

Purusothmn Nair S Bhasker Nair

March 2022

LIST OF TABLES

Table 1-1: Summary of the literature review regarding existing climate change and global warming situation 3

Table 1-2: Summary of the literature review regarding the impacts of climate change 5

Table 1-3: Summary of the literature review regarding the mitigation responses toward limiting global warming 9

Table 2-1: Summary of the literature review on the pinch-based approach in the development of CEPA.....15

Table 2-2: Summary of the literature review on mathematical programming approaches in the work concerning CO_2 emissions reduction. 17

Table 2-3: Summary of literature review on CEPA application 19

Table 2-4: Overview of various NETs 24

Table 3-1: Data for Example 1.....30

Table 3-2: Energy and CO_2 emissions from energy sources for Example 1 (revisited, after Steps (2) and (3)) 41

Table 3-3: Final energy sources and total CO_2 emissions for Example 1 (Revisited).....46

Table 3-4: Data for Example 2.....47

Table 3-5: Final energy sources and total CO_2 emissions for Example 2.....51

Table 4-1: Energy and CO_2 Intensities for energy sources after CCS deployment (after Steps (5) and (6)) 63

Table 5-1: Basic structure of an energy cascade table for EP-NETs deployment without CCS77

Table 5-2: Energy cascade table for targeting EP-NETs deployment for Example 1 82

Table 5-3: Basic structure of energy cascade table with deployment of CCS and renewable energy sources 83

Table 5-4: Energy cascade table for Example 1 (Revisited), with renewable energy sources of C_{COMP} = 0 kg CO_2/kWh (Scenario 1).....88

Table 5-5: Energy cascade table for Example 1 (Revisited), with renewable energy sources of C_{COMP} = 0.15 Mt CO2/TWh (Scenario 2) 90

Table 5-6: Energy cascade table for targeting EP-NETs and CCS deployment for Example 1 (Revisited) 93

Table 5-7: Basic structure of energy cascade table for deployment of EC-NETs without CCS 95

Table 5-8: Energy cascade table for EC-NETs deployment without CCS (Scenario 1) 98

Table 5-9: Energy cascade table for EC-NETs deployment with CCS (Scenario 2)..... 100

Table 6-1: Industrial plant data for (a) Period 1, (b) Period 2 and (c) Period 3 111

Table 6-2: Availability and CO_2 intensities of energy sources 114

Table 6-3: Optimal allocation of energy sources for Scenario 1..... 119

Table 6-4: Optimal allocation of energy sources for Scenario 2..... 123

LIST OF FIGURES

Figure 1-1: Superstructural representation of energy planning problem involving NETs and CCS 11

Figure 2-1: Pinch analysis in graphical targeting technique (Tan and Foo, 2007) 13

Figure 2-2: Pinch analysis in graphical targeting technique with CCS deployment (Tan et al., 2009b) 14

Figure 2-3: Arrangement of EW and ocean alkalinisation technology 21

Figure 2-4: Arrangement of DAC technology 21

Figure 2-5: Arrangement of biochar technology 22

Figure 2-6: Arrangement of BECCS technology 22

Figure 2-7: General research methodology 27

Figure 3-1: EPPD for planning EP-NETs deployment: (a) infeasible EPPD and (b) feasible EPPD 29

Figure 3-2: EPPD for Example 1: (a) infeasible EPPD and (b) feasible EPPD 32

Figure 3-3: EPPD for targeting of CCS system 34

Figure 3-4: Revised EPPD: (a) With CCS deployment and (b) Initial EP-NETs target (after Steps (4) and (5)) 35

Figure 3-5: Revised EPPD: (a) With CCS deployment and (b) Revised EP-NETs target (after Steps 6 and 7) 37

Figure 3-6: Flowchart for targeting the minimum deployment of CCS and EP-NETs 40

Figure 3-7: Revised EPPD with CCS deployment for Example 1 (Revisited, after Step (4)) 42

Figure 3-8: EPPD with CCS and EP-NETs deployment for Example 1 (Revisited, after Step (5)) 42

Figure 3-9: Revised EPPD with CCS and EP-NETs deployment for Example 1 (Revisited, after Step (7)) 44

Figure 3-10: Revised EPPD with CCS and EP-NETs deployment for Example 1 (Revisited, after Step (9)) 45

Figure 3-11: Final EPPD with CCS and EP-NETs deployment for Example 1 46

Figure 3-12: Revised EPPD with CCS deployment for Example 2 (after Steps (3) and (4)).....48

Figure 3-13: EPPD with CCS and EP-NETs deployment for Example 2 (after Step (5)).....49

Figure 3-14: Revised EPPD with CCS and EP-NETs deployment for Example 2 (after Step (7)) 50

Figure 3-15: Revised EPPD with CCS and EP-NETs deployment for Example 2 (after Step (9)) 50

Figure 4-1: Infeasible EPPD for the targeting of EC-NETs without CCS deployment.....54

Figure 4-2: Infeasible EPPD for targeting of EC-NETs without CCS deployment (after EC-NETs targeting).....55

Figure 4-3: Feasible EPPD for targeting of EC-NETs without CCS deployment.....56

Figure 4-4: EPPD for DAC deployment without CCS: (a) infeasible EPPD, (b) targeting for the minimum deployment of DAC, and (c) feasible EPPD with minimum DAC and compensatory energy requirements 58

Figure 4-5: Infeasible EPPD: (a) with CCS deployment and (b) with CCS and EC-NETs deployment.....61

Figure 4-6: Feasible EPPD with CCS and EC-NETs deployment.....62

Figure 4-7: Revised EPPD post-CCS deployment for case study (after Step (7)) 64

Figure 4-8: EPPD for case study (DAC and CCS deployment): (a) infeasible EPPD with CCS and DAC targeting, (b) feasible EPPD with CCS, DAC and renewable energy targeting.....65

Figure 4-9: Loci of EC-NETs and EP-NETs 67

Figure 4-10: Targeting the deployment of EC-NETs and EP-NETs without CCS.....68

Figure 4-11: EPPD for case study (Revisited): (a) Preliminary EPPD, (b) loci for BECCS and DAC and (c) feasible EPPD with BECCS and DAC targeting.....70

Figure 4-12: Preliminary EPPD for the targeting of EP-NETs and EC-NETs with CCS deployment 71

Figure 4-13: Infeasible EPPD for the targeting of EP-NETs and EC-NETs with CCS deployment 72

Figure 4-14: Revised EPPD post-CCS deployment for case study (Infeasible).....73

Figure 4-15: EPPD for case study: (a) infeasible EPPD with BECCS as the compensatory energy ; (b) feasible EPPD with BECCS and DAC targeting; (c) zoom-in section for feasible EPPD in (b) 75

Figure 5-1: Energy planning pinch diagram for the scenario with C_{COMP} of 0.15 Mt/TWh 91

Figure 5-2: EPPD for EC-NETs Deployment without CCS (Scenario 1).....99

Figure 5-3: EPPD for CCS and EC-NETs Deployment (Scenario 2).....101

Figure 6-1: Basic frameworks for multiperiod energy planning: (a) Superstructural model and (b) ATM 104

Figure 6-2: ATM results for Scenario 1 118

Figure 6-3: Energy mix and CO_2 load contribution from the power generation industry (PG1-PG4) for Scenario 1 121

Figure 6-4: ATM results for Scenario 2 122

Figure 6-5: CO_2 load transfer for Scenario 2.....124

Figure 6-6: Energy mix and CO_2 load contribution from the oleochemical industry (O1 – O5) for Scenario 2.....125

ABBREVIATIONS

CO_2	Carbon dioxide
GHGs	Greenhouse gases
NDCs	Nationally Determined Contributions
CDR	Carbon dioxide removal
NETs	Negative emissions technologies
CCS	CO_2 capture and storage
DAC	Direct air capture
EW	Enhanced weathering
BECCS	Bioenergy with CO_2 capture and storage
EC-NETs	Energy-consuming negative emissions technologies
EP-NETs	Energy-producing negative emissions technologies
EU	European Union
CCEP	Carbon constrained energy planning
CEPA	Carbon emissions pinch analysis
EPPD	Energy planning pinch diagram
ATM	Automated targeting method
MILP	Mixed-integer linear programming

NOMENCLATURE

$F_{S,i}$	Energy provided by energy source *i*
$F_{D,j}$	Energy requirement of energy demand *j*
$C_{S,i}$	CO_2 intensity of energy source *i*
$C_{D,j}$	CO_2 intensity of energy demand *j*
$C_{R,i}$	CO_2 intensity of energy source *i* after CCS retrofit
C_{COMP}	CO_2 Intensity of the compensatory energy source
$C_{EC\text{-}NET}$	CO_2 Intensity of EC-NETs
Δm_L	Aggregate CO_2 emissions limit of a specified geographical location
Δm_T	Cumulative CO_2 emissions of all energy sources
Δm_R	Total target CO_2 emissions reduction
$\Delta m_{R,i}$	Target CO_2 emissions reduction from energy source *i*
$\Delta m_{R,\ EP\text{-}NET}$	CO_2 emissions removal by EP-NETs
$\Delta m_{R,\ EC\text{-}NET}$	CO_2 emissions removal by EC-NETs
$\Delta m_{D,j}$	Maximum CO_2 emissions by energy demand *j*
RR	Removal ratio of CCS system
X	Parasitic power loss of CCS system
$F_{EP\text{-}NET}$	Minimum deployment of EP-NETs
$F_{EC\text{-}NET}$	Minimum deployment of EC-NETs
F_{BM}	Energy generated from biomass combustion
F_{EX}	Excess energy to be phased out
F_{DF}	Energy deficit gap
$F_{TR,k}$	Theoretical extent of CCS retrofit at level *k*
$\Delta F_{TR,k}$	Theoretical extent of CCS retrofit at level *k* to be elevated to level *k*-1 with a lower CO_2 intensity
$F_{AR,k}$	Actual extent of CCS retrofit at level *k*
$F_{R,i}$	Extent of CCS retrofit on energy source *i*
$F_{NR,i}$	Net energy available from energy source *i* with CCS retrofit
$F_{NS,i}$	Net energy available from energy source *i* without CCS retrofit
$F_{NetR,k}$	Net energy available at level *k* with and without CCS retrofit
$F_{N,k}$	Net energy at level *k*

$F_{E,k}$	Net energy available at level *k*
F_{COMP}	Minimum deployment of compensatory energy
L_T	Revised total CO_2 emissions after CCS and NETs deployment
Y_i	Minimum theoretical reduction of CCS retrofit extent on energy source *i*
ΔY_i	Remaining reduction of the extent of CCS retrofit on energy source *i*
A_i	Feasible reduction of CCS retrofit extent on energy source *i*
Z_i	Minimum theoretical addition of CCS retrofit extent on energy source *i*
ΔZ_i	Remaining addition of extent of CCS retrofit on energy source *i*
B_i	Feasible addition to CCS retrofit extent on energy source *i*
M_k	Theoretical energy reduction at level *k*
ΔM_k	Net energy to be elevated to level *k*-1 with a lower CO_2 intensity
N_k	Feasible energy reduction at level *k*
$FS_{i,t}$	The deployment of energy source *i* in period *t*
$A_{i,t}$	Maximum availability of energy source *i* in period *t*
$C_{S,i,t}$	CO_2 intensity of energy source *i* in period *t*
$C_{R,i,t}$	CO_2 intensity of energy source *i* with CCS retrofit in period *t*
$RR_{i,t}$	Removal ratio of energy source *i* in period *t*
$X_{i,t}$	Parasitic power loss of energy source *i* in period *t*
$FNR_{i,t}$	Net energy of energy source *i* with CCS retrofit in period *t*
$FNS_{i,t}$	Net energy of energy source *i* without CCS retrofit in period *t*
$FR_{i,t}$	Amount of energy source *i* subjected to CCS retrofit in period *t*
$FD_{j,t}$	Energy demand of energy sink *j* in period *t*
$FNR_{i,j,t}$	Net energy of energy source *i* for energy sink *j* with CCS retrofit in period *t*
$FNS_{i,j,t}$	Net energy of energy source *i* for energy sink *j* without CCS retrofit in period *t*
$L_{j,t}$	CO_2 emission limit of energy sink *j* in period *t*
$B_{i,j,t}$	Binary variable for the deployment of energy source *i* without CCS retrofit to energy sink *j*
$C_{i,j,t}$	Binary variable for the deployment of energy source *i* with CCS retrofit to energy sink *j*
$ET_{i,t\rightarrow t+1}$	CO_2 load transfer of energy source *i* from period *t* to period *t*+1.

Chapter 1: INTRODUCTION

1.1 Research Motivation

The rapid growth of the world population, as well as the expansion of the global economy, has led to a steady rise in energy demand and generation. According to Paice (2022), the world population is expected to reach 9.5 billion by year 2050; a quarter of which would be confined to the African regions. These statistics second the forecast by the International Energy Agency that the global energy demand will rise by 1.3% annually until year 2030 (IEA, 2021a). The modernisation of global economies translates to key trends, notably the electrification of transportation and a rise in digital infrastructure (IEA, 2021a). Consequently, the global electricity demand is projected to grow almost twice the rate of the energy demand at 2.4% annually until year 2030 (IEA, 2021a). By the end of year 2030, electricity is forecasted to account for 22% of the total final energy consumption in comparison to 20% in year 2021 (IEA, 2021a).

Parallel to this growth is the rise in carbon dioxide (CO_2) emissions. According to the World Meteorological Organization (2020), the atmospheric levels of CO_2 had consistently been on an upwards trend ever since it breached the 400 ppm mark in year 2015. By the end of year 2020, the global average CO_2 concentration was approximately 412.5 ppm, an increase from 410.5 ppm as observed by the end of year 2019 (IEA, 2021a). Although the usage of coal and oil for energy generation declined in year 2020 due to the COVID-19 pandemic, a similar trend did not continue in the subsequent year. The year 2021 saw a large rebound in the usage of coal and oil, thus resulting in the second-largest annual increase of CO_2 emissions in history (IEA, 2021a). As of year 2020, the electricity sector alone contributed 36% of the global CO_2 emissions equivalent to 12.3 Gt CO_2 (IEA, 2021a). While coal and natural gas contributed 70% of the global electricity generation, renewable energy sources e.g., nuclear, hydroelectric, wind and solar energy made up the remaining 30% (IEA, 2021a). Note that coal was only responsible for the generation of one-third of the global electricity supply in year 2020. However, its high CO_2 intensity meant that coal alone contributed 75% of the total CO_2 emissions originating from the electricity sector in year 2020 (IEA, 2021a). Meanwhile, natural gas was the second-largest emitter of CO_2 in the electricity sector for year 2020 (IEA, 2021a).

The continuous rise of greenhouse gases (GHGs) concentrations had resulted in the global mean surface temperature being 1.1 °C above the pre-industrial level for years 2016 to 2020 (World Meteorological Organization, 2020). The global average surface temperature for years 2016 to 2020 was 0.24 °C warmer versus years 2011 to 2015 (World Meteorological Organization, 2020). Between years 2006 and 2015, IPCC (2019a) reported that the global mean surface temperature of both land and ocean had increased by 0.87 °C, in comparison to the pre-industrial period from years 1850 to 1900. The rate of warming for the land alone within the same period were almost twice higher, with an observed temperature rise of 1.53 °C, in comparison to the pre-industrial period (IPCC, 2019a). At the current trajectory, it is unlikely that limiting global warming to within 2 °C above the pre-industrial level by the end of this century, as set during the Paris Agreement would be achievable (IPCC, 2018). According to the United Nations Environment Programme (2019), the GHGs emissions are forecasted to hit 60 Gt CO_2-eq by year 2030 with existing policies in place. By implementing the unconditional and conditional Nationally Determined Contributions (NDCs), the global GHGs emissions are projected to decrease by 4 and 6 Gt CO_2-eq, respectively, by year 2030 (United Nations Environment Programme, 2019). However, a large emissions gap persists in terms of climate change management to safe levels (United Nations Environment Programme, 2019). Despite a full deployment of the unconditional NDCs, there would be a gap of 32 and 15 Gt CO_2-eq between the cumulative emissions in year 2030 and limiting pathways of 1.5 °C and 2 °C respectively. In other words, the full deployment of unconditional NDCs would most likely limit global warming to within 3.2 °C by year 2100, far short of the Paris Agreement target of 1.5–2 °C (IPCC, 2018; United Nations Environment Programme, 2019).

In response to the Paris Agreement, Project Drawdown was founded in year 2014 to evaluate the period with an observed decline in the concentrations of GHGs in the atmosphere (Project Drawdown, 2020). There were two scenarios modelled under Project Drawdown. The less ambitious Scenario 1 modelled a rise of CO_2-eq concentrations to approximately 540 ppm by year 2050, resulting in a rise of the average surface temperature by 1.74 °C, relative to the pre-industrial level (Project Drawdown, 2020). The average surface temperature is projected to further rise to 1.85 °C above the pre-industrial level by year 2060, due to the time lag between

GHGs emissions and planetary warming (Project Drawdown, 2020). By contrast, the more ambitious Scenario 2 aims to limit the rise of the average surface temperature by the end of this century to 1.5 °C, relative to the pre-industrial level. In Scenario 2, the CO_2-eq concentration is expected to peak at 490 ppm in mid-2040, before falling to 485 ppm by year 2050 (Project Drawdown, 2020). According to the Drawdown Review (Project Drawdown, 2020), the CO_2 concentration in the atmosphere as of early year 2020 was 410 ppm. Considering other GHGs such as methane (CH_4), nitrous oxide (N_2O), and chlorofluorocarbons (CFCs), the CO_2-eq concentrations were estimated at 460 ppm (Project Drawdown, 2020). In other words, the CO_2-eq concentrations are projected to hit the 540 ppm mark in year 2050, mimicking the less ambitious Scenario 1 (Project Drawdown, 2020). Table 1-1 presents a summary of the literature review regarding existing climate change and global warming situation.

Table 1-1: Summary of the literature review regarding existing climate change and global warming situation

Summary	Literature
Between years 2006 and 2015, the global mean surface temperature of land and ocean was 0.87 °C higher than the pre-industrial level. The rate of warming of land alone was twice higher at 1.53 °C	(IPCC, 2019a)
Between years 2016 and 2020, the global mean surface temperature was 1.1 °C higher than the pre-industrial level; 0.24 °C warmer than years 2011 and 2015	(World Meteorological Organization, 2020)
Global average CO_2 concentration at 412.5 ppm by the end of year 2020	(IEA, 2021a)
Electricity sector contributed 36% of global CO_2 emissions in year 2020 where 75% of it was contributed by coal	(IEA, 2021a)
2nd largest annual increase of CO_2 emissions in history in year 2021	(IEA, 2021a)

GHGs emissions are projected to hit 60 Gt CO_2-eq by year 2030	(United Nations Environment Programme, 2019)
CO_2-eq concentration is projected to hit 540 ppm by year 2050, translating to a temperature rise of 1.74 °C (year 2050) and 1.85 °C (year 2060)	(Project Drawdown, 2020)
Global warming is projected to hit 3.2 °C in year 2100 despite the full deployment of unconditional NDCs	(IPCC, 2018; United Nations Environment Programme, 2019)

Speaking of climate change impacts, global warming has resulted in an increased occurrence of heat-related events (droughts), a loss of sea ice sheets and glaciers (IPCC, 2019b), decreased snow cover (IPCC, 2019b) and heavy precipitations (IPCC, 2019a). IPCC (2019a) reported that 1.5 °C global warming is projected to impact 178 million people by year 2050 due to water stress, habitat degradation and desertification. A further rise in global warming to 2 °C and 3 °C above the pre-industrial level will potentially impact 220 and 277 million people respectively (IPCC, 2019a). Among all continents, Asia and Africa are most likely to be impacted by desertification, resulting in a decline in crop yield (IPCC, 2019a). Aside from desertification, global warming also led to an average loss of 278 Gt y^{-1} of ice mass at the Greenland Ice Sheet (IPCC, 2019a). Between years 1967 to 2018, the June snow cover at the Artic declined by 13.4% per decade, translating to an approximate loss of 2.5 million km^2 of snow (IPCC, 2019a). Climate change impacts often extend beyond environmental consequences. The accumulation of GHGs in the atmosphere is parallel to the rise of air pollution, accelerating health impacts such as pneumonia and asthma (Project Drawdown, 2020). Both environmental and health impacts lead to economic and social consequences such as the loss of human and social rights (Levvy and Patz, 2015). Low-income countries are highly probable to suffer greater consequences of climate change despite emitting the least amount of GHGs (Levvy and Patz, 2015). Table 1-2 presents a summary of the literature review regarding the impacts of climate change.

Table 1-2: Summary of the literature review regarding the impacts of climate change

Summary	Literature
Loss of sea ice sheets & glaciers, decreased snow cover and heavy precipitations	(IPCC, 2019b, 2019a)
Global warming of 1.5, 2 and 3 °C is projected to impact 178, 220 and 277 million people respectively	(IPCC, 2019a)
An average loss of 278 Gt y^{-1} of ice mass at the Greenland Ice Sheet	(IPCC, 2019b)
June snow cover at the Artic decreased by 13.4% per decade between years 1967 and 2018	(IPCC, 2019b)
Increased air pollution, thus resulting in health impacts	(Project Drawdown, 2020)
Loss of human and social rights	(Levvy and Patz, 2015)

Rapid mitigation actions are needed to manage the imminent impacts of climate change and global warming. The Paris Climate agreement aimed at limiting the rise of the average surface temperature to well below 2 °C, relative to the pre-industrial level, while pursuing efforts in limiting the rise of the average surface temperature to within 1.5 °C above the pre-industrial level (IPCC, 2018). While it is forecasted that the initial implementation costs of mitigation responses on a global scale to be in the range of $ 23.4 to $ 26.2 trillion, the benefits of climate change solutions, valued in the range of $ 96.4 to $ 143.5 trillion far outweigh the external costs (Project Drawdown, 2020). The benefits valuation does not include other co-benefits such as increased savings in healthcare due to reduced air pollution and minimisation of agriculture losses, proving that climate change solutions offer significant benefits to mankind despite a high initial investment (Project Drawdown, 2020). According to the IPCC, the net global CO_2 emissions must fall by 45% in year 2030 in comparison to year 2010 levels, before subsequently achieving net-zero emissions in year 2050 (IPCC, 2018). On a broader scale, two strategies may be employed in limiting global warming, comprising of *mitigation responses* and *carbon dioxide removal* (CDR) (IPCC, 2018). The former would either prevent or at least minimise the emissions of GHGs. One example of a mitigation response is the increased usage of renewable energy sources in the

power generation sector. Presently, fossil fuels such as coal and natural gas dominate the electricity generation mix due to their technological maturity and higher reliability. By contrast, renewable energy sources such as solar and wind are dependent on environmental conditions such as the speed of the wind, intensity of sunlight, seasonal changes and geographical location (Stram, 2016). Additionally, solar energy requires a high capital expenditure due to costly solar photovoltaic (PV) cells (Stram, 2016). While electricity demand remains on the rise, inconsistent power generation leads to lower dependency and thus reduced confidence in renewable energy sources. The intermittency of renewable energy sources necessitates the need for storage technology to act as a buffer, entailing additional operating costs (Stram, 2016). However, a heavy reliance on traditional fossil fuels translates to ever-rising CO_2 emissions, forcing a trend to incorporate renewable energy sources for electricity generation. Over the last decade, a sharp decline in the cost of solar PV cells and wind turbines accelerated the incorporation of renewable energy sources into the power generation mix (IEA, 2021a). It is projected that a minimum of 500 GW of solar PV and wind energy would be added annually at least until year 2030 (IEA, 2021a). Looking into the future, the increased integration of renewable energy sources into the power generation mix alongside traditional fossil fuels would aid in the reduction of total GHGs emissions. Over the next two decades, the renewable energy sector is forecasted to experience a steeper growth. By the end of year 2040, renewable energy sources are projected to contribute 52.5% of the total electricity generation with the oil sector no longer in the mix (IEA, 2019).

As part of the mitigation actions, Project Drawdown proposed a wide range of potential initiatives that could be undertaken to minimise the rise of the average surface temperature to within 1.5 °C above the pre-industrial level, covering aspects such as electricity production, agricultural and land usage, transportation and buildings (Project Drawdown, 2020). In terms of electricity generation, it is necessary to shift away from traditional fossil-based sources such as oil, coal and natural gas while incorporating renewable energy sources. The latter includes the use of hydropower, solar power, geothermal and wind energy, and is forecasted to draw down approximately 163.8 – 397 Gt CO_2-eq between years 2020 and 2050 (Project Drawdown, 2020). While electricity generation from renewable energy sources is usually viewed as carbon-neutral, Life Cycle Assessment (LCA) shows otherwise (Ludin et al., 2018). Consequently, the dependency

on renewable energy sources alone is not sufficient in minimising GHGs emissions, hence requiring further mitigation strategies such as CO_2 Capture and Storage (CCS) deployment. Traditional fossil fuels such as coal and natural gas have high CO_2 intensities, i.e., approximately 1 and 0.5 Mt TWh^{-1} respectively (Ooi et al., 2013). The use of CCS decreases these high CO_2 intensities of fossil fuels by over 80% (Ooi et al., 2013). It is forecasted that CCS could potentially draw down approximately 2.2 – 4.4 Gt CO_2-eq between years 2020 and 2050 (Project Drawdown, 2020). Typically, *carbon capture* technologies may be categorised as post-combustion capture, pre-combustion capture and oxyfuel capture (Gibbins and Chalmers, 2008). The captured CO_2 is then compressed before being stored in depleted oil fields and saline aquifers (Gibbins and Chalmers, 2008). By the end of year 2021, there was only one large-scale operational CCS project (with 30 other new plants in the development stage), with a capacity of sequestering approximately 1 Mt CO_2 y^{-1}. Considering all CO_2 capture plants in the development pipeline, the CO_2 capture capacity would only hit 60 Mt CO_2 y^{-1} in year 2030. Note that this projection is far off from the target of sequestering approximately 430 Mt CO_2 y^{-1} in efforts to achieve net-zero emissions by year 2050 (Fajardy, 2021). Nevertheless, IEA reported that recent policy developments and technology innovations may drive the growth of CCS deployment (Fajardy, 2021). Despite the high costs of CO_2 compressions and additional capital expenditure, CCS deployment is vital for a cumulative reduction of GHGs.

Most recently, the COP26 in Glasgow proved to be vital in further driving the efforts to mitigate climate change impacts. The Glasgow Climate Pact finalised the pledges made in the Paris Agreement to ensure that the initial target of limiting global warming to within 1.5 °C above the pre-industrial level remains achievable if all countries are jointly united in fulfilling their pledges (United Nations Climate Change, 2021a). Through the Glasgow Climate Pact, 153 countries, covering 80% of the global GHGs emissions had revised their NDCs. The revised NDCs imply that more than 90% of the world's gross domestic product and approximately 90% of the world's GHGs emissions are now included in the scope of net-zero commitment (United Nations Climate Change, 2021a). Additionally, countries have jointly agreed to further improvise and strengthen their year 2030 targets in year 2022. At the current progress, the projected GHGs emission by year 2030 would be approximately 5Gt lower than initially predicted (United Nations Climate

Change, 2021a). Although some countries were not aligned in the net-zero commitment, an agreement had been achieved to accelerate the deployment of mitigation actions for managing climate change impacts. One of the important milestones of COP26 was phasing down unabated coal. A total of 190 countries had agreed to reduce coal burning due to its high CO_2 intensity (United Nations Climate Change, 2021a). This also means that countries are striving for energy transition to achieve their net-zero targets. On the other hand, under the Global Methane Pledge, more than 100 countries have jointly agreed to reduce methane emissions by 30% by year 2030, covering 46% of global methane emissions (United Nations Climate Change, 2021a). Methane is a hazardous greenhouse gas due to its ability to capture heat up to 25 times greater than CO_2 (United States Environmental Protection Agency, 2021). Therefore, the commitment for methane reduction has come promptly. Other milestones include halting deforestation and accelerating migration to electric vehicles (United Nations Climate Change, 2021a). For the latter effort, the increased usage of electric vehicles as part of the effort to decarbonise the road transportation sector could potentially reduce 2.6 Gt CO_2 by year 2030 (United Nations Climate Change, 2021a). Meanwhile, halting deforestation would allow forests to capture GHGs from the atmosphere, aside from preserving the habitat for animals. The pledges made under the Paris Agreement and Glasgow Climate Pact focused on the drastic reduction of GHGs emissions. Table 1-3 presents the summary of the literature review regarding the mitigation responses toward limiting global warming.

Table 1-3: Summary of the literature review regarding the mitigation responses toward limiting global warming

Summary	Literature
Deploying renewable energy sources e.g., hydropower, solar power, geothermal and wind energy into the power generation mix. Estimated drawdown potential of approximately 163.8 – 397 Gt CO_2-eq between years 2020 and 2050	(Project Drawdown, 2020)
CCS deployment with an estimated drawdown potential of approximately 2.2 – 4.4 Gt CO_2-eq between years 2020 and 2050	(Project Drawdown, 2020)
CCS deployment is required to sequester approximately 430 Mt CO_2 y^{-1} to achieve the net-zero emissions target by year 2050	(Fajardy, 2021)
Phasing down unabated coal, 30% methane emissions reduction target by year 2030, deforestation halting and migration to electric vehicles to reduce 2.6 Gt CO_2 by year 2030 (COP26)	(United Nations Climate Change, 2021b)

Although these actions are commendable in mitigating climate change impacts, much more needs to be done to limit global warming to within 2 °C, and possible 1.5 °C above the pre-industrial level. Phasing down unabated coal alone would be insufficient in meeting climate change targets. As part of the global goal to achieve net-zero emissions, it would require the removal of GHGs from the atmosphere to complement the GHGs emissions reduction strategy. The background work regarding CDR and negative emission technologies (NETs) would be provided in the next chapter.

1.2 Research Scope

This research will focus on the deployment of NETs, alongside CCS and renewable energy sources during *carbon-constrained energy planning* (CCEP) to systematically address issues related to CO_2 emissions reduction. The research scope involves the development of pinch analysis and mathematical optimisation approaches for the deployment of NETs and CCS techniques during CCEP. For the pinch analysis approach, new targeting techniques i.e., graphical, and algebraic

targeting techniques are developed to determine the minimum deployment of energy-producing NETs (EP-NETs), energy-consuming NETs (EC-NETs) and CCS, alongside renewable energy sources for the satisfaction of the CO_2 emissions limit within a specified geographical region. On the other hand, the mathematical optimisation approach is used for the development of a detailed multiperiod energy planning model of NETs.

1.3 Research Aims and Objectives

The aims and objectives of this research are given as follows:

i. To determine the minimum deployment of EP-NETs alongside CCS and renewable energy sources during the energy planning stage using a graphical targeting technique **(Chapter 3)**.

ii. To determine the minimum deployment of EC-NETs alongside EP-NETs, CCS, and renewable energy sources during the energy planning stage by developing a graphical targeting technique **(Chapter 4)**.

iii. To develop a novel algebraic targeting technique to determine the target deployment of renewable energy sources, CCS and NETs during energy planning **(Chapter 5)**.

iv. To develop a mathematical optimisation approach involving multiperiod energy planning for the deployment of renewable energy sources, CCS and NETs involving CO_2 intensive industries **(Chapter 6)**.

1.4 Problem Statement

The energy planning problem with the deployment of NETs during CCEP is formally stated as follows:

- Given a set of energy sources $i \in I$ comprise of either fossil-based sources e.g., coal, oil, or natural gas, renewable energy sources e.g., tidal, wind, hydropower etc. or EP-NETs e.g., bioenergy with CCS (BECCS) and biochar. Energy source i has a given amount of energy, $F_{S,i}$, and its respective CO_2 intensity, $C_{S,i}$. The product of its energy amount and CO_2 intensity yields the CO_2 emissions for energy source i. The total CO_2 emissions of all energy sources are given as Δm_T.

- Given a set of energy demand $j \in J$ comprise of geographical regions/economic sectors and EC-NETs e.g., direct air capture (DAC), ocean liming, enhanced weathering (EW) etc. each with its energy requirement, $F_{D,j}$, and maximum CO_2 emissions, $\Delta m_{D,j}$. Dividing the latter with the former yields the CO_2 intensity of energy demand j, $C_{D,j}$.
- It is desired to reduce the CO_2 emissions for a given region/sector. Hence, an aggregate CO_2 emissions limit, Δm_L is set. The difference between Δm_T and Δm_L represents the target reduction of CO_2 emissions, Δm_R.
- The energy planners may utilise NETs, CCS, renewable energy sources, or a combination of them for the satisfaction of the maximum CO_2 emissions limit, Δm_L.
- This work identifies minimum deployment of renewable energy sources, CCS and NETs to achieve Δm_L for a given energy planning problem. Both parasitic power losses (X) and removal ratio (RR) of the CCS system are assumed to remain constant. The compensatory energy consists of either renewable energy sources or EP-NETs to make up for power losses during CCS.

A superstructural representation for the above planning problem may be given in Figure 1-1.

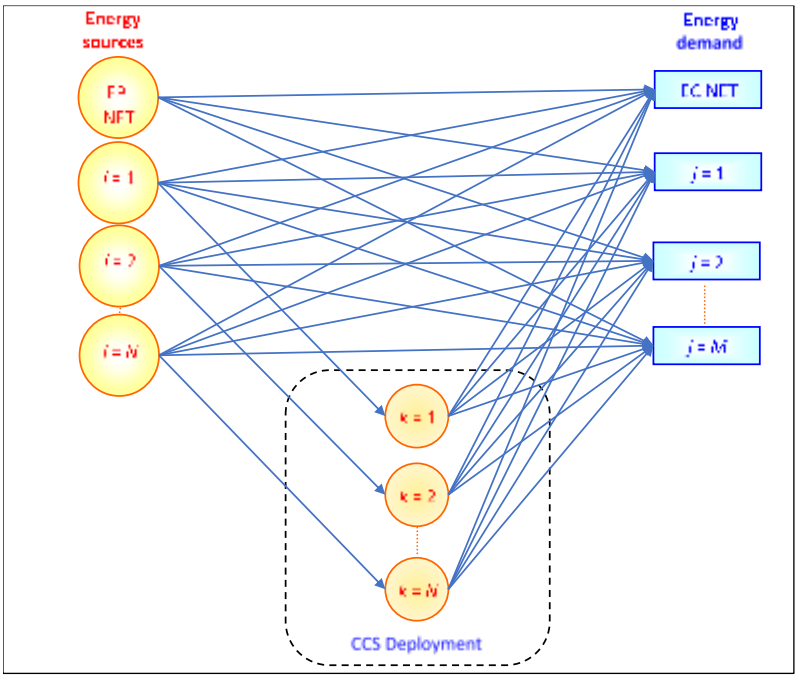


Figure 1-1: Superstructural representation of energy planning problem involving NETs and CCS

Chapter 2: LITERATURE SURVEY

2.1 Pinch Analysis

The concept of pinch analysis was first introduced in the 1970s when Hohmann (1971) synthesised heat exchanger networks for optimum energy recovery. The *pinch analysis* concept was first introduced in this via a graphical technique for determining optimal energy utility targets. Improved pinch methodology was developed in subsequent work (Linnhoff and Flower, 1978; Umeda et al., 1978). Later, Linnhoff *et al.* (1982) documented the use of pinch analysis for energy integration under the branch of process integration which was subsequently incorporated into mainstream process design (Smith, 2016). El-Halwagi and Manousiouthakis (1989) extended the pinch analysis concept for *mass exchange networks*, leading to *mass integration* (El-Halwagi, 2012) and subsequently *material resource conservation networks* (Foo, 2012). These early extensions were based on similarities between heat and mass transfer; subsequent developments in pinch analysis have resulted from similar analogies. Recently, Klemeš *et al.* (2018) surveyed the application of pinch analysis to tackle diverse sustainability challenges. In these early works of heat and mass integration, the pinch analysis concept allows the identification of system targets ahead of detailed design, e.g., hot, and cold utilities for heat exchanger networks, minimum fresh resources for material resource conservation network, etc. Also, Linnhoff and Dhole (1993) utilised the pinch analysis concept to perform a total site integration which eventually lead to the first reporting of CO_2 emissions reduction. In short, pinch analysis is beneficial in identifying process improvement targets, as well as specific measures for improving the performances of existing systems.

2.2 Carbon Emissions Pinch Analysis (CEPA)

CEPA is a key fundamental technique for CCEP. Utilising the targeting philosophy of *pinch analysis*, Tan and Foo (2007) pioneered the *energy planning pinch diagram* (EPPD) in Figure 2-1 to determine the minimum deployment of renewable or low-carbon energy sources needed to meet the CO_2 emissions limit.

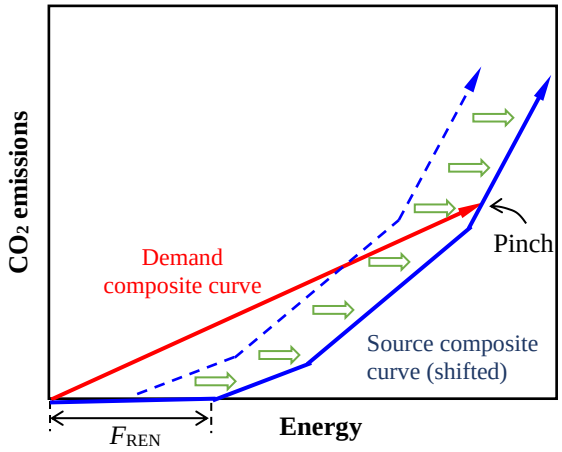


Figure 2-1: Pinch analysis in graphical targeting technique (Tan and Foo, 2007)

Based on the EPPD in Figure 2-1, the deployment target of renewable energy sources (F_{REN}) is obtained by shifting the source composite curve until it stays entirely to the right and below the demand composite curve. The point where the demand and source composite curves touch each other is the *pinch point*. The latter is viewed as the bottleneck of the energy planning system in determining the minimum deployment of renewable energy sources in meeting the CO_2 emissions limit (Tan and Foo, 2007). In other words, if lesser renewable energy sources are deployed, the CO_2 emissions limit would be violated. Therefore, the pinch analysis concept is vital in providing the best possible targets for an energy planning scenario. Aside from the EPPD, various CEPA targeting techniques were extended from these early works of energy and mass integration mentioned in Chapter 2.1. For instance, the algebraic targeting techniques i.e., *cascade analysis* (Foo et al., 2008) and *composite table algorithm* (Shenoy, 2010) were developed in the same manner, that the *problem table algorithm* was used in heat integration (Linnhoff et al., 1982). While Lee *et al.* (2009) developed a novel automated targeting approach for the targeting of low-carbon energy sources, Bandyopadhyay *et al.* (2010) developed *segregated planning approaches* for optimum allocation of specific energy resources to various sectors.

2.3 Planning of CO_2 Capture and Storage in CEPA

The graphical targeting technique of EPPD was later extended by Tan et al. (2009b) to deploy CCS, where renewable energy sources served as compensatory energy; shown in Figure 2-2.

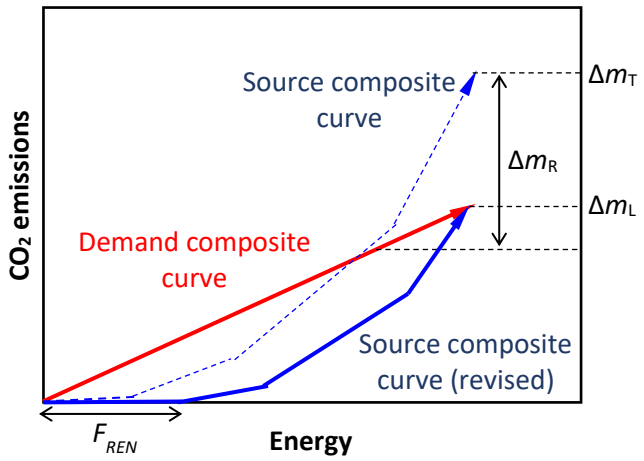


Figure 2-2: Pinch analysis in graphical targeting technique with CCS deployment (Tan et al., 2009b)

Based on Figure 2-2, note that the total target CO_2 emissions reduction (Δm_R) is greater than the difference between the cumulative CO_2 emissions of all energy sources (Δm_T) and the aggregate CO_2 emissions limit (Δm_L). This is due to the parasitic power losses during CCS deployment. Consequently, renewable energy sources (F_{REN}) with the assumption of zero CO_2 intensity were deployed as compensatory energy. The limitation of the graphical targeting technique led to the utilisation of the automated targeting method (ATM) for CCS deployment by Ooi *et al.* (2013). In the latter work, Ooi *et al.* (2013) minimised the deployment of compensatory energy, which was to be served by renewable energy sources. Subsequently, Ooi et al. (2014) further improvised the work to incorporate a multiperiod energy planning model. By utilising either the graphical targeting technique or ATM, the model would determine the optimum deployment of renewable energy sources and CCS technology for each period. Note that in this multiperiod work, the CO_2 emissions limit may be violated in earlier periods provided that the limit is satisfied at the end of the energy planning horizon (Ooi et al., 2014). Later, Sahu *et al.* (2014) developed an algebraic targeting technique to minimise the use of compensatory energy during CCS deployment, using both renewable energy and fossil-based sources. In another work of CCS planning by Thengane *et al.* (2019), a graphical pinch approach was used to determine the optimum allocation of captured CO_2 with available geological reservoirs. A method for planning electricity trading systems was also introduced by Lopez et al. (2021) to minimise the requirement for renewable

energy sources. Table 2-1 presents a summary of the literature review on the pinch-based approach in the development of CEPA.

Table 2-1: Summary of the literature review on the pinch-based approach in the development of CEPA

Brief Summary	Literature
Development of pinch analysis concept	(Hohmann, 1971)
Pinch analysis for energy integration	(Linnhoff et al., 1982)
Pinch analysis for mass exchange networks	(El-Halwagi and Manousiouthakis, 1989)
Pinch analysis for total site integration	(Linnhoff and Dhole, 1993)
Development of EPPD	(Tan and Foo, 2007)
Development of cascade analysis technique	(Foo et al., 2008)
Development of an automated targeting approach	(Lee et al., 2009)
EPPD for CCS deployment	(Tan et al., 2009b)
Development of composite table algorithm and nearest neighbour algorithm	(Shenoy, 2010)
Segregated targeting of multiple resource networks	(Bandyopadhyay et al., 2010)
Pinch analysis for mass integration	(El-Halwagi, 2012)
Pinch analysis for conservation of various material resources	(Foo, 2012)
ATM for CCS deployment	(Ooi et al., 2013)
Graphical targeting technique & ATM for multiperiod energy planning	(Ooi et al., 2014)
Development of algebraic targeting technique	(Sahu et al., 2014)
Pinch analysis for process design	(Smith, 2016)
Graphical pinch approach for CCS planning	(Thengane et al., 2019)
Electricity trading	(Lopez et al., 2021)

2.4 Mathematical Optimisation Approaches in CO_2 Emissions Reduction

The work concerning CO_2 emissions reduction was also performed using mathematical programming approaches. A superstructural model was developed by Pekala *et al.* (2010) to develop an energy planning scenario subject to CO_2 emissions and land footprint constraints. In this work, liquid biofuels and CCS technology were included in the energy planning model for the mitigation of CO_2 emissions (Pękala et al., 2010). Meanwhile, Tan *et al.* (2013) developed a mixed-integer linear programming (MILP) model to match the CO_2 sources to available CO_2 sinks i.e., reservoirs. This work is particularly useful in handling CCS systems during energy planning (Tan et al., 2013). Later, carbon integration networks purposed for industrial parks were developed for both single period (Al-Mohannadi and Linke, 2016) and multiperiod (Al-Mohannadi et al., 2016) energy planning models. The optimisation-based approach focused on the development of low-cost carbon networks that satisfied the CO_2 emissions constraints within an industrial cluster (Al-Mohannadi et al., 2016; Al-Mohannadi and Linke, 2016). Tan (2016) also developed a MILP model for biochar-based systems that minimises the total carbon footprint while ensuring that the parameters of the soil quality remain unimpacted. Behrens et al. (2016) equally developed a mathematical model for the planning of Portugal's electricity system using a high proportion of renewable energy sources i.e., hydropower. Later, P-graph and Monte Carlo simulation approaches were adopted for CCEP, while considering CCS deployment (Tan et al., 2017). The P-graph technique ensured the generation of robust and near-optimal carbon management networks (Tan et al., 2017). A linear programming model was also developed to optimise the enhanced weathering (EW) network (Tan and Aviso, 2019). This optimisation model considered source-sink constraints for the use of EW in the acceleration of carbon fixation while minimising CO_2 emissions (Tan and Aviso, 2019). Most recently, Mohd Idris and Hashim (2021) successfully modelled the integration of biomass co-firing alongside coal to achieve a significant reduction in CO_2 emissions. Table 2-2 presents a summary of the literature review on the use of the mathematical programming approaches in the work concerning CO_2 emissions reduction.

Table 2-2: Summary of the literature review on mathematical programming approaches in the work concerning CO_2 emissions reduction.

Brief Summary	Literature
Superstructural model	(Pękala et al., 2010)
MILP model for CCS systems	(Tan et al., 2013)
Carbon integration networks for industrial parks (single period)	(Al-Mohannadi and Linke, 2016)
Carbon integration networks for industrial parks (multiperiod)	(Al-Mohannadi et al., 2016)
MILP model for biochar-based systems	(Tan, 2016)
Mathematical model for Portugal's electricity system	(Behrens et al., 2016)
P-graph and Monte Carlo simulation approaches for CCEP	(Tan et al., 2017)
Linear programming model for EW networks	(Tan and Aviso, 2019)
Modelling of biomass co-firing with coal	(Mohd Idris and Hashim, 2021)

2.5 Applications of CEPA

The application of CEPA is evident globally. Crilly and Zhelev (2008, 2010) outlined the significance of CEPA in determining the optimal fuel mix for Ireland's electricity generation sector. Additionally, Atkins et al. (2010) and Walmsley *et al.* (2014, 2015) reported the usage of CEPA for the reduction of CO_2 emissions from the power generation and transportation sectors in New Zealand. Additionally, CEPA was utilised to assess the target of generating one-third of the electricity production in California via renewable energy sources (Walmsley et al., 2015a). Liang and Lu (2015) utilised CEPA to determine the minimum deployment of renewable energy sources to meet China's emissions constraints. Salman et al. (2019) adopted CEPA for energy sector planning in Nigeria. The utilisation of CEPA is evident in Baltic countries (Baležentis et al., 2019). Baležentis *et al.* (2019) reported the usage of biomass in Estonia and Latvia, and wind energy in Lithuania, both obtained from CEPA. In India, Priya and Bandyopadhyay (2013) conducted a

power system planning for the Indian electricity sector based on CEPA principles. Aside from that, CEPA was used to determine the energy mix for the electricity generation sector in various countries within the European Union (Poland, Netherlands, Germany, Italy, the United Kingdom, Spain, France and Sweden) (Su et al., 2020). Most recently, Cossutta et al. (2021) applied CEPA to achieve net-zero emissions in the United Kingdom by year 2050.

Additionally, CEPA was utilised to assess the year 2050 target for the United Arab Emirates in terms of its CO_2 emissions while considering the energy return on investment and water footprint (Lim et al., 2018). In other words, the pinch analysis philosophy allows CEPA to be readily extended for various energy planning aspects, i.e., land (Foo et al., 2008), water (Tan et al., 2009a) and product carbon footprint (Tjan et al., 2010; Yap et al., 2020). Additionally, a paper by Tan et al. (2018) demonstrated the combination of CEPA alongside input-output analysis to measure the economic performance of a country. The CEPA technique is now relatively mature and can be found in a review paper (Foo and Tan, 2016), an encyclopaedia chapter (Tan and Foo, 2017), a handbook chapter (Tan and Foo, 2013) and even in a monograph (Foo and Tan, 2020). Critically, Andiappan et al. (2019) demonstrated the use of CEPA as guidance for policymaking in the energy sector. Table 2-3 presents a summary of the literature mentioned in the application of CEPA.

Table 2-3: Summary of literature review on CEPA application

Brief Summary	Literature
CEPA in Ireland	(Crilly and Zhelev, 2010, 2008)
Pinch analysis for water footprint	(Tan et al., 2009a)
CEPA for New Zealand's electricity sector	(Atkins et al., 2010)
CEPA for chemical processes	(Tjan et al., 2010)
CEPA for India based on prioritised cost	(Priya and Bandyopadhyay, 2013)
Combination of CEPA and energy return on investment for New Zealand's electricity sector	(Walmsley et al., 2014)
CEPA for New Zealand's transportation sector	(Walmsley et al., 2015b)
CEPA for China	(Liang and Lu, 2015)
CEPA for the USA	(Walmsley et al., 2015a)
CEPA technique in a review paper	(Foo and Tan, 2016)
CEPA in an encyclopaedia chapter	(Tan and Foo, 2017)
CEPA for the UAE	(Lim et al., 2018)
CEPA for economic systems	(Tan et al., 2018)
CEPA for Nigeria	(Salman et al., 2019)
CEPA for Baltic states	(Baležentis et al., 2019)
CEPA for Malaysia	(Ramli et al., 2019)
CEPA for policymaking	(Andiappan et al., 2019)
CEPA in a monograph	(Foo and Tan, 2020)
CEPA in multi-product plants	(Yap et al., 2020)
CEPA for the EU	(Su et al., 2020)
CEPA for the UK	(Cossutta et al., 2021)
CEPA for Trinidad and Tobago	(Ramsook et al., 2022)

2.6 Negative Emissions Technologies

According to the IPCC (2018), the deployment of CDR would be required in the range of 100 to 1,000 Gt CO_2 throughout the 21st century. CDR can be achieved using NETs through different physical, chemical, or biological pathways (McGlashan et al., 2012). Nevertheless, the reliance on CDR for achieving climate change targets requires a significant decline in CO_2 emissions by year 2030 (IPCC, 2018). Therefore, previous efforts in decarbonising the global economy can help to ensure a successful deployment of CDR. NETs offer the opportunity to offset positive emissions originating from sectors that are hard to decarbonise e.g., transportation and agricultural sectors (McGlashan et al., 2012). NETs can be categorised according to their capture methods and storage mechanisms (McLaren, 2012). The two capture methods are *direct capture* and *indirect capture* (McLaren, 2012). The direct capture method involves the utilisation of chemicals for the absorption of CO_2 from the air e.g., EW, DAC, and ocean liming. By contrast, indirect capture methods such as biochar and BECCS rely on photosynthesis by plants for CO_2 removal from the air, eventually forming biomass.

EW refers to the dispersion of large quantities of silicate or carbonate minerals into the soil for accelerated reactions with carbonic acid originating from dissolved CO_2 in rainwater (Bach et al., 2019). The soluble end products of EW are ultimately carried by runoff into bodies of water (McLaren, 2012). Like EW, ocean alkalinisation involves the addition of lime generated from lime kilns to the surface layers of the ocean (McGlashan et al., 2012). The lime reacts with atmospheric CO_2 resulting in the rise of the water pH (McGlashan et al., 2012). Consequently, more CO_2 is absorbed by the alkaline seawater. One benefit of ocean alkalinisation is that no CO_2 compression is required since the absorption is readily taking place in the ocean (McGlashan et al., 2012). Figure 2-3 presents the arrangement of EW and ocean alkalinisation technology.

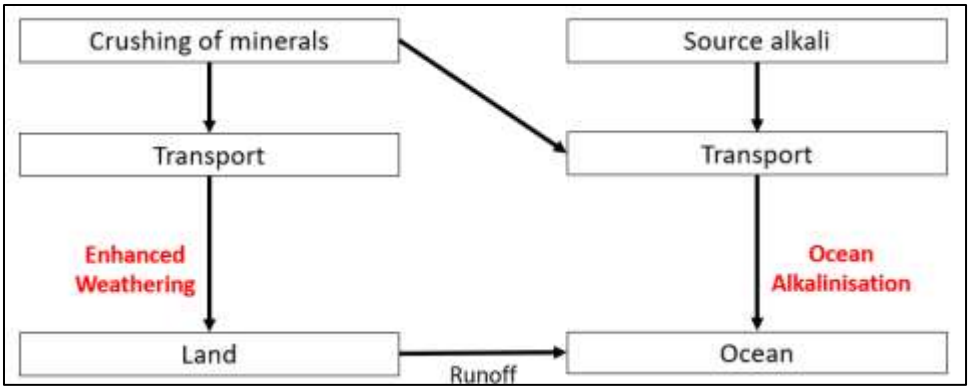


Figure 2-3: Arrangement of EW and ocean alkalinisation technology

On the other hand, DAC also referred to as artificial trees, utilises sorbents for the separation of CO_2 from the air (McGlashan et al., 2012). Upon saturation, the sorbent is regenerated for CO_2 separation, which is then pressurised for storage (McGlashan et al., 2012). Figure 2-4 presents the arrangement of the DAC technology.

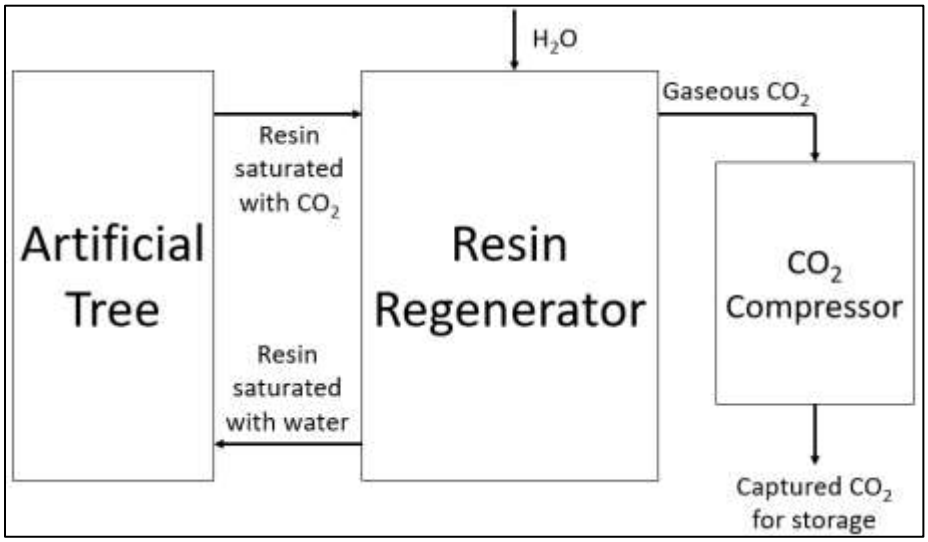


Figure 2-4: Arrangement of DAC technology

As for the indirect capture method, biochar involves slow pyrolysis of biomass under an oxygen-deficient environment (McGlashan et al., 2012). The usage of biomass is considered as NETs since it previously captured atmospheric CO_2 via purpose-grown energy crops. The biochar is applied to the soil for property enhancement (McGlashan et al., 2012). The recalcitrant carbon content of the biochar is effectively sequestered in the soil in a solid form. The slow pyrolysis also

generates liquid and gaseous energy resources, which may be combusted for heat and power generation (McGlashan et al., 2012). Figure 2-5 presents the arrangement of biochar technology.

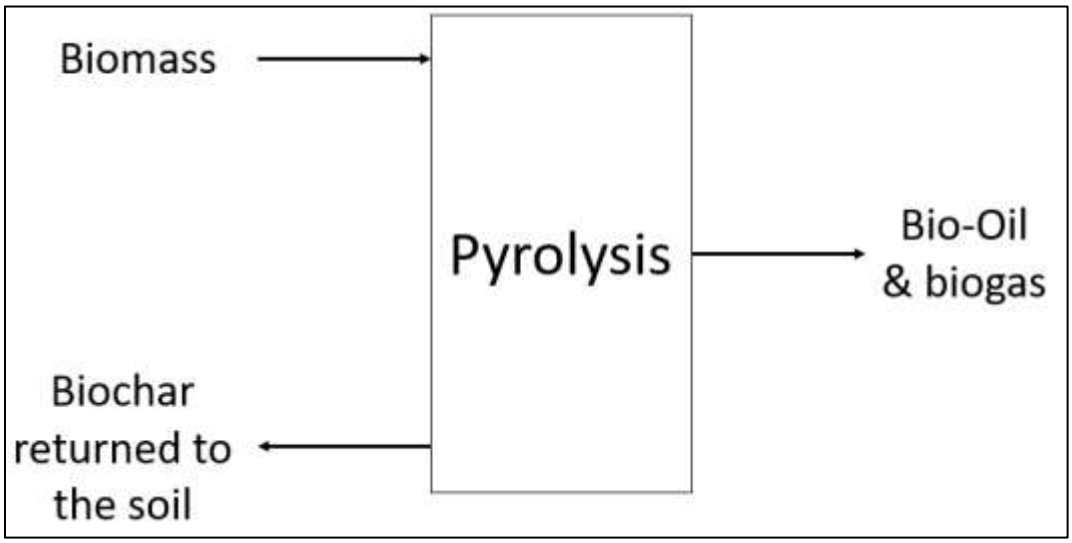


Figure 2-5: Arrangement of biochar technology

On the other hand, BECCS is the combustion of biomass in power plants retrofitted with CCS (McGlashan et al., 2012). Without CCS, power generation through biomass combustion alone may be regarded as carbon-neutral (or as a low carbon process). Therefore, retrofitting power plants with CCS makes BECCS a carbon-negative process. Figure 2-6 presents the arrangement of the BECCS technology.

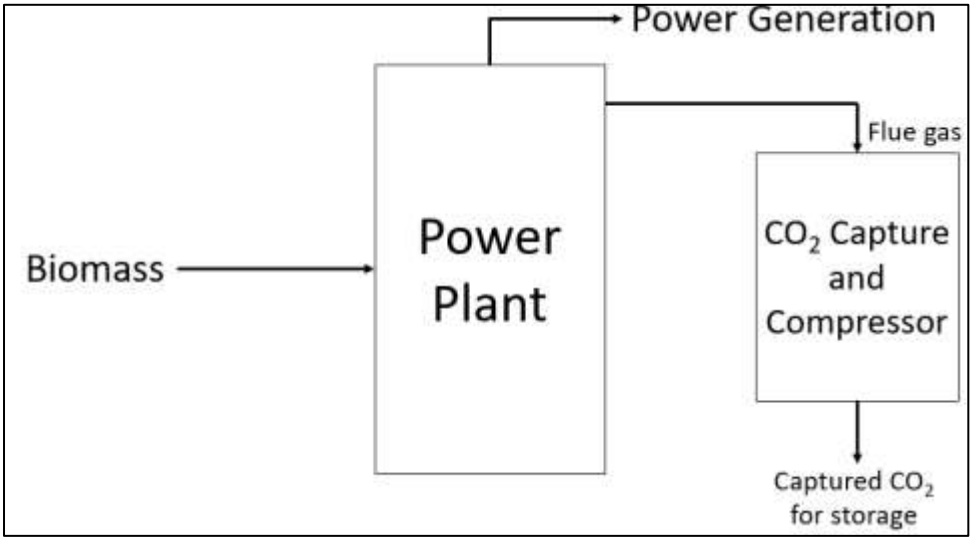


Figure 2-6: Arrangement of BECCS technology

Table 2-4 presents an overview of various NETs. Based on Table 2-4, each NETs has its respective advantages and disadvantages with various applications. Aside from the overview of various NETs in Table 2-4, NETs can also be classified into four different storage categories, such as mineral, pressurised, oceanic and biotic (McLaren, 2012). Mineral storage involves the formation of bonds between CO_2 molecules in a mineral form (McLaren, 2012). Examples of mineral storage are EW and biochar. On the other hand, pressurised storage such as DAC and BECCS involves the storage of pressurised CO_2 in depleted oil wells or saline aquifers (Gibbins and Chalmers, 2008; McLaren, 2012). Ocean liming is categorised under oceanic storage, where carbon binds with naturally occurring minerals in the ocean (McLaren, 2012). Lastly, biotic storage ensures the carbon is held in a stable form. The usage of timber in construction, burial of biomass, and reforestation are classified under biotic storage (McLaren, 2012). Therefore, it is important to develop rigorous models to prioritise and optimise the usage of NETs before incorporating them into a carbon management plan.

Table 2-4: Overview of various NETs

Type of Capture Method	Examples	Description	Advantages	Disadvantages	Literature
Direct Capture	Enhanced Weathering	Enhanced reaction with dissolved CO_2 from rainwater due to mineral addition to the soil	- Lower storage cost due to the absence of pressurised CO_2 storage - Minimal land requirement	- Dependent on the availability of suitable land - Requires significant energy input for CO_2 removal, thus higher operating cost	(Bach et al., 2019; McLaren, 2012)
	Direct Air Capture	Utilising absorbents for CO_2 absorption from the air	- Can be located at any geographical location - Direct absorption of CO_2 from the atmosphere using resins	- Higher storage cost due to pressurised CO_2 storage - Requires significant energy input for CO_2 removal, thus higher operating cost - Requires an abundant water source for the regeneration of the resin	(McGlashan et al., 2012; Smith et al., 2016a)
	Ocean Liming	Addition of lime kiln to the surface layer of the ocean to react with atmospheric CO_2	- Lower storage cost due to the absence of pressurised CO_2 storage - Traps CO_2 in its natural mineral form	- Requires transportation of lime kiln to the middle of the ocean, thus higher operating cost - Possesses a risk of interfering with the natural balance of the ocean ecosystem	(Bach et al., 2019; McGlashan et al., 2012)
Indirect Capture	Biochar	Slow pyrolysis of biomass under an oxygen-deficient environment	- The solid form of biochar may be utilised for soil reinforcements - Lower CO_2 emissions from the agriculture sector due to reduced fertiliser usage - Emissions avoidance via the substitution of fossil fuels with biofuels	- Uncertainty of large-scale implementation - Lack of understanding regarding the interaction of biochar with various kinds of soils	(McGlashan et al., 2012)
	Bioenergy with CCS	Biomass combustion in a CCS retrofitted power plant	- High technology maturity - Net energy output during CO_2 removal	- Dependent on the availability of suitable energy crops - Competition of land area between food and energy crops - High water and nutrient requirement	(McGlashan et al., 2012; Smith et al., 2016a)

The usage of NETs CO_2 removal from the atmosphere in limiting global warming is pivotal. It is projected that the deployment of BECCS and DAC could potentially remove 3.3 Gt CO_2-eq y^{-1} in year 2100 (Smith et al., 2016a). By contrast, the potential CO_2-eq removal capacity of EW is significantly lower at 1 Gt CO_2-eq y^{-1} (Smith et al., 2016a). Despite having great potential CO_2 removal capacity, there are several challenges and constraints associated with NETs. While BECCS is estimated to produce energy equivalent to 170 EJ by the end of the century, the estimated energy requirement for DAC in year 2100 is 156 EJ yr^{-1} (Smith et al., 2016a). In other words, DAC and EW are classified as EC-NETs while BECCS and biochar are categorised under EP-NETs. Meanwhile, the land, water and nutrient requirements for BECCS are higher than DAC and EW (Smith et al., 2016a). Additionally, BECCS is limited to certain regions. Therefore, the interface of NETs with the background energy system is an important consideration in their deployment (Creutzig et al., 2019). Although a full-scale deployment of NETs into the existing power sector is not feasible presently due to the lack of maturity in the associated technologies, a recent assessment demonstrated that as much as 89.8% of the annual emissions in Scotland may be removed via NETs (Alcalde et al., 2018). By contrast, a recent assessment projected a reduction of the total annual emissions in the range of 7.6% to 32.1% for the United Kingdom via NETs (Smith et al., 2016b). Since Scotland has a vast land area, combined with relatively low emission per capita, the deployment of NETs proved to be instrumental in achieving climate change targets. More recently, Galán-Martín *et al.* (2021) used a linear programming model to determine that early deployment of BECCS and DAC can avoid long-term economic penalties to meet the emissions targets for the European Union (EU). These studies illustrate how the deployment of NETs can be incorporated into a full-scale carbon management strategy.

2.7 Research Gap

To date, all work concerning CO_2 emissions reduction using CEPA and mathematical optimisation approaches had focused solely on the deployment of CCS and renewable energy sources toward meeting relevant climate change targets. Although CCS deployment has proven to be instrumental in lowering CO_2 emissions, complete reliance on a single technology would be insufficient in achieving GHGs drawdown. As iterated during COP26, the achievement of the net-zero emissions target by mid-century would require CDR, which is typically achieved via NETs

(United Nations Climate Change, 2021a). Despite several drawbacks of NETs deployment, its importance for CDR given the long-term goal of managing climate change is crucial. Policymakers and governments should readily be incorporating NETs into existing industries and power generating sectors in the bid of cutting emissions. Additionally, NETs should complement existing strategies in place for GHGs emissions reduction. As mentioned by Bednar et al. (2021), the availability of a carbon budget for limiting global warming to within 1.5 °C above the pre-industrial level would be exhausted in this decade. According to the IPCC (2021), an additional emission of 500 Gt of CO_2 would drive the temperature rise to within 1.5 °C above the pre-industrial level. At the current rate, only a decade (from year 2022) remains for countries to exhaust the carbon budget (Fischetti, 2021). Even if countries agree to limit global warming to within 2 °C, it implies that only 1,350 Gt of CO_2 may be emitted (Fischetti, 2021). Further emissions would result in global warming exceeding the 2 °C target. If the similar trajectory of 42 Gt of CO_2 emissions in year 2018 persists moving forward, the 2 °C target would be violated in year 2052 (Fischetti, 2021). With the criticality of the ongoing climate crisis, there is very little space for poor decisions. Accurate targets with proper methodologies are needed to prevent any avoidable adverse consequences.

Therefore, this research aims to extend the CEPA-based and mathematical optimisation approaches for the deployment of NETs in the development of realistic energy planning. Different characteristics of NETs versus CCS and renewable energy sources mean that previous targeting methodologies are no longer suitable for the development of realistic energy planning. The CEPA-based graphical targeting technique developed in this work could form a viable energy planning framework for the deployment of NETs into existing energy systems. CEPA can provide a high-level, low-resolution approach to complement the mathematical programming models used for more detailed but less transparent planning. Figure 2-7 presents the general picture of the research methodology, highlighting previous work done relevant to CO_2 emissions reduction and the novelty of this research.

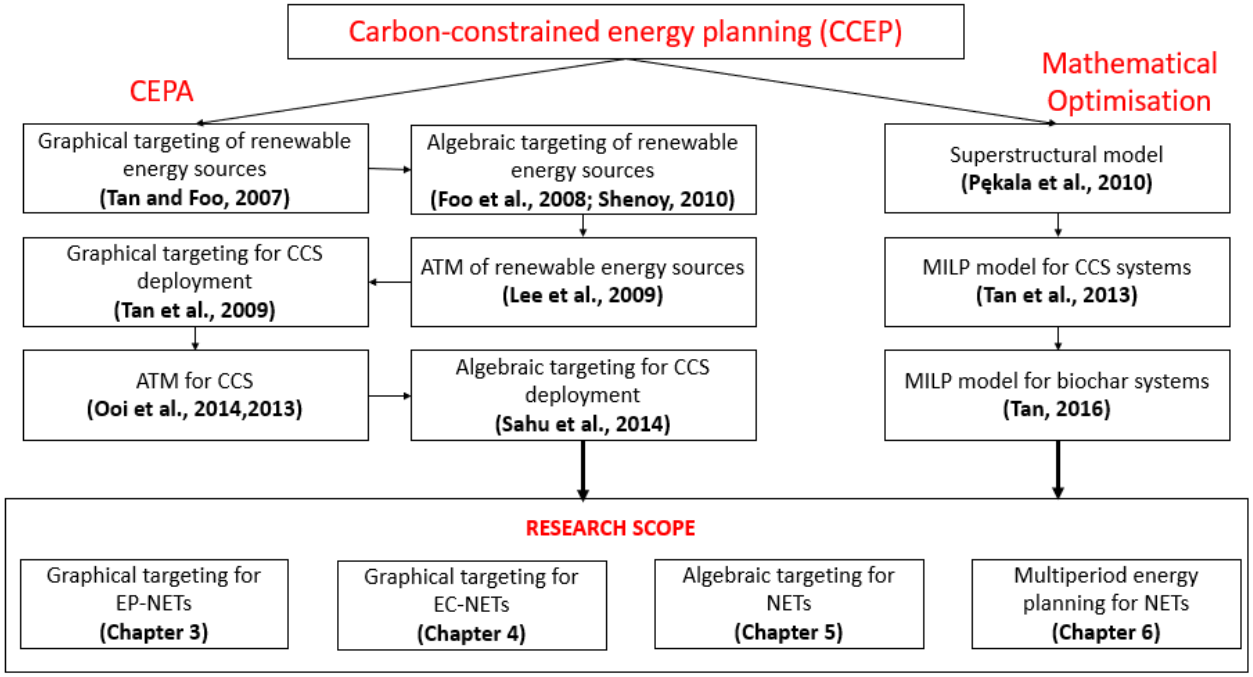


Figure 2-7: General research methodology

Based on Figure 2-7, a graphical targeting technique would initially be developed for the targeting of EP-NETs (Chapter 3) and EC-NETs (Chapter 4). Later, a robust algebraic targeting technique capable of handling large sets of problems is developed to improve the accuracy during energy planning (Chapter 5). The latter technique determines the target deployment of both EP-NETs and EC-NETs during CCEP. Finally, a hybrid approach making the combined use of ATM and *superstructural* models is developed for energy planning involving CO_2-intensive industries (Chapter 6). The methodologies developed through this research would aid in the development of realistic and sustainable energy planning for nations and industries.

Chapter 3: GRAPHICAL TARGETING TECHNIQUE FOR THE DEPLOYMENT OF ENERGY-PRODUCING NEGATIVE EMISSIONS TECHNOLOGIES

This chapter presents the results associated with the development of an extended graphical targeting technique for the deployment of EP-NETs and/or CCS. As mentioned in Chapter 2.6, EP-NETs are technologies that allow CO_2 emissions removal, while generating energy. Some examples of EP-NETs are BECCS and biochar. Since biomass had previously absorbed atmospheric CO_2, the CO_2 captured from the combustion of flue gases essentially makes it a carbon-negative process. The graphical targeting technique for EP-NETs deployment is demonstrated using two examples.

3.1 Targeting Technique without the Deployment of CO_2 Capture and Storage

In the seminal work for CEPA, the EPPD was developed by Tan and Foo (2007) to identify the minimum deployment of renewable energy sources in an energy planning scenario. The work was later extended for the planning of CCS deployment where the minimum extent of CCS retrofit and minimised parasitic power losses were determined (Tan et al., 2009b). In this work, the EPPD is utilised for the planning of EP-NETs deployment. However, due to the different characteristics of EP-NETs, the earlier targeting procedures (Tan et al., 2009b; Tan and Foo, 2007) have to be revamped completely. The step-by-step targeting technique to determine the minimum EP-NETs target with the revised graphical targeting technique is outlined for two different scenarios that follow. The deployment of EP-NETs is kept to a minimum since it is less established. One main underlying assumption for this work is that BECCS is assumed as the chosen EP-NETs, due to its greatest technology maturity, allowing its easy incorporation into existing energy systems (McGlashan et al., 2012). In this case, it is assumed that CCS is not utilised in fossil-fuel-based power plants, due to reasons such as economic considerations, the lack of a site for CO_2 storage, etc. In this case, it is also assumed that BECCS consists of new power plants built to cater for the use of biomass as fuel. The newly, purposeful built power plants would consist of CCS facilities to cater for long-term sustainability, thus ensuring a positive return on investment. Additionally, retrofitting existing fossil-fuel power plants e.g., coal and natural gas to cater for the use of biomass and CCS is capital intensive and may require shift in existing operation. Hence, an energy

planner can only make use of EP-NETs to achieve the aggregate CO_2 emissions limit (Δm_L) in this case. As mentioned earlier, the EPPD (Tan and Foo, 2007) is used for the planning of EP-NETs deployment here. A generic EPPD is shown in Figure 3-1.

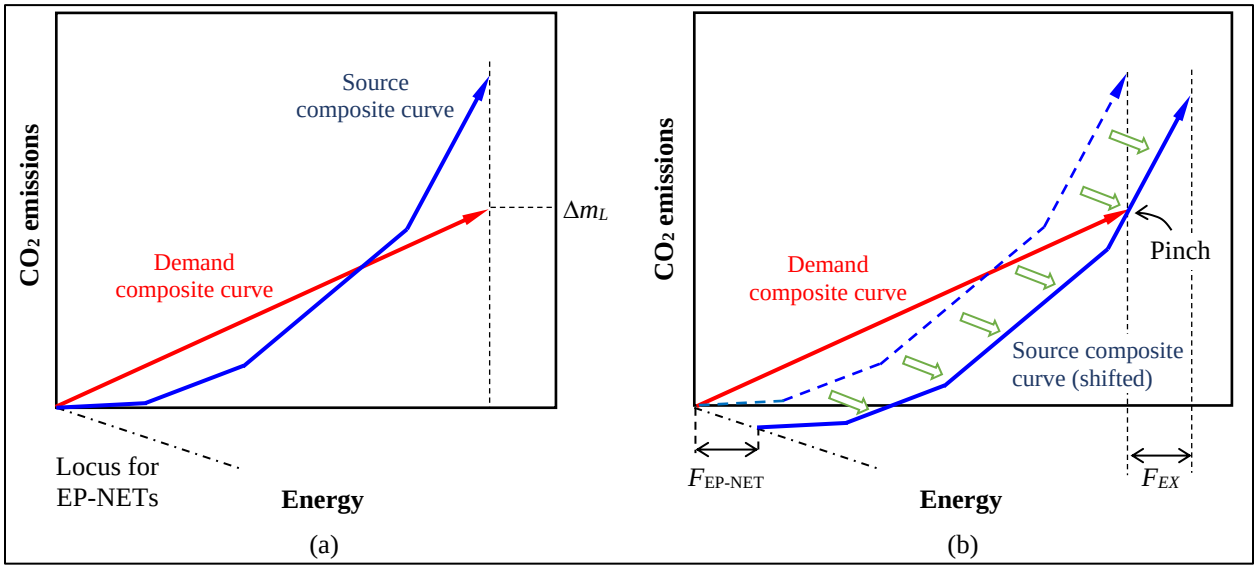


Figure 3-1: EPPD for planning EP-NETs deployment: (a) infeasible EPPD and (b) feasible EPPD

As shown in Figure 3-1, the *source composite curve* is plotted on the EPPD by its cumulative CO_2 emissions versus the cumulative energy of all energy sources; the latter are arranged in ascending order of their CO_2 intensity values. The total CO_2 emissions are indicated by the vertical distance of the source composite curve, while its horizontal distance indicates the total amount of energy required by the system. On the other hand, the CO_2 emissions limit (Δm_L) is represented by the *demand composite curve*, which has a smaller vertical distance as compared to the source composite curve. When the demand composite curve stays below the source composite curve, the system is considered infeasible (Figure 3-1(a)). To restore the feasibility, the source composite curve needs to stay entirely to the right and below the demand composite curve. This entails the use of EP-NETs in the system. To determine the minimum EP-NETs deployment, the targeting technique for this scenario is given as follows:

i. A locus is added at the origin of the EPPD, with a negative slope that corresponds to the negative CO_2 intensity of EP-NETs. In other words, CO_2 emissions will be removed when EP-NETs is deployed.

ii. The source composite curve is slid along the negative-slope locus until it stays entirely below and to the right of the demand composite curve, to form the feasible EPPD. The point that the two composite curves touch is the pinch of the given energy planning problem (Figure 3-1(b)).

iii. The horizontal distance of the opening of the leftmost part of the EPPD represents the minimum EP-NETs deployment ($F_{\text{EP-NET}}$).

iv. The horizontal distance of the extension of the source composite curve on the rightmost part of the EPPD constitutes the excess energy (F_{EX}). These energy sources are to be phased out given the CO_2 emissions limit.

v. Note that $F_{\text{EP-NET}}$ represents the net energy requirement from EP-NETs to meet both power and emission constraints. The amount of energy that should be generated from biomass combustion (F_{BM}) is calculated from Equation 3-1, considering the parasitic power losses during CCS.

$$F_{\text{BM}} = \frac{F_{\text{EP-NET}}}{1 - X} \qquad \text{Equation 3-1}$$

Example 1 illustrates the graphical targeting technique without CCS deployment.

3.1.1 Example 1

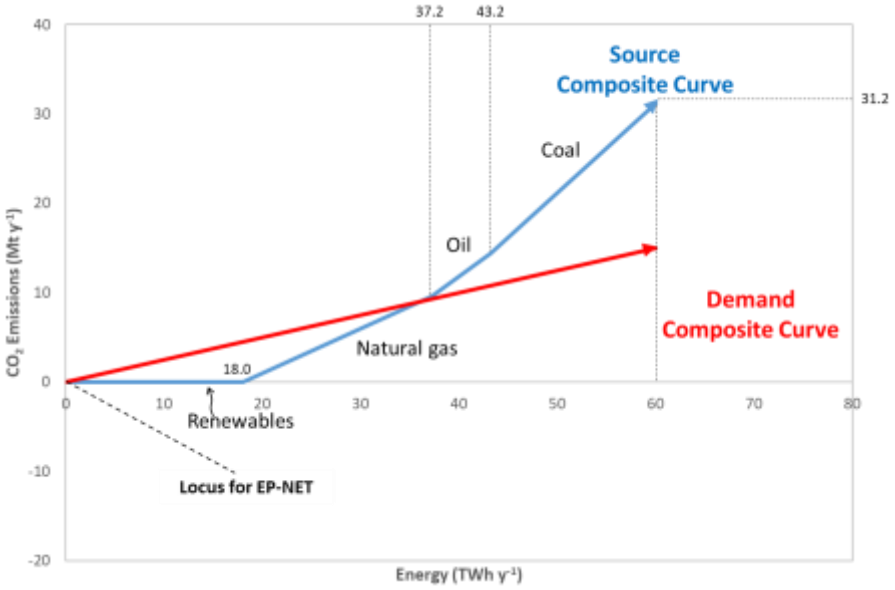
The power generation sector of the Philippines which was originally reported by Tan et al. (2009b) is used to illustrate the deployment of EP-NETs during energy planning without CCS deployment. Table 3-1 presents the data for Example 1.

Table 3-1: Data for Example 1

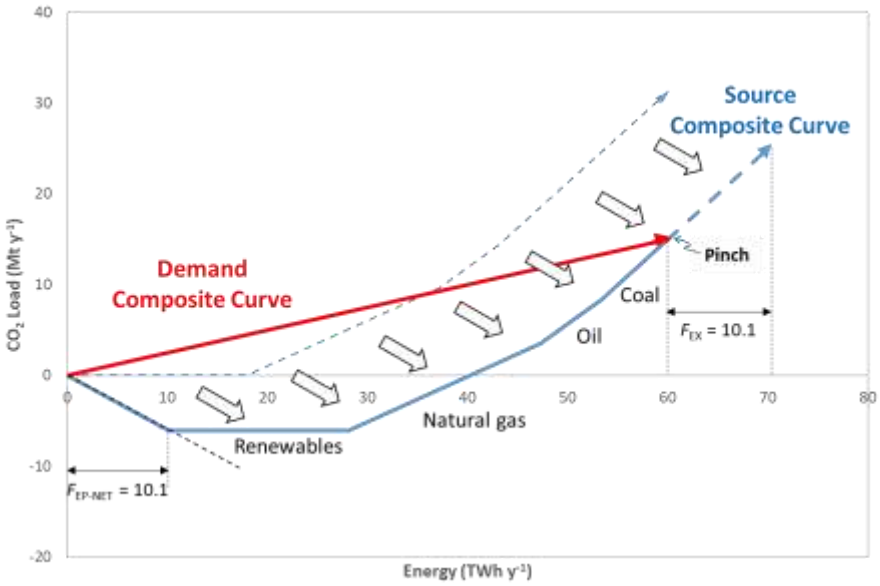
Energy Source *i*	$F_{S,i}$ **(TWh y^{-1})**	$C_{S,i}$ **(Mt CO$_2$ TWh^{-1})**	$F_{S,i}\,C_{S,i}$ **(Mt CO$_2$ y^{-1})**
Renewables	18.0	0	0
Natural Gas	19.2	0.5	9.6
Oil	6.0	0.8	4.8
Coal	16.8	1.0	16.8
	$\sum_i F_{S,i}$ = 60.0		**Δm_T = 31.2**

Based on Table 3-1, renewable energy sources (carbon-neutral sources) and three fossil-based sources were used to satisfy the total power demand of the Philippines (Tan et al., 2009b), equivalent to 60 TWh y^{-1}. Renewable energy sources consisted mostly of geothermal power and hydroelectric power (Tan et al., 2009b). The total CO_2 emissions (Δm_T) amounted to 31.2 Mt y^{-1}. The CO_2 emissions limit (Δm_L) was set to 15 Mt y^{-1} (Tan et al., 2009b). Hence, the CO_2 emissions reduction target (Δm_R) is determined as 16.2 Mt y^{-1} (= 31.2 – 15 Mt y^{-1}), which is to be achieved by utilising BECCS alone; the latter is assumed to have a CO_2 intensity of -0.6 Mt CO_2 $(TWh)^{-1}$ (Ooi et al., 2013). Following Step (i) of the graphical targeting technique, an infeasible EPPD is first plotted in Figure 3-2(a). The source composite curve is slid along the negative slope locus until it stays entirely below and to the right of the demand composite curve (Step (ii)). Figure 3-2(b) shows the feasible EPPD where the minimum EP-NETs deployment is determined, and the CO_2 emissions limit is observed. As shown, 10.1 TWh y^{-1} of EP-NETs is needed ($F_{EP\text{-}NET}$) to meet the CO_2 emissions limit (Δm_L) of 15 Mt y^{-1} (Step (iii)). The same amount of excess energy (F_{EX}) is identified from the extension of the source composite curve on the rightmost part of the EPPD i.e., 10.1 TWh y^{-1}, which is to be originated from the coal sector (Step (iv)). In other words, only 6.7 TWh y^{-1} (= 16.8 – 10.1 TWh y^{-1}) of energy is to be generated from the coal sector instead of the original plan with 16.8 TWh y^{-1} (see Table 3-1).

Note that the reduction in energy generation from the coal sector is consistent with its highest CO_2 intensity among the three fossil-based sources. If the energy generation from the oil or natural gas sector were to be reduced instead of the coal sector, more energy would be required from BECCS. This is because the oil and natural gas sectors have lower CO_2 intensities, which results in a greater extent of compensatory energy, in view of the CO_2 emissions limit. Also, note that the results obtained from Figure 3-2(b) represent the net energy requirement from BECCS to meet both power and emission constraints for Example 1. Assuming that the parasitic power loss (X) during biomass combustion is 0.15, the amount of energy that should be produced from biomass combustion (F_{BM}) is calculated from Equation 3-1, equating to 11.9 TWh y^{-1} (Step (v)). Note that F_{BM} is higher than $F_{EP\text{-}NET}$ due to the parasitic power losses during CCS.



(a)



(b)

Figure 3-2: EPPD for Example 1: (a) infeasible EPPD and (b) feasible EPPD

3.2 Targeting Technique with the Deployment of CO_2 Capture and Storage

For this case, it is assumed that both CCS and EP-NETs are deployed for an energy planning problem. It is further assumed that the use of CCS is prioritised over EP-NETs since CCS is relatively mature. In other words, CCS is first deployed to achieve the desired CO_2 emissions limit

(Δm_L) before EP-NETs is used. Note that the use of CCS entails some energy losses. Subsequently, EP-NETs may be utilised as the compensatory energy to cater to the parasitic power losses during CCS deployment. Since EP-NETs has a negative CO_2 intensity, the graphical targeting technique for CCS deployment proposed by Tan et al. (2009b) has to be modified to determine the various system targets for this energy planning problem, e.g., minimum EP-NETs deployment, the extent of CCS retrofit, etc. The revised targeting technique is given as follows:

1. The EPPD is first used to determine the targets associated with CCS. As shown in Figure 3-3, it may be observed that the total CO_2 emissions to be removed from the system (Δm_R) is greater than the difference between the total CO_2 emissions (Δm_T) and the CO_2 emissions limit (Δm_L). This is due to the removal ratio (*RR*) of the CCS technique. The readers may refer to the original work for detailed procedures (Tan et al., 2009b). For a given CCS technique with specific *RR*, the total CO_2 emissions removal (Δm_R) may be calculated from Equation 3-2. Note that in this case, the CO_2 emissions removed from energy source *i* ($\Delta m_{R,i}$) must satisfy the constraints given as in Equation 3-3 and Equation 3-4.

$$\Delta m_{\mathrm{R}} = \frac{\Delta m_{\mathrm{T}} - \Delta m_{\mathrm{L}}}{\mathrm{RR}} \qquad \text{Equation 3-2}$$

$$\Delta m_{\mathrm{R},i} \leq F_i \times C_{\mathrm{S},i} \quad \forall i \qquad \text{Equation 3-3}$$

$$\sum_{i=1}^{n} \Delta m_{\mathrm{R},i} = \Delta m_{\mathrm{R}} \qquad \text{Equation 3-4}$$

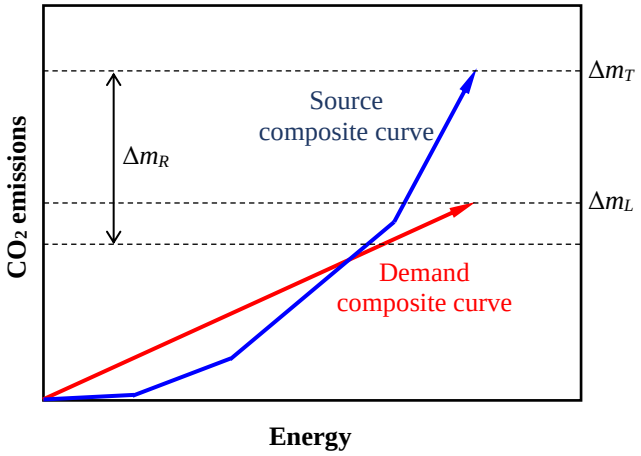


Figure 3-3: EPPD for targeting of CCS system

2. The initial extent of CCS retrofit ($F_{R,i}$) and CO_2 intensity of energy source *i* after CCS retrofit ($C_{R,i}$) are calculated using the methodology proposed by Tan et al. (2009b) and Ooi *et al.* (2013) as shown in Equation 3-5 and Equation 3-6 respectively.

$$F_{\mathrm{R},i} = \frac{\Delta m_{\mathrm{R},i}}{C_{\mathrm{S},i}} \qquad \forall i \qquad \text{Equation 3-5}$$

$$C_{\mathrm{R},i} = \frac{C_{\mathrm{S},i} \times (1 - RR)}{1 - X} \qquad \forall i \qquad \text{Equation 3-6}$$

where *X* in Equation 3-6 is the parasitic power loss of the CCS system (see discussion in Tan et al. (2009b)).

3. Once the initial targets are determined in Steps (1) and (2), the *net energy* from energy source *i* with ($F_{NR,i}$) and without CCS retrofit ($F_{NS,i}$) are calculated from Equation 3-7 and Equation 3-8 respectively.

$$F_{\mathrm{NR},i} = F_{\mathrm{R},i} \times (1 - X) \qquad \forall i \qquad \text{Equation 3-7}$$

$$F_{\mathrm{NS},i} = F_{\mathrm{S},i} - F_{\mathrm{R},i} \qquad \forall i \qquad \text{Equation 3-8}$$

4. A revised source composite curve is re-plotted for the EPPD, as shown in Figure 3-4(a). For this case, the source composite curve will include all energy sources with and without CCS retrofit. Since the energy sources are to be plotted in ascending order of CO_2 intensities, the segments for energy sources that have been retrofitted with CCS will have a leaner slope, as compared to those without CCS retrofit. Note also that there exists an energy deficit gap (F_{DF}) at the right end of the EPPD (Figure 3-4(a)), which is due to the parasitic power losses during CCS.

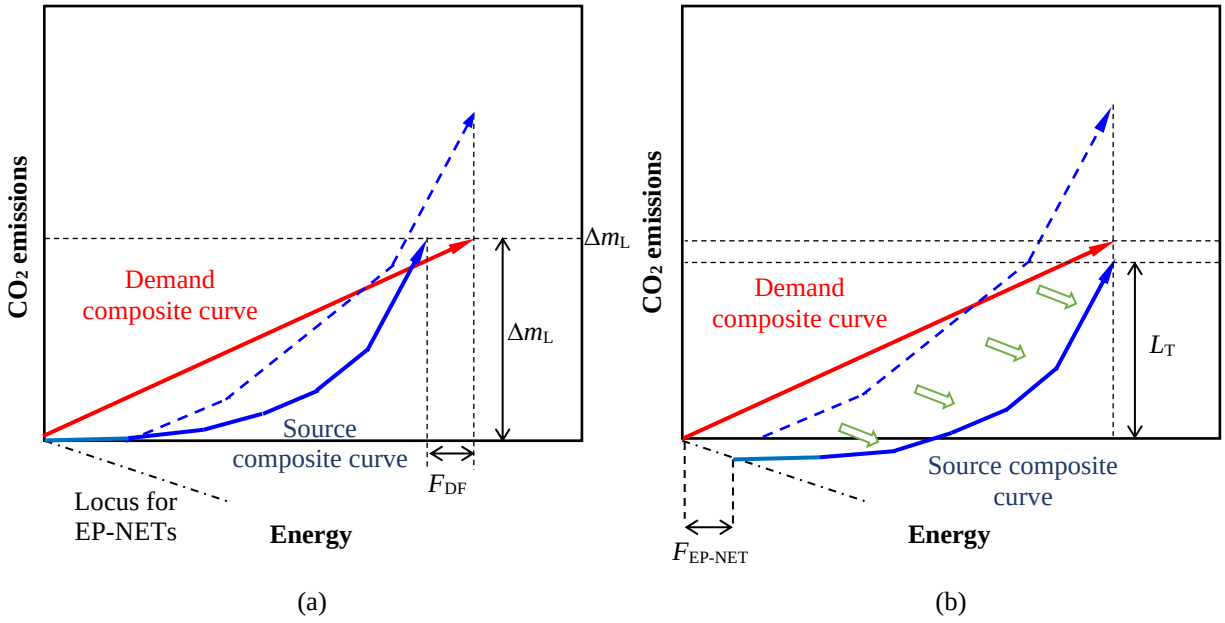


Figure 3-4: Revised EPPD: (a) With CCS deployment and (b) Initial EP-NETs target (after Steps (4) and (5))

5. The initial amount of EP-NETs is next determined. A locus with a negative slope (corresponds to the CO_2 intensity of EP-NETs) is added at the origin of the EPPD. The source composite curve is slid along the negative-slope locus until it reaches the right end of the demand composite curve, as demonstrated in Figure 3-4(b). Doing this will fulfil the total demand of the system (represented by the horizontal distance of the demand composite curve). The opening of the leftmost end of the EPPD determines the initial deployment of EP-NETs, to be used as the compensatory energy of the CCS system ($F_{EP\text{-}NET}$). Note that in the revised EPPD (Figure 3-4(b)), the shifted source composite curve does not touch the demand composite curve. This is because the source composite curve

was shifted downwards along the negative slope locus. The vertical distance of the shifted source composite curve from the horizontal axis indicates the *revised total CO_2 emissions* (L_T).

6. Due to the negative CO_2 intensity of EP-NETs, L_T would initially be lower than the CO_2 emissions limit (Δm_L). Therefore, the initial extent of CCS retrofit ($F_{R,i}$) determined in Step (2) may be reduced. In other words, a lesser amount of fossil-fuel-based power plants will need to be retrofitted with CCS. The exact extent of CCS retrofit is to be determined in the following sub-steps.
   i. To determine the *minimum theoretical reduction* in the extent of CCS retrofit on energy source *i* (Y_i), beginning the calculation procedure for an energy source with the lowest CO_2 intensity (i.e., the cleanest energy source) is proposed. The minimum theoretical reduction may be determined using Equation 3-9.

$$Y_i = \frac{\Delta m_L - L_T}{C_{S,i} \times RR} \qquad i = 1 \qquad \text{Equation 3-9}$$

   ii. Note that the *maximum possible reduction* in the extent of CCS retrofit on energy source *i* should not exceed $F_{R,i}$ that was determined in Step (2). For cases where Y_i is larger than $F_{R,i}$, the remaining reduction, (ΔY_i) is cascaded to energy source *i* with higher CO_2 intensity, as demonstrated in Equation 3-10 and Equation 3-11. Equation 3-10 also shows that for cases where Y_i is smaller than $F_{R,i}$, no further calculations are necessary.

$$\Delta Y_i = \begin{cases} Y_i - F_{R,i}, & Y_i > F_{R,i} \\ 0, & Y_i \leq F_{R,i} \end{cases} \quad \forall i \qquad \text{Equation 3-10}$$

$$Y_{i+1} = \frac{\Delta Y_i \times C_{S,i}}{C_{S,i+1}} \; i = 1, 2, \dots, n-1 \qquad \text{Equation 3-11}$$

   iii. By comparing Y_i and $F_{R,i}$, the *feasible reduction* in the extent of CCS retrofit on energy source *i* (A_i) is determined from Equation 3-12.

$$A_i = \begin{cases} Y_i, & Y_i < F_{\mathrm{R},i} \\ F_{\mathrm{R},i}, & Y_i \geq F_{\mathrm{R},i} \end{cases} \quad \forall i \qquad \text{Equation 3-12}$$

iv. Equation 3-13 is used to determine the revised $F_{R,i}$.

$$F_{\mathrm{R},i} = F_{\mathrm{R},i} - A_i \quad \forall i \qquad \text{Equation 3-13}$$

7. The net energies from energy source *i* with ($F_{NR,i}$) and without CCS retrofit ($F_{NS,i}$) are re-calculated using Equation 3-7 and Equation 3-8 respectively. Based on the revised values of $F_{NR,i}$ and $F_{NS,i}$, the revised source composite curve is again plotted on the EPPD, as shown in Figure 3-5(a). Note that the previously determined energy contribution from EP-NETs (Step 5) is to be revised, and hence is excluded from the source composite curve. Similar to Step (5), the source composite curve is once again slid along the EP-NETs locus until it reaches the right end of the demand composite curve, as demonstrated in Figure 3-5(b).

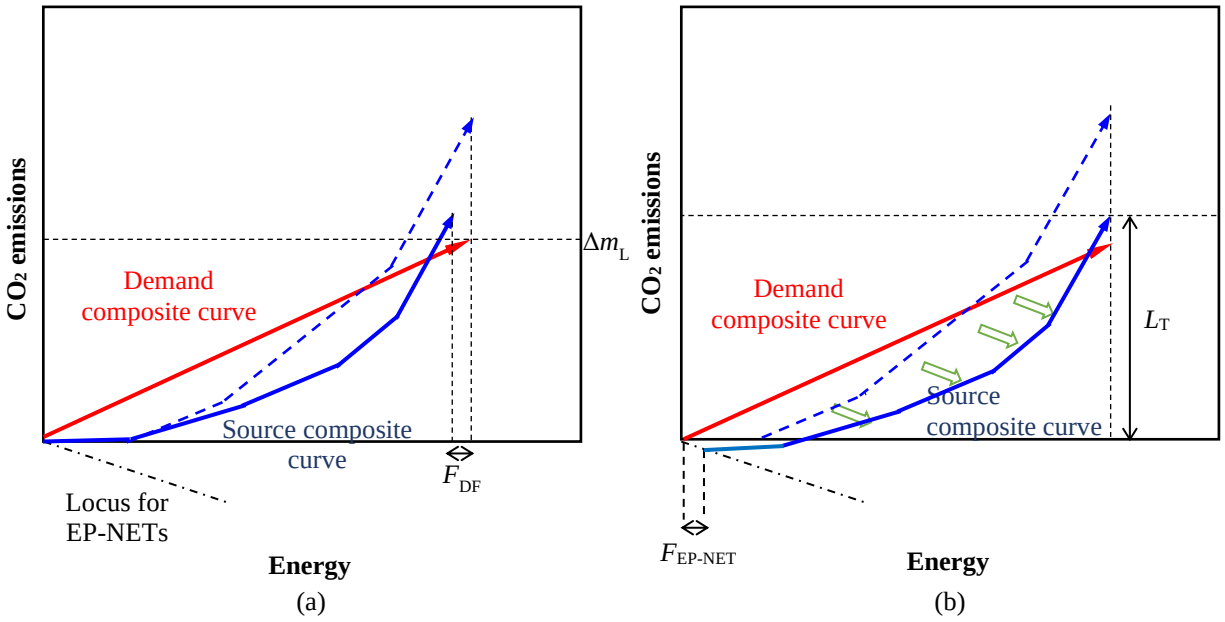


Figure 3-5: Revised EPPD: (a) With CCS deployment and (b) Revised EP-NETs target (after Steps 6 and 7)

8. For cases where L_T is higher than Δm_L, the $F_{R,i}$ value must be increased. In other words, a greater amount of fossil-fuel-based power plants are to be retrofitted with CCS.

i. Equation 3-9 is modified to determine the *minimum theoretical addition* to the extent of CCS retrofit on energy source *i*, i.e., Z_i. Note that in this case, the technique commences from energy source *i* with the highest CO_2 intensity, as demonstrated in Equation 3-14.

$$Z_i = \frac{L_{\mathrm{T}} - \Delta m_{\mathrm{L}}}{C_{\mathrm{S},i} \times RR} \qquad i = n \qquad \text{Equation 3-14}$$

ii. The *maximum possible addition* of CCS retrofit extent on energy source *i* should not exceed $F_{\mathrm{NS},i}$. If Z_i is larger than $F_{\mathrm{NS},i}$, the difference, (ΔZ_i) is cascaded to energy source *i* with lower CO_2 intensity, as demonstrated in Equation 3-15 and Equation 3-16; note that the latter equations were modified based on Equation 3-10 and Equation 3-11 respectively. Equation 3-15 also shows that for cases where Z_i is smaller than $F_{\mathrm{NS},i}$, no further calculation is necessary.

$$\Delta Z_i = \begin{cases} Z_i - F_{\mathrm{NS},i}, & Z_i > F_{\mathrm{NS},i} \\ 0, & Z_i \leq F_{\mathrm{NS},i} \end{cases} \quad \forall i \qquad \text{Equation 3-15}$$

$$Z_i = \frac{\Delta Z_{i+1} \times C_{\mathrm{S},i+1}}{C_{\mathrm{S},i}} \; i = n-1, n-2, \ldots, 1 \qquad \text{Equation 3-16}$$

iii. By comparing Z_i and $F_{\mathrm{NS},i}$, Equation 3-12 is modified to determine the *feasible addition* to the extent of CCS retrofit on energy source *i* (B_i), as demonstrated in Equation 3-17.

$$B_i = \begin{cases} Z_i, & Z_i < F_{\mathrm{NS},i} \\ F_{\mathrm{NS},i}, & Z_i \geq F_{\mathrm{NS},i} \end{cases} \quad \forall i \qquad \text{Equation 3-17}$$

iv. Equation 3-13 is modified as Equation 3-18 to determine the revised $F_{R,i}$.

$$F_{R,i} = F_{R,i} + B_i \quad \forall i$$ Equation 3-18

9. Steps (3) and (7) are now repeated to determine the revised values of $F_{EP\text{-}NET}$ and $L_{T.}$ The latter value is compared to Δm_L. Steps (6) to (8) are repeated until L_T matches the value of Δm_L.

Figure 3-6 demonstrates the iterative procedure of this graphical targeting technique to determine the various system targets (e.g., minimum EP-NETs usage, minimum extent of CCS retrofit) where CCS and EP-NETs are deployed for energy planning problems. Note that in the above procedure, Steps (1) – (3) were originally reported by Tan et al. (2009b) while the other steps are newly proposed in this work.

Example 1 is revisited to illustrate the graphical targeting technique with the deployment of both CCS and EP-NETs during energy planning.

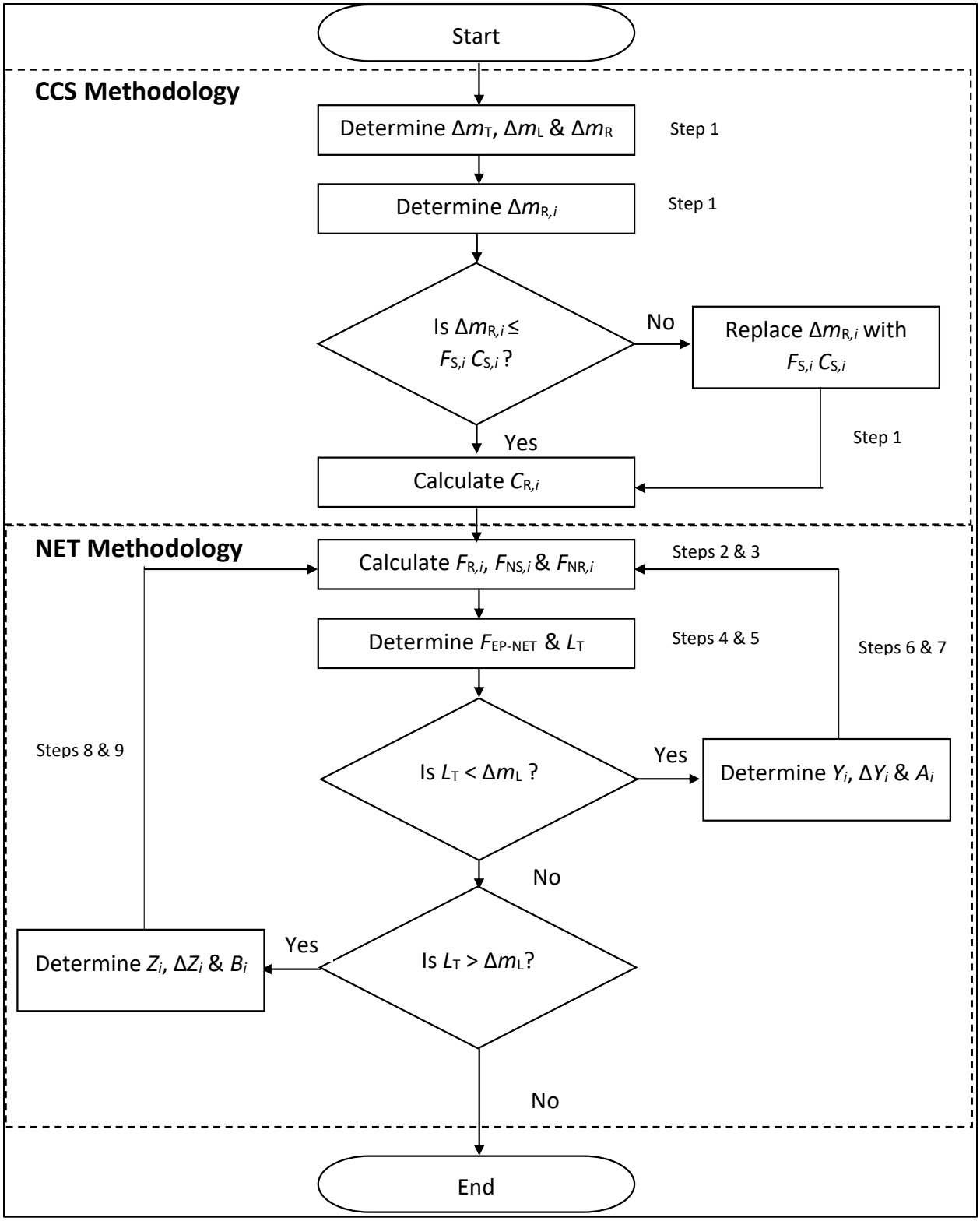


Figure 3-6: Flowchart for targeting the minimum deployment of CCS and EP-NETs

3.2.1 Example 1 (Revisited)

Example 1 is revisited to illustrate the deployment of CCS and EP-NETs during energy planning. The CO_2 emissions limit (Δm_L) was kept at 15 Mt y^{-1}. With the assumption that the removal ratio (RR) and parasitic power losses (X) of the CCS system are set to 0.85 and 0.15, respectively, the CO_2 emissions removal (Δm_R) is calculated using Equation 3-2 (Step (1)) as 19.06 Mt y^{-1} (= (31.2 – 15)/0.85 Mt y^{-1}). Since the coal sector has the highest CO_2 intensity, its total CO_2 emissions of 16.8 Mt y^{-1} is captured entirely, leaving a remainder of 2.26 Mt CO_2 y^{-1} (= 19.06 – 16.8 Mt y^{-1}) to be captured from the oil sector. The initial extent of CCS retrofit ($F_{R,i}$) for the coal and oil sectors are then calculated using Equation 3-5 (Step (2)), as 16.8 and 2.82 TWh y^{-1}, respectively. Table 3-2 presents the energy contribution and CO_2 emissions from all energy sources with and without CCS retrofit, calculated following Steps (2) and (3).

Table 3-2: Energy and CO_2 emissions from energy sources for Example 1 (revisited, after Steps (2) and (3))

Energy source *i*	$F_{NS,i}$ / $F_{NR,i}$ (TWh y^{-1})	$C_{S,i}$ / $C_{R,i}$ (Mt CO_2 TWh^{-1})	Total CO_2 emissions (Mt CO_2 y^{-1})
Renewables	18.00	0	0
Oil (with CCS retrofit)	2.40	0.14	0.34
Coal (with CCS retrofit)	14.28	0.18	2.52
Natural gas	19.20	0.50	9.60
Oil	3.18	0.80	2.54
Coal	0	1.00	0
	$\sum_i F_{S,i}$ = 57.06		**L_T = 15.00**

From Table 3-2, the total CO_2 emissions post-CCS is observed to match the CO_2 emissions limit (Δm_L) of 15 Mt y^{-1}. Note however that the net energies from the oil and coal sectors have been reduced to 2.4 and 14.28 TWh y^{-1}, respectively, due to the parasitic power losses during CCS. This leads to a lower amount of total energy, i.e., 57.06 TWh y^{-1} instead of its original value of 60 TWh y^{-1} (see Table 3-1) i.e., a reduction of 2.94 TWh y^{-1}. The revised EPPD after CCS deployment in

Figure 3-7 (Step (4)) shows that an energy deficit (F_{DF}) of 2.94 TWh y^{-1} is observed at the right end of the EPPD.

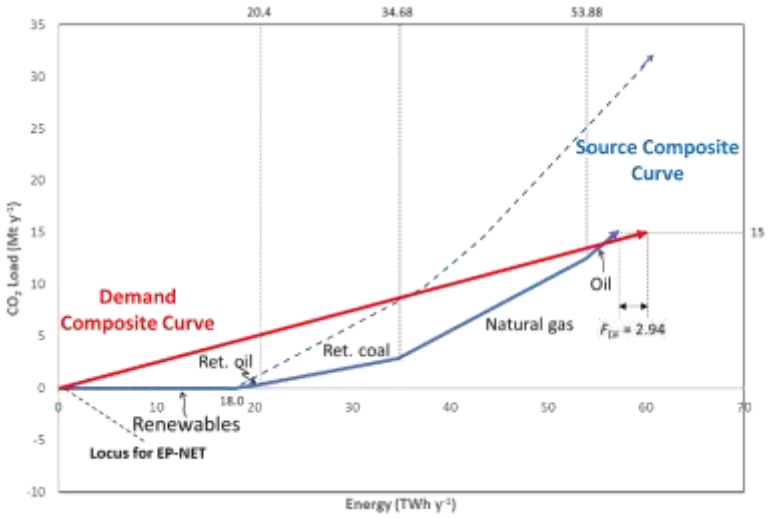


Figure 3-7: Revised EPPD with CCS deployment for Example 1 (Revisited, after Step (4))

Step (5) is next followed to determine the revised EP-NETs requirement. As shown in Figure 3-8, the source composite curve is slid along the EP-NETs locus until it reaches the right end of the demand composite curve.

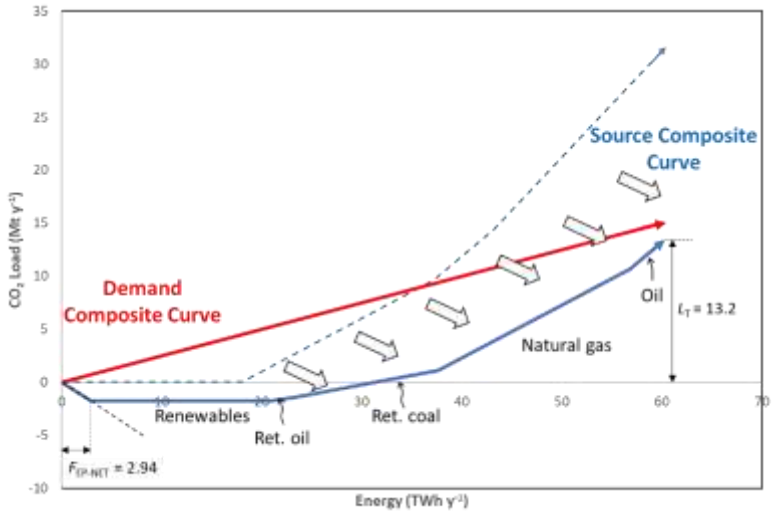


Figure 3-8: EPPD with CCS and EP-NETs deployment for Example 1 (Revisited, after Step (5))

The horizontal opening of the leftmost end of the EPPD in Figure 3-8 indicates that an initial EP-NETs amount ($F_{EP\text{-}NET}$) of 2.94 TWh y^{-1} is required as the compensatory energy. However, the

revised total CO_2 emissions (L_T) is determined as 13.2 Mt y^{-1}, which is lower than the Δm_L value of 15 Mt y^{-1}. Therefore, the initial extent of CCS retrofit determined earlier may be reduced. This is to be done following Step (6) i.e., commencing from the natural gas sector due to its lowest CO_2 intensity.

By applying Equation 3-9 (Step (6)(i)), the minimum theoretical reduction to the extent of CCS retrofit on the natural gas sector (Y_1) is calculated as 4.16 TWh y^{-1}. However, since the power plants in the natural gas sector were not CCS retrofitted previously ($F_{R,1} = 0$), the reduction to the extent of CCS retrofit is hence cascaded to the power plants in the oil sector with a higher CO_2 intensity. The minimum theoretical reduction to the extent of CCS retrofit on the oil sector (Y_2) is calculated as 2.60 TWh y^{-1} from Equation 3-11 (Step (6)(ii)). Note that Y_2 is lesser than Y_1 by 1.56 TWh y^{-1} (= 4.16 – 2.6 TWh y^{-1}). Also note that when energy source *i* with a higher CO_2 intensity is utilised for the reduction in the extent of CCS retrofit, lesser energy is required from energy source *i* to fulfil the CO_2 emissions gap. Since the extent of CCS retrofit on the oil sector ($F_{R,2}$) was 2.82 TWh y^{-1}, a reduction of 2.60 TWh y^{-1} is feasible; thus, requiring no changes to the extent of CCS retrofit in the coal sector. Subsequently, the feasible reduction to the extent of CCS retrofit on the natural gas (A_1) and oil (A_2) sectors are determined from Equation 3-12 as 0 and 2.6 TWh y^{-1} respectively (Step (6)(iii)). The revised extent of CCS retrofit on the natural gas ($F_{R,1}$) and oil ($F_{R,2}$) sectors are calculated from Equation 3-13 (Step (6)(iv)). While no reduction occurs to $F_{R,1}$, $F_{R,2}$ decreases to 0.23 TWh y^{-1} (= 2.83 – 2.6 TWh y^{-1}). The net energies from the oil sector with ($F_{NR,2}$) and without CCS retrofit ($F_{NS,2}$) are re-calculated from Equation 3-7 and Equation 3-8 (Step (7)) as 0.19 and 5.77 TWh y^{-1}, respectively.

A revised source composite curve is next re-plotted in ascending order of CO_2 intensities for all energy sources with and without CCS retrofit but excluding the EP-NETs contribution of 2.94 TWh y^{-1} determined in Step (5). The EP-NETs amount is re-determined following Step (7) and shown in the revised EPPD in Figure 3-9.

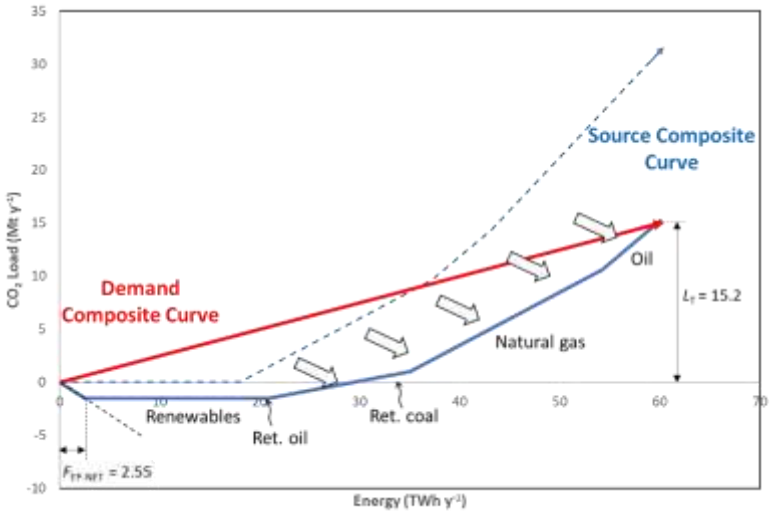


Figure 3-9: Revised EPPD with CCS and EP-NETs deployment for Example 1 (Revisited, after Step (7))

Based on Figure 3-9, $F_{EP\text{-}NET}$ decreased to 2.55 TWh y^{-1} (from 2.94 TWh y^{-1} in Figure 3-8). While the power demand is satisfied, the L_T value exceeded Δm_L by 0.23 Mt y^{-1} (= 15.23 – 15 Mt y^{-1}). Therefore, the extent of CCS retrofit on energy source *i* must be increased, commencing from the coal sector due to its highest CO_2 intensity (Step (8)). First, the minimum theoretical addition to the extent of CCS retrofit on the coal sector (Z_3) is calculated from Equation 3-14, equating to 0.28 TWh y^{-1} (Step (8)(i)). With no coal sector available for further CCS retrofitting, the difference between Z_3 and the net energy available from the coal sector (ΔZ_3), equating to 0.28 TWh y^{-1} is cascaded to the oil sector with a lower CO_2 intensity. Equation 3-16 is next used to determine the minimum theoretical addition to the extent of CCS retrofit on the oil sector (Z_2) as 0.34 TWh y^{-1} (Step (8)(ii)). Since Z_2 is lower than the net energy available from the oil sector ($F_{NS,2}$ = 5.77), the addition of 0.34 TWh y^{-1} to its minimum extent of CCS retrofit ($F_{R,2}$) is feasible. Consequently, there is no requirement for CCS retrofit on power plants in the natural gas sector. Following this, the feasible addition to the extent of CCS retrofit on coal (B_3) and oil (B_2) sectors are determined from Equation 3-17 as 0 and 0.34 TWh y^{-1} respectively (Step (8)(iii)). The revised minimum extent of CCS retrofit on oil ($F_{R,2}$) and coal ($F_{R,3}$) sectors are calculated from Equation 3-18 (Step (8)(iv)). No changes occurred in the coal sector but $F_{R,2}$ for the oil sector increased from 0.23 to 0.57 TWh y^{-1}.

Following Step (9), the net energies from the oil sector with ($F_{NR,2}$) and without ($F_{NS,2}$) CCS retrofit are re-calculated from Equation 3-7 and Equation 3-8 as 0.48 and 5.43 TWh y^{-1} respectively. The source composite curve is re-plotted in ascending order of CO_2 intensities for all energy sources with and without CCS retrofit, while the EP-NETs amount is re-determined using the revised EPPD in Figure 3-10.

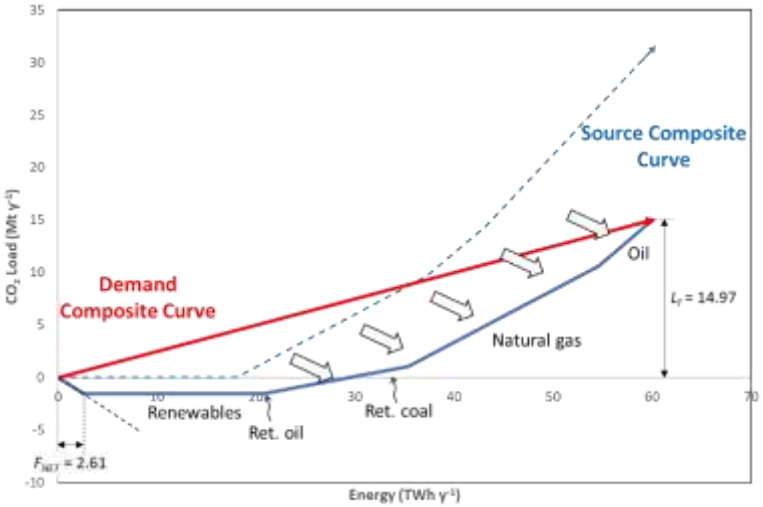


Figure 3-10: Revised EPPD with CCS and EP-NETs deployment for Example 1 (Revisited, after Step (9))

Based on Figure 3-10, the minimum EP-NETs requirement ($F_{EP\text{-}NET}$) increased from 2.55 TWh y^{-1} (Figure 3-9) to 2.61 TWh y^{-1}, thus satisfying the power demand. The additional negative CO_2 emission contribution from EP-NETs resulted in L_T lower than the aggregate CO_2 emissions limit (Δm_L) by 0.03 Mt y^{-1}. Therefore, Step (6) is repeated to reduce the extent of CCS retrofit on energy source *i*. The iterative procedures are repeated for three rounds until L_T matches the Δm_L value of 15 Mt y^{-1}. Table 3-3 presents the final energy contribution and CO_2 emissions from all energy sources for this example.

Table 3-3: Final energy sources and total CO_2 emissions for Example 1 (Revisited)

Energy Source *i*	$F_{NS,i}$ / $F_{NR,i}$ (TWh y^{-1})	$C_{S,i}$ / $C_{R,i}$ (Mt CO_2 TWh^{-1})	Total CO_2 Emissions (Mt CO_2 y^{-1})
EP-NETs	2.60	-0.60	-1.56
Renewables	18.00	0	0
Oil (retrofit)	0.45	0.14	0.06
Coal (retrofit)	14.28	0.18	2.52
Natural gas	19.20	0.50	9.60
Oil	5.48	0.80	4.38
	F_D = 60.00		**L_T = 15.00**

From Table 3-3, it may be observed that both the energy demand (60 TWh y^{-1}) and CO_2 emissions limit (15 Mt y^{-1}) of the energy planning problem have been fulfilled. The final EPPD for the deployment of CCS and EP-NETs is presented in Figure 3-11.

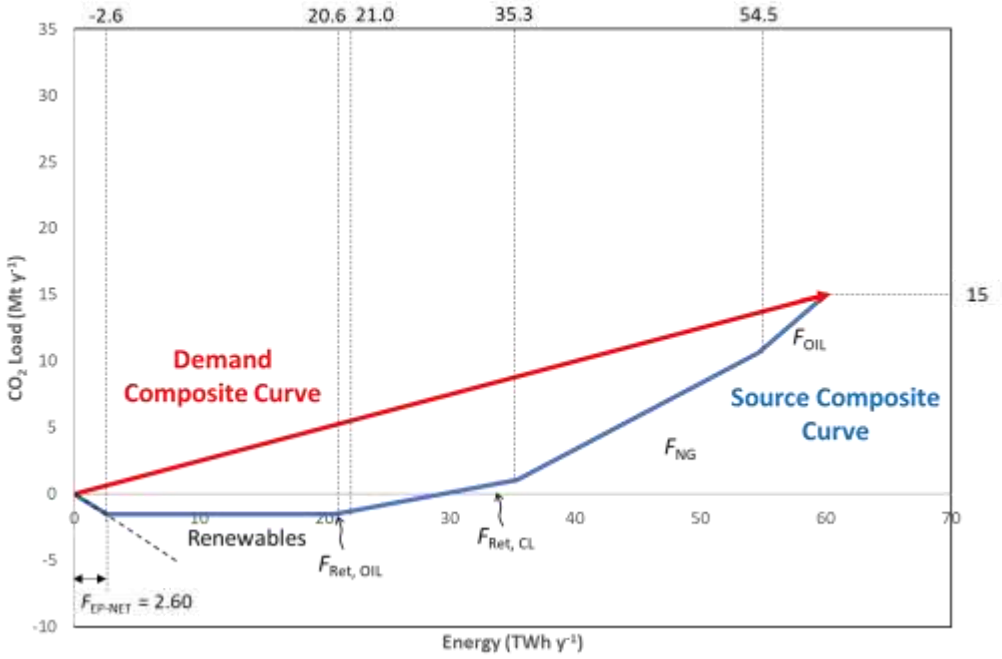


Figure 3-11: Final EPPD with CCS and EP-NETs deployment for Example 1

It is worth comparing the system with and without CCS deployment. For the latter, Figure 3-2(b) shows that 10.1 TWh y^{-1} of EP-NETs is required. On the other hand, Figure 3-11 shows that the deployment of EP-NETs is reduced by approximately 75% (to 2.61 TWh y^{-1}) when CCS is deployed, as compared to that in Figure 3-2(b). A big portion of the CO_2 emission is captured via CCS, which leads to a lesser deployment of EP-NETs being required to fulfil the CO_2 emissions limit.

3.2.2 Example 2

Example 2 adopts a hypothetical example to illustrate the deployment of CCS and EP-NETs as compensatory energy during energy planning, with data are shown in Table 3-4. The purpose of this example is to demonstrate the robustness of the newly developed graphical targeting technique in determining various system targets i.e., minimum deployment of EP-NETs, the extent of CCS retrofit etc. Additionally, the example would demonstrate the use of the graphical targeting technique in situations with stringent CO_2 emissions limits, thus requiring CCS deployment on all energy sources. As shown in Table 3-4, renewable energy sources (carbon neutral) and three fossil-based sources were utilised to satisfy the energy demand of 55 TWh y^{-1}. The total CO_2 emissions (Δm_T) amounted to 33.1 Mt y^{-1}, to which more than 90% is contributed by the coal sector. The CO_2 emissions limit (Δm_L) was set to 5 Mt y^{-1}.

Table 3-4: Data for Example 2

Energy Source *i*	$F_{S,i}$ **(TWh y^{-1})**	$C_{S,i}$ **(Mt CO_2 TWh^{-1})**	$F_{S,i}\,C_{S,i}$ **(Mt CO_2 y^{-1})**
Renewables	20	0	0
Natural Gas	3	0.5	1.5
Oil	2	0.8	1.6
Coal	30	1.0	30.0
	$\sum_i F_{S,i}$ = 55		**Δm_T = 33.1**

To achieve the targeted Δm_L value of 5 Mt y^{-1}, the CO_2 emissions removal (Δm_R) is calculated using Equation 3-2 (Step (1)) as 33.06 Mt y^{-1} (= (33.1 – 5)/0.85 Mt y^{-1}), indicating that almost 100% of the fossil-based power plants require CCS retrofit (unlike Example 1 where only coal and oil

sectors were subjected to CCS retrofitting). Like Example 1, the *RR* and *X* values are assumed as 0.85 and 0.15 respectively. The CO_2 emissions from both coal (30 Mt y^{-1}) and oil (1.6 Mt y^{-1}) sectors are captured entirely, while the remaining CO_2 emissions are to be removed from the natural gas sector ($\Delta m_{R,1}$) i.e., 1.46 Mt y^{-1} (= 33.06 – 30 – 1.6 Mt y^{-1}). The minimum extent of CCS retrofit ($F_{R,i}$) for coal, oil and natural gas sectors are calculated from Equation 3-5 (Step (2)), equating to 30, 2 and 2.92 TWh y^{-1} respectively. Figure 3-12 presents the revised EPPD after CCS deployment, following Steps (3) and (4).

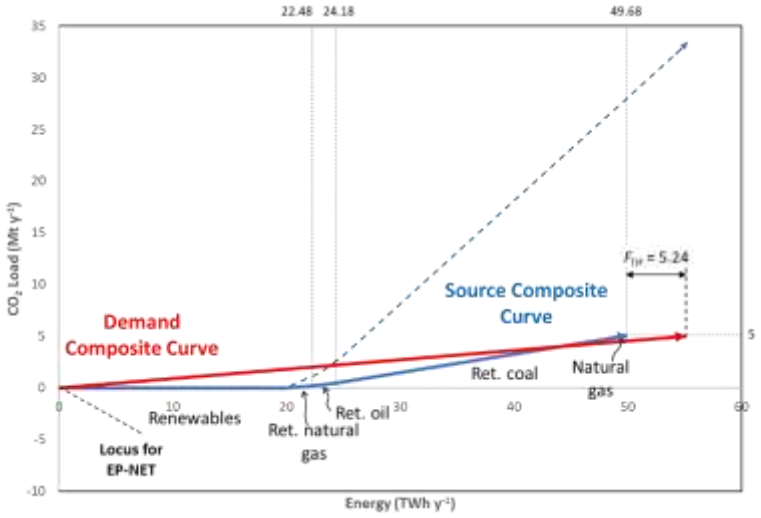


Figure 3-12: Revised EPPD with CCS deployment for Example 2 (after Steps (3) and (4))

Based on Figure 3-12, it is evident that the total CO_2 emissions has achieved the desired CO_2 emissions limit, i.e., 5 Mt y^{-1}. However, an energy deficit of 5.24 TWh y^{-1} is observed due to parasitic power losses during CCS. To overcome the energy deficit, the same amount of EP-NETs is to be used, as shown in the revised EPPD in Figure 3-13. Like Example 1, BECCS with an assumed CO_2 intensity of -0.6 Mt CO_2 $(TWh)^{-1}$ is deployed to aid in CO_2 emissions removal (Ooi et al., 2013).

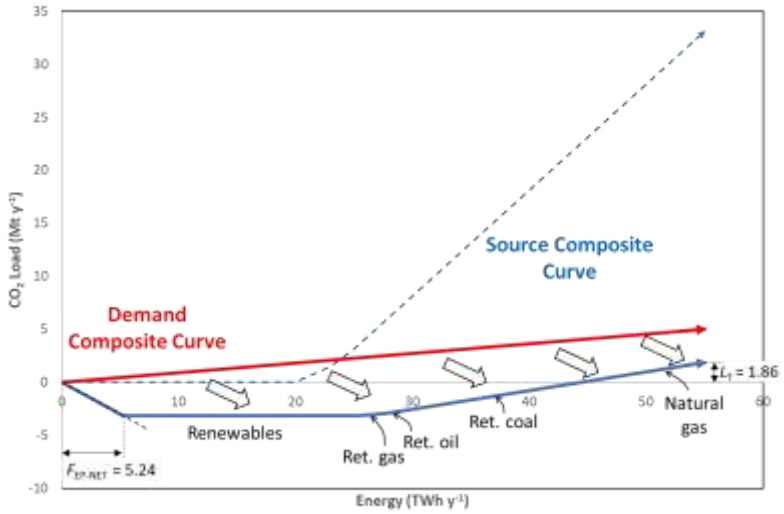


Figure 3-13: EPPD with CCS and EP-NETs deployment for Example 2 (after Step (5))

Figure 3-13 however shows that the L_T value is determined as 1.86 Mt y^{-1}, which is much lower than the Δm_L value. Therefore, the initial extent of CCS retrofit on energy source *i* determined earlier may be reduced following Step (6), i.e., commencing from the natural gas sector with the lowest CO_2 intensity.

By applying Equation 3-9 (Step (6)(i)), the minimum theoretical reduction to the extent of CCS retrofit on the natural gas sector (Y_1) is calculated as 7.39 TWh y^{-1}. Since only 2.92 TWh y^{-1} of the natural gas sector was previously CCS retrofitted, the difference between Y_1 and $F_{R,1}$ (ΔY_1), i.e., 4.48 TWh y^{-1} (= 7.39 – 2.92 TWh y^{-1}) is cascaded to the oil sector of higher CO_2 intensity. Based on Equation 3-11, Y_2 is calculated as 2.80 TWh y^{-1} (Step (6)(ii)). Once again, since only 2 TWh y^{-1} of the plants in the oil sectors were retrofitted with CCS previously, the difference (ΔY_2) of 0.8 TWh y^{-1} (= 2.8 – 2 TWh y^{-1}) is cascaded to the coal sector. Equation 3-11 next calculated that Y_3 (coal) as 0.64 TWh y^{-1} (Step (6)(ii)). The feasible extent of CCS retrofit (A_i) for natural gas, oil and coal sectors are determined from Equation 3-12 as 2.92, 2 and 0.64 TWh y^{-1}, respectively (Step (6)(iii)). The revised $F_{R,i}$ is calculated from Equation 3-13 (Step (6)(iv)). While both natural gas and oil sectors are no longer subjected to CCS retrofit, $F_{R,3}$ (coal) decreases to 29.36 TWh y^{-1} (= 30 – 0.64 TWh y^{-1}).

Following Step (7), the net energies from the coal sector with ($F_{NR,3}$) without CCS retrofit ($F_{NS,3}$) are re-calculated from Equation 3-7 and Equation 3-8, equating to 24.96 TWh y^{-1} and 0.64 TWh

y^{-1} (= 30 – 29.36), respectively. The revised EPPD is replotted to determine the revised $F_{EP\text{-}NET}$ value as 4.4 TWh y^{-1}, as shown in Figure 3-14.

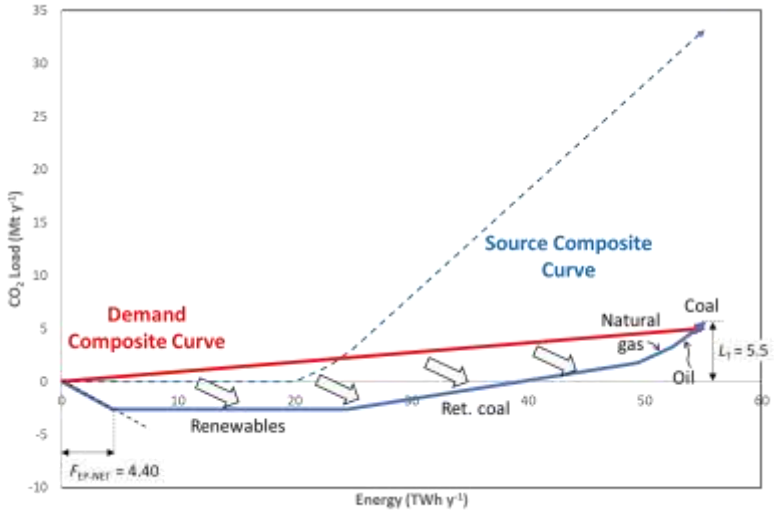


Figure 3-14: Revised EPPD with CCS and EP-NETs deployment for Example 2 (after Step (7))

While the power demand is satisfied, Figure 3-14 shows that the L_T value has now exceeded Δm_L by 0.5 Mt y^{-1} (= 5.5 – 5 TWh y^{-1}). Therefore, the extent of CCS retrofit must be increased, commencing from the coal sector with the highest CO_2 intensity (Step (8)). The methodology of Step (8) is identical to those listed in Example 1. The revised EPPD is replotted in Figure 3-15 following Step (9), with the $F_{EP\text{-}NET}$ value increased to 4.49 TWh y^{-1} to satisfy the power demand.

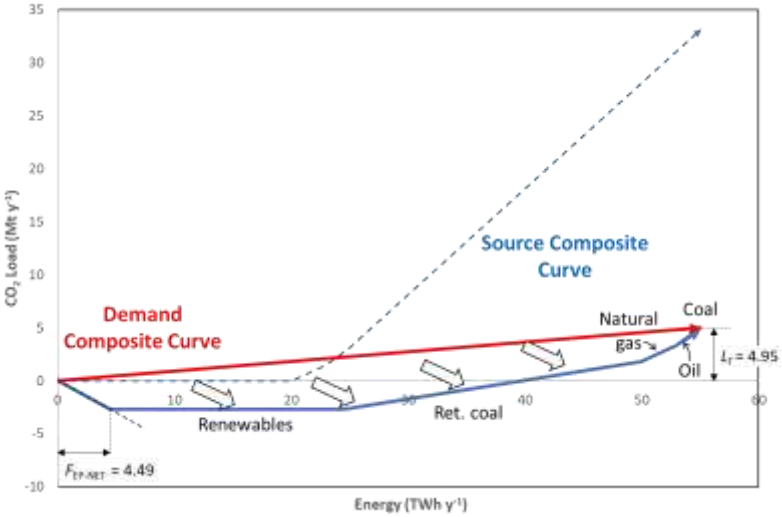


Figure 3-15: Revised EPPD with CCS and EP-NETs deployment for Example 2 (after Step (9))

Figure 3-15 shows that the negative CO_2 load contribution from BECCS resulted in L_T lower than the aggregate CO_2 emissions limit (Δm_L) by 0.05 Mt y^{-1}. Therefore, Step (6) is repeated to reduce the extent of CCS retrofit on energy source *i*. The iterative procedures were repeated four times until the L_T value matches at 5 Mt y^{-1}. Table 3-5 presents the summary for Example 2, in which energy demand and CO_2 emissions limit are both fulfilled.

Table 3-5: Final energy sources and total CO_2 emissions for Example 2

Energy source *i*	$F_{NS,i}$ / $F_{NR,i}$ (TWh y^{-1})	$C_{S,i}$ / $C_{R,i}$ (Mt CO_2 TWh^{-1})	Total CO_2 Emissions (Mt CO_2 y^{-1})
BECCS	4.48	-0.60	-2.69
Renewables	20.00	0	0
Coal (retrofit)	25.41	0.18	4.48
Natural gas	3.00	0.50	1.50
Oil	2.00	0.80	1.60
Coal	0.11	1.00	0.11
	F_D = 55.00		**L_T = 5.00**

Based on Table 3-5, CCS was deployed in the coal sector alone. These results are consistent with previous explanations that CCS deployment should commence from the energy source with the highest CO_2 intensity (i.e., dirtiest energy source). In other words, the CO_2 emissions from the coal sector must be initially mitigated before addressing the emissions from sectors with lower CO_2 intensities i.e., oil and natural gas sectors. Suppose that the natural gas or the oil sector was CCS retrofitted in Example 2, the minimum deployment of BECCS would have been higher than 4.48 TWh y^{-1}, thus undesirable. Also note that once again (like Example 1), CCS deployment aided in CO_2 removal, thus reducing the minimum deployment of BECCS.

3.3 Chapter Summary

A novel graphical method for the deployment of EP-NETs during energy planning has been developed and demonstrated with two scenarios. The graphical method is an extension of a previous study (Tan et al., 2009b) but with EP-NETs integrated as part of energy planning. In the

first example, EP-NETs are directly employed to reduce the total CO_2 emissions during power generation, without the use of CCS. The remaining example deploys EP-NETs as the compensatory energy during CCS. Therefore, both EP-NETs and CCS retrofit extent are to be minimised for the sources while fulfilling the total CO_2 emissions limit. The graphical targeting technique provides intuitive insights into the minimum deployment of EP-NETs and the optimum CCS retrofit allocation for each energy source. Aside from prioritising the energy source with the highest CO_2 intensity for CCS deployment, the graphical targeting technique can demonstrate the effectiveness of CDR which is evident through the negative slope of EP-NETs.

Chapter 4: GRAPHICAL TARGETING TECHNIQUE FOR THE DEPLOYMENT OF ENERGY-CONSUMING NEGATIVE EMISSIONS TECHNOLOGIES

This chapter presents the results associated with the development of a graphical targeting technique for the deployment of EC-NETs and/or CCS. The different characteristics of EC-NETs require a revamp of the targeting techniques employed for the deployment of EP-NETs. Note that deployment of EC-NETs is kept to a minimum, as it is relatively immature (as compared to renewable energy sources and CCS technologies), aside from having higher operating costs. It is assumed that DAC is the chosen EC-NETs for this work due to its widely available literature data (House et al., 2011; McLaren, 2012; Smith et al., 2016a). Additionally, DAC is close to a full-scale commercial deployment with ongoing development in the United States. It is projected that this DAC plant would capture 1 Mt CO_2 annually by year 2023 (IEA, 2021b).

4.1 Targeting Technique of Energy-Consuming Negative Emissions Technologies without the Deployment of CO_2 Capture and Storage

In this case, it is assumed that CCS will not be deployed, due to the high capital expenditure involved in retrofitting existing fossil-based power plants. Therefore, only DAC would be deployed to achieve the aggregate CO_2 emissions limit (Δm_L). Note however that the energy requirement of DAC for CO_2 emissions removal results in insufficient energy to meet the existing power demand. Therefore, renewable energy sources are deployed as compensatory energy; from a holistic perspective, this incremental capacity is part of the deployment of EC-NETs systems.

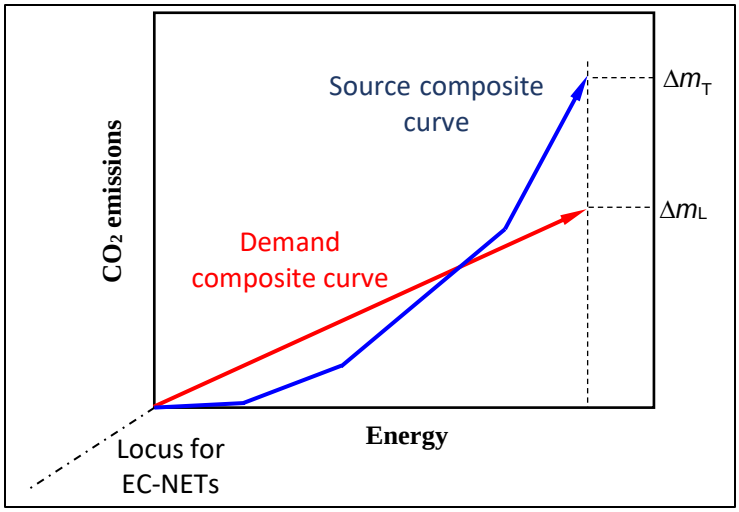


Figure 4-1: Infeasible EPPD for the targeting of EC-NETs without CCS deployment

The minimum deployment of EC-NETs via graphical targeting technique is given as follows:

1. The *source composite curve* is plotted on CO_2 emissions versus the energy diagram. The vertical axis is the cumulative CO_2 emissions, while the horizontal axis is the cumulative energy of all energy sources in order of increasing CO_2 intensities. The total CO_2 emissions emitted from all energy sources (Δm_T) is illustrated by the vertical distance while the horizontal distance of the source composite curve constitutes the total energy available in the planning system, as shown in Figure 4-1.

2. The vertical axis of the *demand composite curve* is the CO_2 emissions limit, while the horizontal axis is the total demand of the energy planning system. The demand composite curve has a smaller vertical distance, in comparison to the source composite curve indicating the CO_2 emissions limit (Δm_L). Figure 4-1 represents an infeasible EPPD since the demand composite curve is located below and to the right of the source composite curve.

3. A locus with a positive slope is added diagonally from the EPPD origin, with its slope corresponding to the EC-NETs' absolute CO_2 intensity. This slope indicates that the system will experience a decline in net energy when CO_2 emissions are removed by EC-NETs.

4. The source composite curve is shifted along the EC-NETs locus until the source composite curve reaches the CO_2 emission limit (Δm_L) of the demand composite curve, as shown in Figure 4-2. The minimum deployment of EC-NETs ($F_{EC\text{-}NET}$) is illustrated with the horizontal distance of the opening of the leftmost part of the EPPD.

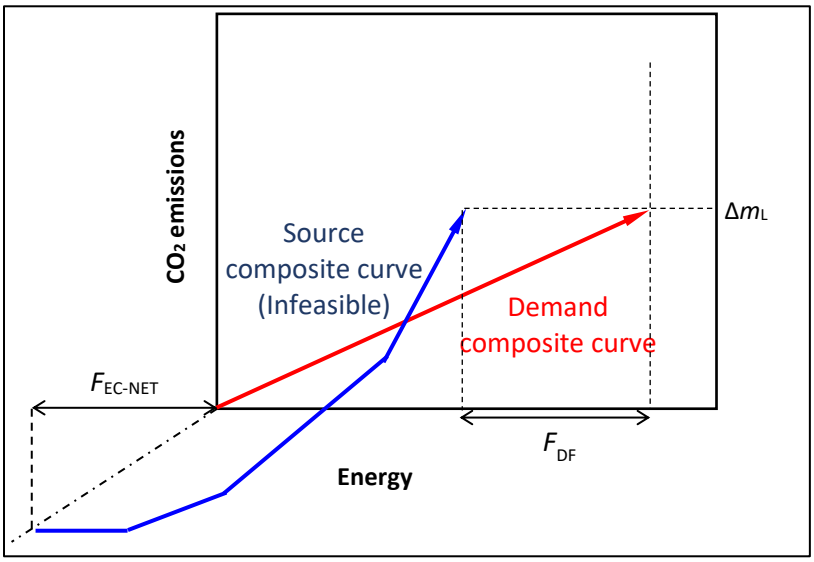


Figure 4-2: Infeasible EPPD for targeting of EC-NETs without CCS deployment (after EC-NETs targeting)

5. The EPPD in Figure 4-2 is still infeasible since the demand composite curve is located to the right of the source composite curve. Note that the energy deficit (F_{DF}) is represented by the horizontal distance between the rightmost ends of the demand and the source composite curve. Therefore, renewable energy sources with zero CO_2 intensity are to be used to restore the feasibility of the EPPD. The source composite curve is then shifted horizontally to the right until it stays entirely to the right and below the demand composite curve, as depicted in Figure 4-3. The minimum deployment of renewable energy sources as compensatory energy (F_{COMP}) is illustrated by the horizontal distance travelled by the source composite curve. In this case, F_{COMP} would always be equal to $F_{EC\text{-}NET}$. In other words, renewable energy sources are used to compensate for the energy demand of EC-NETs during CO_2 emissions removal.

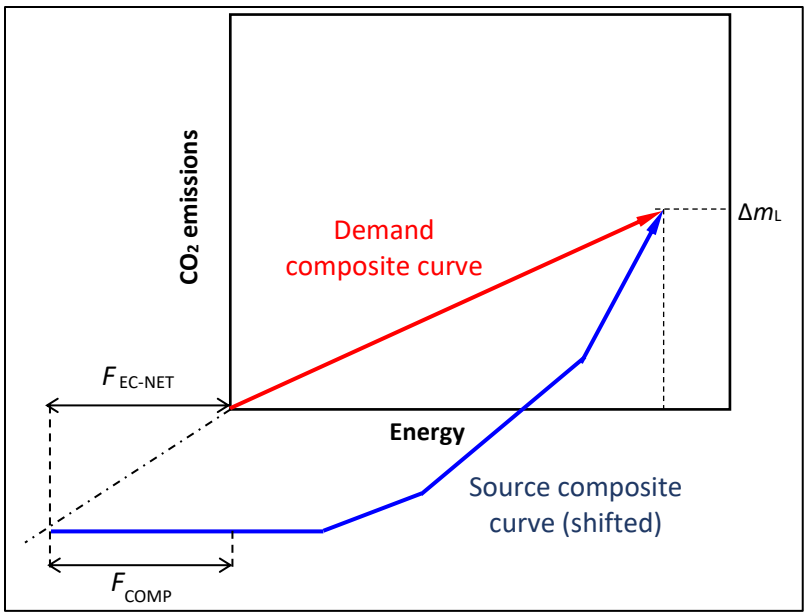


Figure 4-3: Feasible EPPD for targeting of EC-NETs without CCS deployment

The targeting procedure of EC-NETs without CCS deployment is illustrated via a case study.

4.1.1 Case Study

The Philippines's power generation sector case (Tan et al., 2009b) is used to illustrate the graphical targeting technique of EPPD for the deployment of EC-NETs without CCS deployment (see Table 3-1). Based on Table 3-1, 16.2 Mt CO_2 y^{-1} (= 31.2 – 15 Mt CO_2 y^{-1}) is to be removed to achieve an aggregate CO_2 emissions limit of 15 Mt y^{-1}. DAC with a CO_2 intensity of -0.4 Mt CO_2 $(TWh)^{-1}$ (House et al., 2011) is utilised for CDR, indicating that 1 TWh of energy needs to be supplied to EC-NETs to remove 0.4 Mt of CO_2. Hence, the use of DAC should be minimised to reduce its energy consumption. In this work, renewable energy sources with negligible CO_2 intensity are available for use.

The steps for targeting the minimum deployment of DAC are illustrated next. A preliminary EPPD is plotted in Figure 4-4a, based on Steps (1) and (2) of the targeting techniques. The DAC locus with a slope of 0.4 Mt CO_2 $(TWh)^{-1}$ is added diagonally from EPPD origin (Step (3)). Along the DAC locus, the source composite curve is slid until the source composite curve reaches the CO_2 emissions limit (Δm_L) i.e., 15 Mt y^{-1} of the demand composite curve (Step (4)), as shown in Figure 4-4b. Based on the horizontal distance of the opening of the leftmost part of EPPD, a minimum

of 40.5 TWh y^{-1} of DAC deployment ($F_{EC\text{-}NET}$) is necessary (Step (4)). Although the CO_2 emissions limit is satisfied, there is an energy deficit (F_{DF}) experienced by the system, to meet the 60 TWh y^{-1} demand (see Table 3-1). Therefore, renewable energy sources with negligible CO_2 intensity are to be used as compensatory energy, and their consumption is to be determined. Based on Step (5), the source composite curve is shifted horizontally to the right until it stays entirely to the right and below the demand composite curve, as shown in Figure 4-4c. The horizontal distance of the shifted source composite curve indicates the minimum compensatory energy (F_{COMP}) i.e., 40.5 TWh y^{-1} (see Figure 4-4c). For this case study which involves the sole deployment of EC-NETs and renewable energy sources (as compensatory energy), one may divide the total CO_2 emissions to be removed i.e., 16.2 Mt y^{-1} by the absolute CO_2 intensity of DAC i.e., 0.4 Mt CO_2 $(TWh)^{-1}$. Doing this will also lead to the minimum compensatory energy of 40.5 TWh y^{-1}, as is presented in Figure 4-4c. The graphical nature of CEPA through the EPPD allows the energy planner to better communicate the solution in an energy planning scenario. In the following section, the usefulness of graphical CEPA will be further demonstrated for the deployment of EP-NETs and CCS.

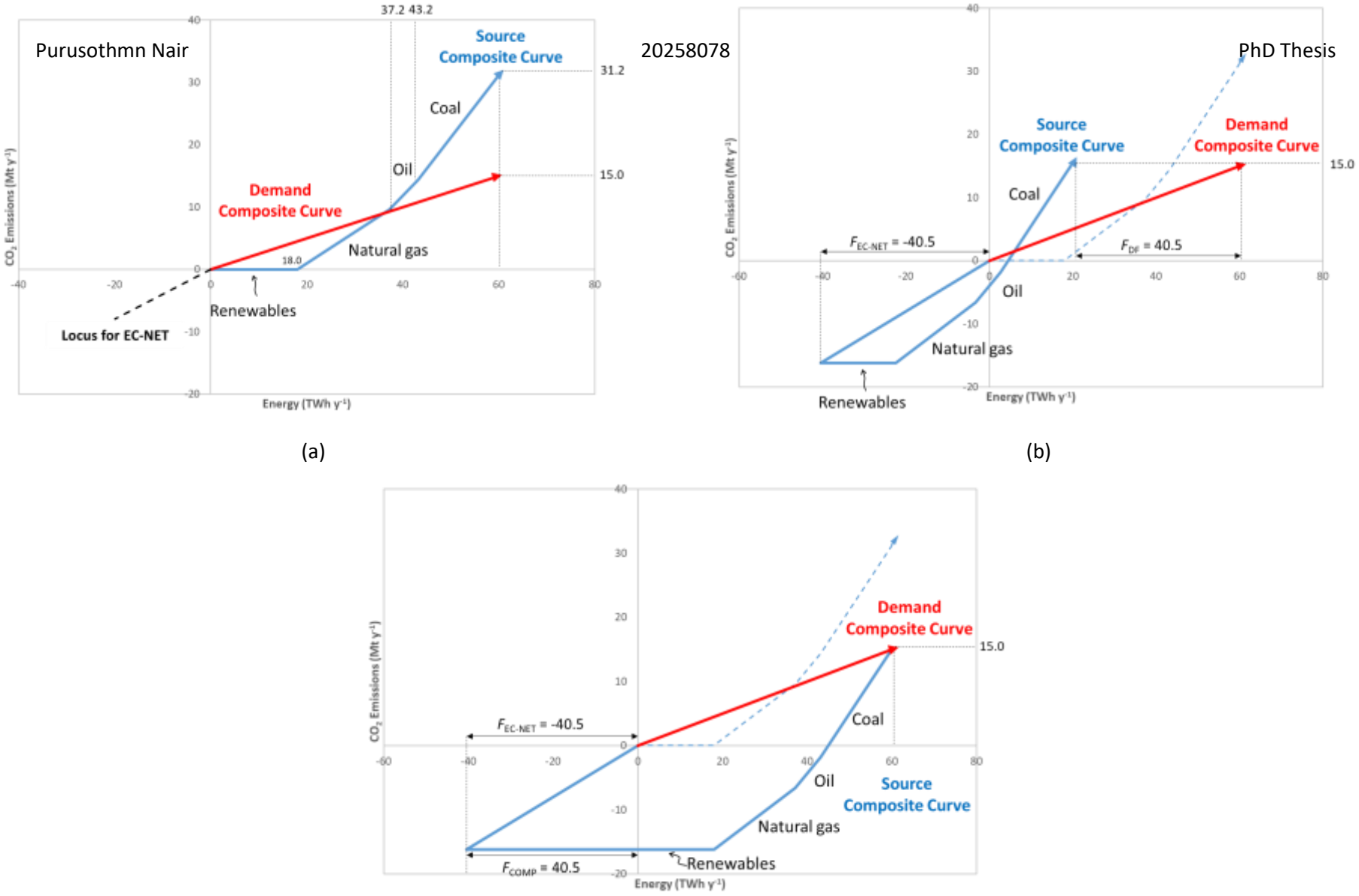


Figure 4-4: EPPD for DAC deployment without CCS: (a) infeasible EPPD, (b) targeting for the minimum deployment of DAC, and (c) feasible EPPD with minimum DAC and compensatory energy requirements

4.2 Targeting Technique of Energy-Consuming Negative Emissions Technologies with the Deployment of CO_2 Capture and Storage

In this case, CCS is deployed in fossil-fuel-based power plants alongside EC-NETs, leading to some parasitic power losses. Therefore, new renewable energy sources must be used as compensatory energy. In Chapter 3.2, EP-NETs (e.g., BECCS) was utilised as the compensatory energy. However, such a case is not feasible for EC-NETs (e.g., DAC) due to its energy-consuming characteristic. Consequently, the targeting technique employed in Chapter 3.2 is modified here for the case of EC-NETs. The target for CCS deployment on fossil-based sectors is determined before the deployment of EC-NETs. CCS deployment is expected to reduce the EC-NETs requirement since a portion of the CO_2 emissions is captured from the fossil-based sectors. The targeting technique is given as follows. The preliminary EPPD for the targeting of EC-NETs with CCS deployment is plotted using Steps (1) and (2) of the targeting techniques involving the deployment of EC-NETs without CCS (see Chapter 4.1) and hence are excluded here.

3. Firstly, the CCS deployment target on fossil-based sectors is determined from Equation 3-2. Once again, note that the total CO_2 emissions to be removed from the system (Δm_R) is greater than the difference between the total CO_2 emissions (Δm_T) and the CO_2 emissions limit (Δm_L). This is due to the removal ratio (RR) of the CCS technique.

4. The CO_2 emissions removal from energy source i ($\Delta m_{R,i}$) is to be calculated. This step is first applied for energy source i with the highest CO_2 intensity, as shown in Equation 4-1. Energy source i with a lower CO_2 intensity would then be retrofitted with CCS if the energy source i of the highest CO_2 intensity is fully CCS retrofitted, as demonstrated in Equation 4-2. Also, note that Equation 4-2 further demonstrates that energy source i will only be retrofitted with CCS if the entire sector is fully retrofitted. In other words, sectors that are partially CCS-retrofitted would be excluded from CCS deployment. It is economically unviable (due to capital requirements) to partially retrofit a fossil-based sector. The lack of funding may dampen the initiative to retrofit fossil-based power plants. Additionally, fully retrofitting fossil-based sectors may

present a better sustainability value to investors, with promising returns in terms of reduction of CO_2 emissions under a carbon market or carbon tax regime.

$$\Delta m_{\mathrm{R},i} = \begin{cases} F_i \times C_{\mathrm{S},i}, & F_i \times C_{\mathrm{S},i} \leq \Delta m_{\mathrm{R}} \\ 0, & F_i \times C_{\mathrm{S},i} > \Delta m_{\mathrm{R}} \end{cases} \quad i = n \qquad \text{Equation 4-1}$$

If $\Delta m_{\mathrm{R},i} \neq 0$,

$$\Delta m_{\mathrm{R},i-1} = \begin{cases} F_{i-1} \times C_{\mathrm{S},i-1}, & F_{i-1} \times C_{\mathrm{S},i-1} \leq \Delta m_{\mathrm{R}} - \sum_{i=n}^{i} \Delta m_{\mathrm{R},i} \\ 0, & F_{i-1} \times C_{\mathrm{S},i-1} > \Delta m_{\mathrm{R}} - \sum_{i=n}^{i} \Delta m_{\mathrm{R},i} \end{cases} \quad i = n, n-1, \ldots, 2 \qquad \text{Equation 4-2}$$

5. Based on the $\Delta m_{R,i}$ values calculated from Equation 4-1 and Equation 4-2, the CCS retrofit extent on energy source *i* ($F_{R,i}$) and CO_2 intensity of CCS retrofitted energy source *i* ($C_{R,i}$) are calculated from Equation 3-5 and Equation 3-6.

6. The deployment of CCS results in parasitic power losses. Therefore, the net energy from energy source *i* with ($F_{NR,i}$) and without CCS retrofit ($F_{NS,i}$) are determined from Equation 3-7 and Equation 3-8 respectively. Based on the values of $F_{NR,i}$ and $F_{NS,i}$, a revised EPPD is plotted, as depicted in Figure 4-5a.

7. Based on Figure 4-5a, energy source *i* retrofitted with CCS has a smaller slope in comparison to energy source *i* without CCS retrofit. At the right end of the EPPD (see Figure 4-5a), there exists an energy deficit gap (F_{DF}) due to the parasitic power losses during CCS deployment. Also, since CCS is only conducted if fossil-based sector(s) is/are fully retrofitted, the total CO_2 emissions of the source composite curve (given by its vertical distance) in Figure 4-5a exceeds the CO_2 emissions limit (Δm_L). In other

words, there is insufficient CCS on the fossil-based sectors to satisfy the CO_2 emissions limit.

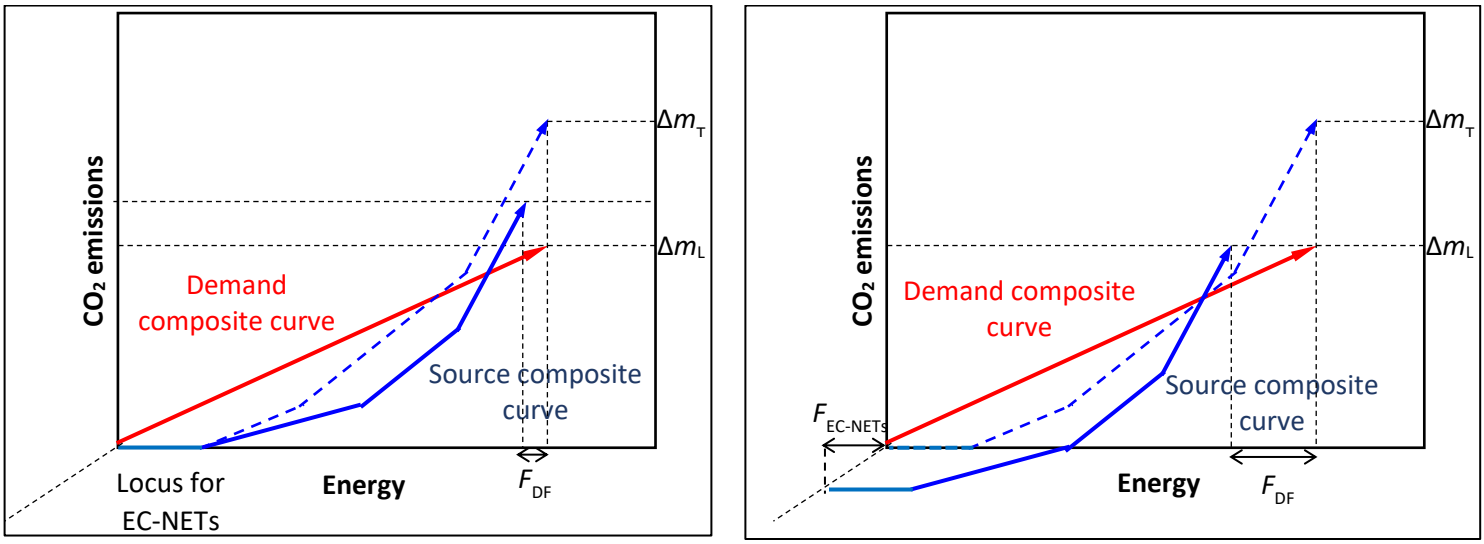


Figure 4-5: Infeasible EPPD: (a) with CCS deployment and (b) with CCS and EC-NETs deployment

8. The next step involves the deployment of EC-NETs to satisfy the CO_2 emissions limit (Δm_L). Steps (3) and (4) of the targeting technique of EC-NETs without CCS deployment (see Chapter 4.1) are repeated to determine the minimum deployment of EC-NETs ($F_{EC\text{-}NET}$), as shown in Figure 4-5b.
9. The EPPD in Figure 4-5b is still infeasible as the demand composite curve is located to the right of the source composite curve. Renewable energy sources with zero CO_2 intensity are used to restore the feasibility of the EPPD. Note that this is essentially the same as Step (5) of the targeting technique of EC-NETs without CCS deployment (Figure 4-3), where the minimum renewable energy sources as compensatory energy (F_{COMP}) is to be determined. Figure 4-6 shows the feasible EPPD with the deployment of CCS and EC-NETs. In comparison to the scenario in Figure 4-3, F_{COMP} is larger in this case than that in Figure 4-3. Note that in the latter scenario, F_{COMP} value is the same as $F_{EC\text{-}NET}$ since renewable energy sources are only used as compensatory energy for EC-NETs, whereas in this case renewable energy sources are also used for compensating the parasitic power losses during CCS deployment.

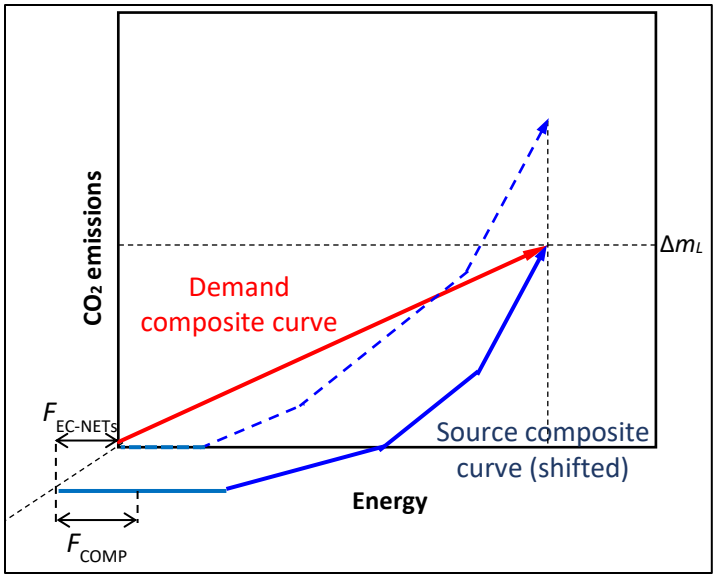


Figure 4-6: Feasible EPPD with CCS and EC-NETs deployment

The targeting technique that involves both EC-NETs and CCS deployment is demonstrated by revising the case study.

4.2.1 Case Study (Revisited)

The targeting technique for EC-NETs and CCS deployment is illustrated by revisiting the previous case study. Note that the CO_2 emissions limit (Δm_L) remains the same as 15 Mt y^{-1}. The *parasitic power loss* (X) and *removal ratio* (RR) of the CCS system are assumed as 0.15 and 0.85 respectively, similar to those used in the literature (Tan et al., 2009b). Firstly, the total CO_2 emissions removal (Δm_R) is determined from Equation 3-2, equating to 19.06 Mt y^{-1} (Step (3)). Equation 4-1 (Step (4)) is then applied to the coal sector due to its highest CO_2 intensity of 1 Mt CO_2 $(TWh)^{-1}$ (see Table 3-1). The CO_2 emissions of the coal sector alone is 16.8 Mt y^{-1} (= 16.8 × 1 Mt y^{-1}). Since this value is lower than Δm_R, the entire coal sector is CCS retrofitted. Based on Equation 4-2 (Step (4)), the remaining CO_2 emissions of 2.26 Mt y^{-1} (= 19.06 – 16.8 Mt y^{-1}) may be captured from the oil sector which has CO_2 emissions of 4.8 Mt y^{-1} (= 6 × 0.8 Mt y^{-1}). However, since it involves partial CCS retrofit, the oil sector is hence excluded. Following this, the CCS retrofit extent on the coal sector is determined from Equation 3-5, equating to 16.8 TWh y^{-1} (= 16.8 ÷ 1 TWh y^{-1}) (Step (5)). Subsequently, the CO_2 intensity of the coal sector post-CCS retrofitting and the net energy available from the coal sector with and without CCS retrofit are

calculated from Equation 3-6 – Equation 3-8 respectively (Steps (5) and (6)). The energy contribution and CO_2 intensities from all energy sources after CCS deployment are presented in Table 4-1.

Table 4-1: Energy and CO_2 Intensities for energy sources after CCS deployment (after Steps (5) and (6))

Energy source *i*	$F_{NS,i}$ / $F_{NR,i}$ (TWh y^{-1})	$C_{S,i}$ / $C_{R,i}$ (Mt CO_2 TWh^{-1})	Total CO_2 emission (Mt CO_2 y^{-1})
Renewable energy	18.00	0	0
CCS retrofitted coal	14.28	0.18	2.52
Natural gas	19.20	0.50	9.60
Oil	6.00	0.80	4.80
Coal	0	1.00	0
	$\sum_i F_i$ = 57.48		**ΔE_T = 16.92**

Based on Table 4-1, the total CO_2 emissions (ΔE_T) exceeded the CO_2 emissions limit by 1.92 Mt y^{-1} (= 16.92 – 15 Mt y^{-1}), due to the absence of CCS retrofit in the oil sector. Also, the parasitic power loss during the CCS retrofit of the coal sector led to an energy deficit gap of 2.52 TWh y^{-1} (=60 – 57.48 TWh y^{-1}). Note that the CO_2 intensity of the coal sector had reduced from 1 to 0.18 Mt CO_2 $(TWh)^{-1}$ post-CCS deployment, indicating that most of the CO_2 emissions from the coal sector are captured via CCS. The revised EPPD post-CCS deployment is presented in Figure 4-7 (Step (7)).

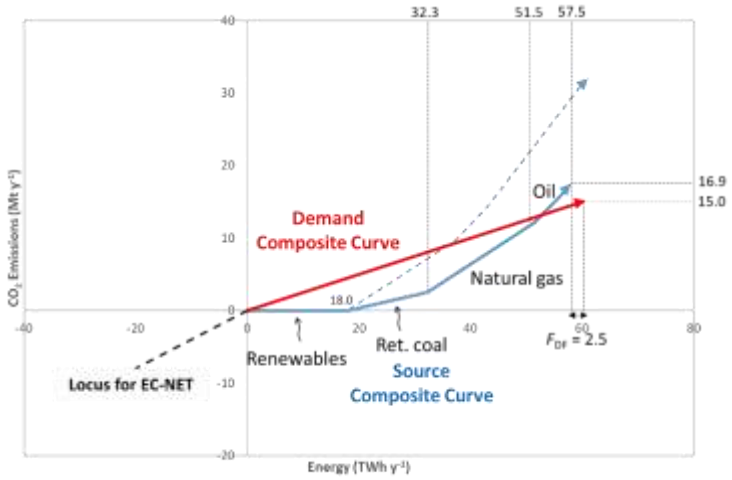
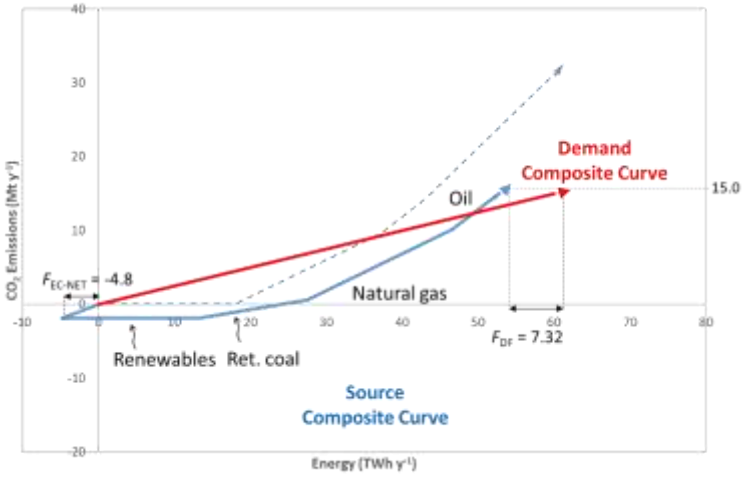


Figure 4-7: Revised EPPD post-CCS deployment for case study (after Step (7))

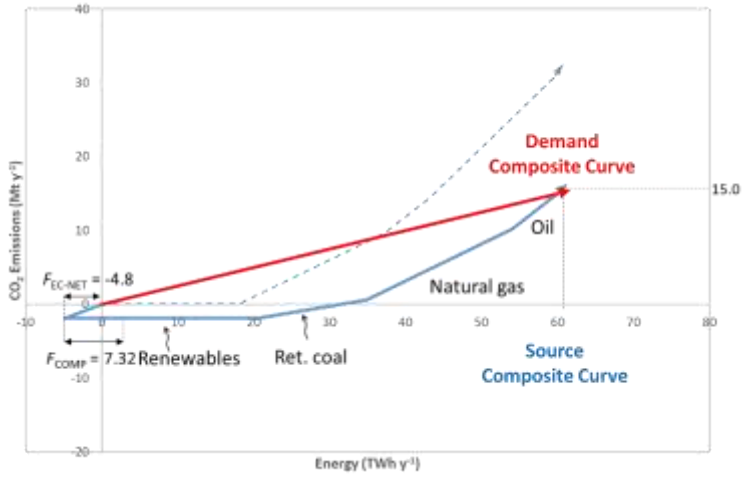
Since the demand composite curve is located on the bottom and to the right side of the source composite curve, the EPPD in Figure 4-7 is deemed infeasible. Therefore, EC-NETs is used to meet the CO_2 emissions limit (Δm_L). The source composite curve is slid along the EC-NETs locus until the source composite curve reaches the CO_2 emissions limit (15 Mt y^{-1}), as depicted in Figure 4-8a (Step (8)). As indicated by the opening of the leftmost part of EPPD in Figure 4-8a, a minimum DAC deployment ($F_{EC\text{-}NET}$) of 4.8 TWh y^{-1} is necessary (Step (8)). Based on Figure 4-8a, the energy deficit gap (F_{DF}) rose from 2.52 TWh y^{-1} (see Figure 4-7) to 7.32 TWh y^{-1} due to the energy requirement for DAC operation. Subsequently, renewable energy sources with zero CO_2 intensity are to be used as the compensatory energy and their consumption is to be determined. Following Step (9), the source composite curve is shifted horizontally to the right until it stays entirely to the right and below the demand composite curve, as shown in Figure 4-8b. The minimum compensatory energy (F_{COMP}) is given by the horizontal distance of the shifted source composite curve, i.e., 7.32 TWh y^{-1} (see Figure 4-8b).

It is also worth comparing the solution in this case with that in Figure 4-4c. For the latter, the energy demand for DAC operation was determined as 40.5 TWh y^{-1} (see Figure 4-4c); it has now been reduced to 4.8 TWh y^{-1}. This is mainly because a large portion of CO_2 emissions has been removed by CCS. Consequently, lesser EC-NETs is required to achieve the CO_2 emissions limit of 15 Mt y^{-1}. Note also that the requirement of compensatory energy (F_{COMP}), i.e., 7.32 TWh y^{-1} is larger than that when DAC alone is deployed, i.e., 4.8 TWh y^{-1} (see Figure 4-8b). In this case, the

renewable energy source is used for complementing both DAC and parasitic power losses during the CCS retrofit. Note that for this case, the approach is important in demonstrating the satisfaction of the CO_2 emissions limit. Upon CCS deployment, both energy demand and CO_2 emissions constraints are now met. The step-by-step CEPA technique ensures both constraints are fulfilled systematically.



(a)



(b)

Figure 4-8: EPPD for case study (DAC and CCS deployment): (a) infeasible EPPD with CCS and DAC targeting, (b) feasible EPPD with CCS, DAC and renewable energy targeting

4.3 Targeting Technique of Energy-Consuming and Energy-Producing Negative Emissions Technologies without the Deployment of CO_2 Capture and Storage

Previous sections described the targeting technique involving EC-NETs e.g., DAC during energy planning. For such cases, renewable energy sources must be deployed as compensatory energy for the EC-NETs. In this section, EC-NETs and EP-NETs are both deployed for the energy planning scenario to achieve the aggregate CO_2 emissions limit (Δm_L). A good candidate for EP-NETs is BECCS due to its technology maturity and relative ease of deployment into existing energy systems (McGlashan et al., 2012). Note that CCS deployment is excluded for this case, due to the reasons mentioned previously. Note also that renewable energy sources are not required as the energy requirement for EC-NETs is to be supplied by EP-NETs. The targeting technique for this case is given as follows. The preliminary EPPD for this case is plotted following Steps (1) and (2) of the targeting techniques involving the deployment of EC-NETs without the use of CCS (see Chapter 4.1) and hence are excluded here.

3. The total CO_2 emissions removal (Δm_R) is determined by the difference between emission limit (Δm_L) and total CO_2 emissions (Δm_T; see Figure 4-9). Two loci of EC-NETs and EP-NETs are added at the leftmost end of the EPPD. As shown in Figure 4-9, the locus for EC-NETs is first added diagonally from the EPPD origin, with a positive slope corresponding to its absolute CO_2 intensity. Next, the locus for EP-NETs with a negative slope (which corresponds to its CO_2 intensity) is added to the EC-NETs locus, such that the vertical distance of these loci will correspond to the total CO_2 emissions removal (Δm_R), as depicted in Figure 4-9. Note that the procedure of determining Δm_R here is different to the techniques applied in Chapter 4.2. Firstly, the absence of CCS deployment, in this case, means Equation 3-3 is not required to consider the *RR* of the CCS system. Secondly, the presence of two types of NETs means that both EP-NETs and EC-NETs must be used simultaneously in determining their target deployment for CO_2 emissions removal.

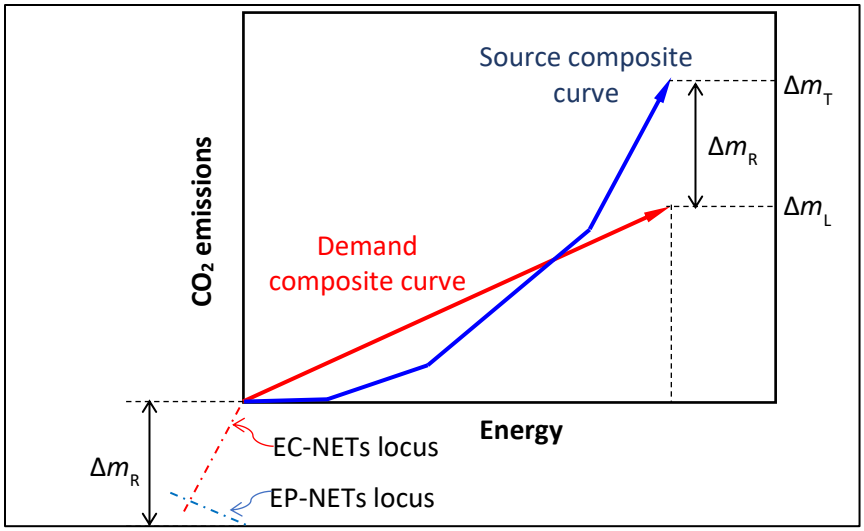


Figure 4-9: Loci of EC-NETs and EP-NETs

4. The source composite curve is first slid along the locus of EC-NETs, and then along the locus of EP-NETs until it covers the total CO_2 emissions removal (Δm_R), as shown in Figure 4-10. Based on Figure 4-10, the intersection between the two loci represents the minimum deployment of each NETs type. The horizontal distance from the origin of the EPPD to the intersection point of the two loci represents the minimum deployment of NETs (F_{NET}) needed for the energy planning scenario. The vertical distances of the two loci in Figure 4-10 represent the CO_2 emissions removed by EP-NETs ($\Delta m_{R,\ EP\text{-}NET}$) and EC-NETs ($\Delta m_{R,\ EC\text{-}NET}$).

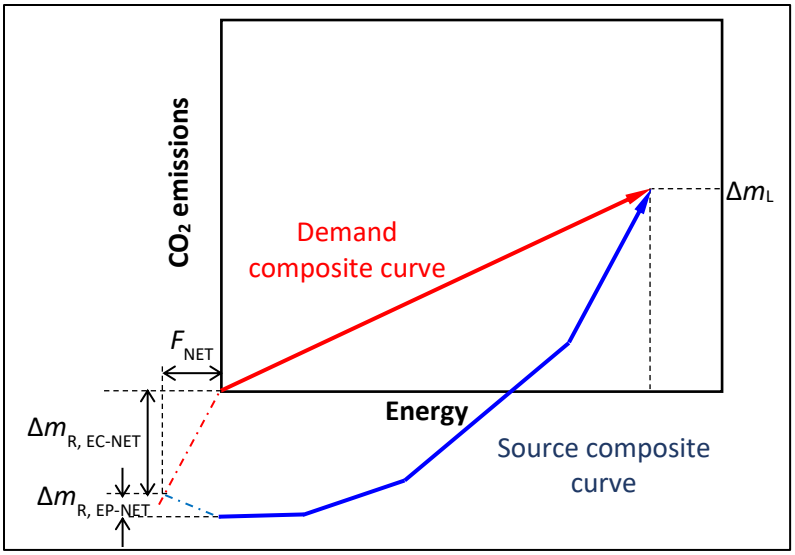


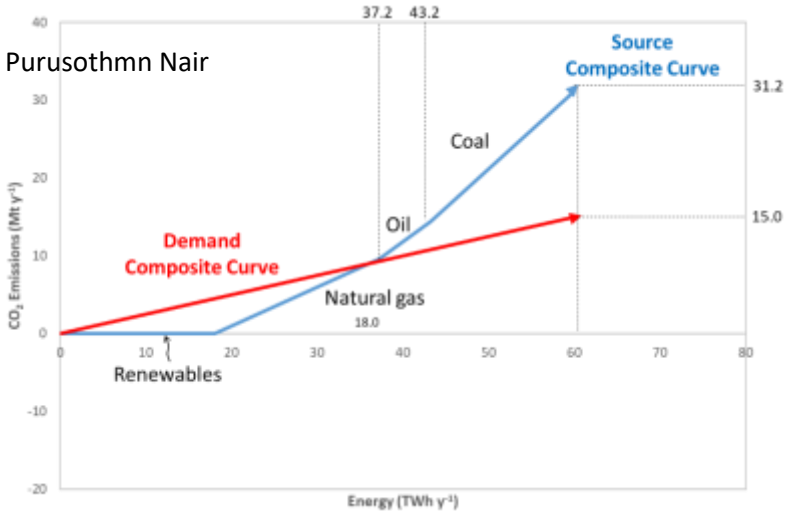
Figure 4-10: Targeting the deployment of EC-NETs and EP-NETs without CCS

The graphical targeting procedure for the deployment of EC-NETs and EP-NETs is illustrated by revisiting the case study.

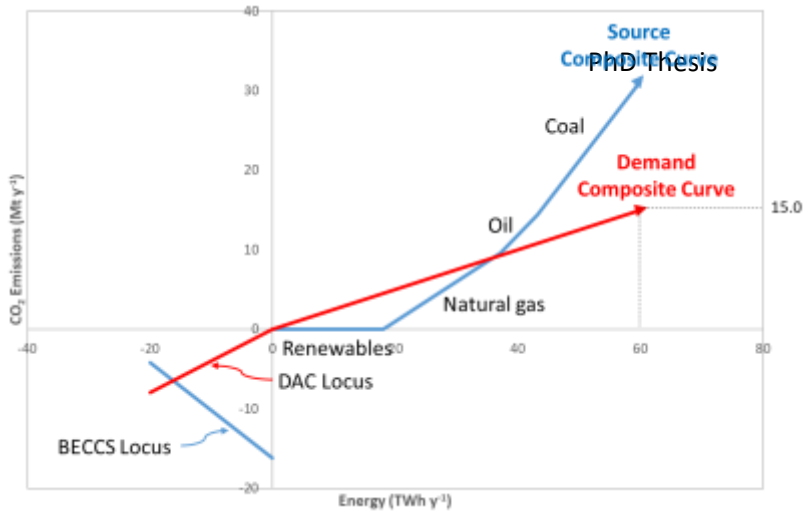
4.3.1 Case Study (Revisited)

The previous case study (Tan et al., 2009b) is revisited, with identical assumptions. In this case, both BECCS (EP-NETs) and DAC (EC-NETs) with respective CO_2 intensities of -0.6 Mt CO_2 $(TWh)^{-1}$ and -0.4 Mt CO_2 $(TWh)^{-1}$ are utilised to achieve a CO_2 emissions reduction (Δm_R) of 16.2 Mt y^{-1} (= 31.2 – 15 Mt y^{-1}). Based on Steps (1) and (2) of the targeting techniques, a preliminary EPPD is plotted in Figure 4-11a. Next, two loci of BECCS and DAC are added to the EPPD, with slopes corresponding to their CO_2 intensities. Hence, the locus of BECCS has a slope of -0.6 Mt CO_2 $(TWh)^{-1}$, while that of DAC has a slope of 0.4 Mt CO_2 $(TWh)^{-1}$, as shown in Figure 4-11b (Step (3)). Figure 4-11c shows a minimum of 16.2 TWh y^{-1} of BECCS deployment for the energy planning scenario. Also, the net CO_2 emissions removal from each NETs may be determined from the vertical distance of the two loci, i.e., 9.72 (BECCS) and 6.48 Mt y^{-1} (DAC) (Step (4)), (see Figure 4-11c). Higher CO_2 intensity of BECCS translated to greater removal of CO_2 emissions in comparison to DAC. Supposedly if EP-NETs with lower CO_2 intensity (e.g., -0.8 Mt CO_2 $(TWh)^{-1}$) is deployed, the minimum deployment of NETs (F_{NET}) would decrease due to its greater CO_2 emissions removal capacity (i.e., higher value of $\Delta m_{R,\ EP\text{-}NETs}$). Similarly, the declining trend of F_{NET} would also be observed if EP-NETs with lower CO_2 intensity (e.g., -0.6 Mt CO_2 $(TWh)^{-1}$) is

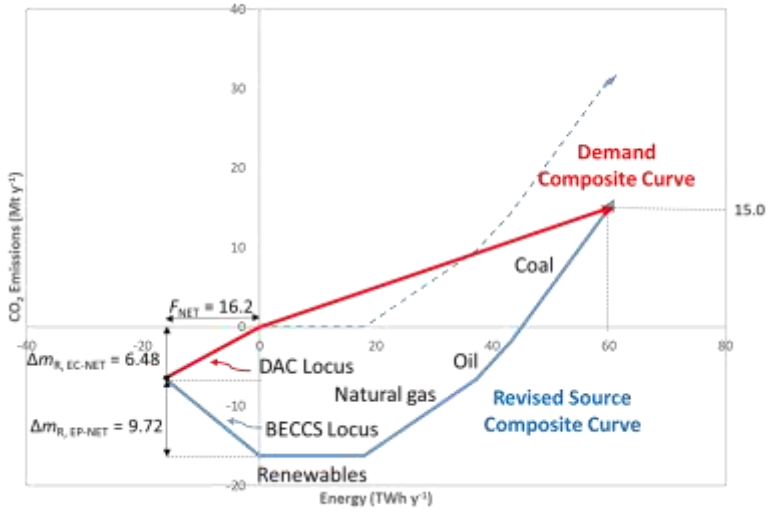
deployed. Also, note that F_{NET} decreased by 60% from 40.5 (see Figure 4-4c) to 16.2 TWh y^{-1} (see Figure 4-11c). The removal of CO_2 emissions via BECCS meant that lesser DAC is required to achieve the CO_2 emissions limit of 15 Mt y^{-1}.



(a)



(b)



(c)

Figure 4-11: EPPD for case study (Revisited): (a) Preliminary EPPD, (b) loci for BECCS and DAC and (c) feasible EPPD with BECCS and DAC targeting

4.4 Targeting Technique of Energy-Consuming and Energy-Producing Negative Emissions Technologies with the Deployment of CO_2 Capture and Storage

It is assumed in this case that CCS is deployed alongside EC-NETs and EP-NETs during energy planning. As will be shown later, with the removal of CO_2 emissions via CCS, a lesser extent of NETs deployment is necessary. The targeting technique for this case is given as follows. Note that Steps (1) to (7) follow the same techniques as the targeting of EC-NETs with CCS deployment (see Chapter 4.2), and hence are excluded here.

8. Due to the parasitic power loss of CCS, EP-NETs is to be used as the compensatory energy of the energy planning system. A locus is added at the EPPD origin, with a slope corresponding to the CO_2 intensity of EP-NETs, as shown in Figure 4-12.

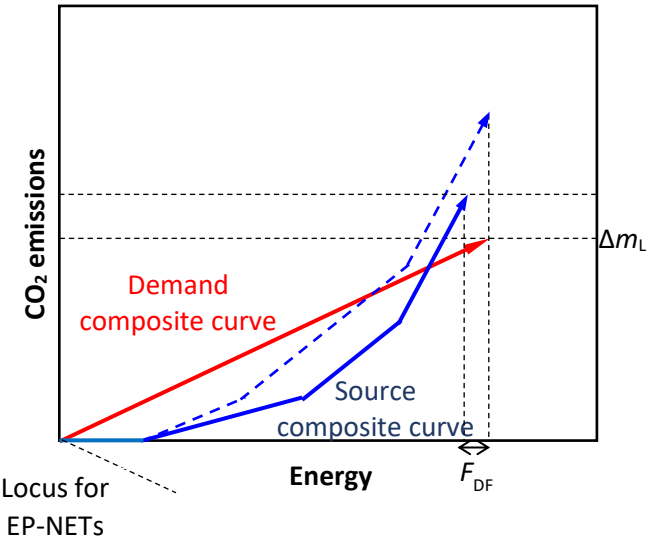


Figure 4-12: Preliminary EPPD for the targeting of EP-NETs and EC-NETs with CCS deployment

9. The source composite curve is slid along the EP-NETs locus until it reaches the right end of the demand composite curve, in which the energy demand of the given energy planning system is satisfied, as shown in Figure 4-13. The minimum deployment of EP-NETs as the compensatory energy for the energy planning system is determined based on the opening of the leftmost end of the EPPD (F_{COMP}).

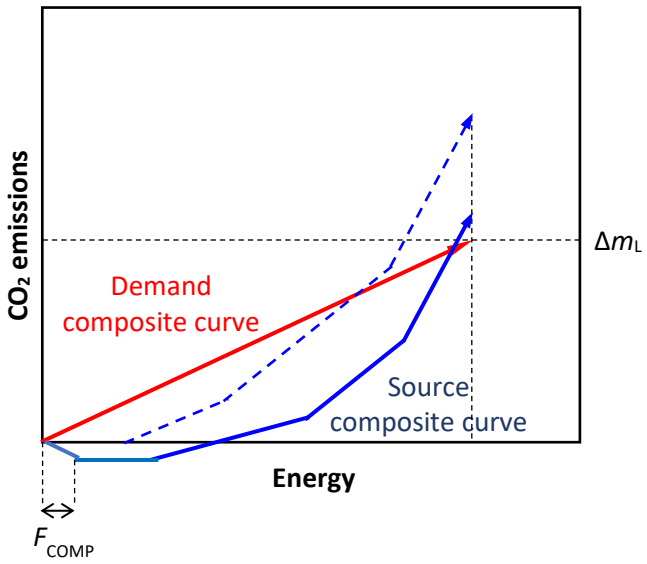


Figure 4-13: Infeasible EPPD for the targeting of EP-NETs and EC-NETs with CCS deployment

10. As observed in Figure 4-13, the vertical distance of the source composite curve (representing the cumulative CO_2 emissions) is still higher than the given CO_2 emissions limit (Δm_L). Therefore, both EC-NETs and EP-NETs are to be used for CO_2 removal.

11. Steps (3) and (4) of the targeting technique of EP-NETs and EC-NETs without CCS deployment (see Chapter 4.3) are then followed to determine the minimum deployment of both NETs.

The targeting technique is illustrated by revisiting the case study.

4.4.1 Case Study (Revisited)

In this case, both EP-NETs and EC-NETs are to be used alongside CCS deployment. The parasitic power loss and removal ratio of the CCS system are assumed as 0.15 and 0.85 respectively (Tan et al., 2009b). The entire coal sector (16.8 TWh y^{-1}) is to be retrofitted with CCS (Steps (3) and (4)). No CCS retrofit of the oil sector takes place, since it involves a partial CCS retrofit. The energy and CO_2 emissions of the energy sources after CCS deployment are like those in Table 4-1 (Steps (5) to (7)). The reduced deployment of CCS retrofit resulted in a higher total CO_2 emission of 16.92 Mt y^{-1}, thus exceeding the CO_2 emissions limit of 15 Mt y^{-1}. Also, note that parasitic power loss during CCS deployment resulted in a lowered energy output of 57.48 TWh y^{-1} (see Table 4-1). In

other words, an energy deficit gap of 2.52 TWh y^{-1} (= 57.48 – 60 TWh y^{-1}) is experienced during CCS deployment. Figure 4-14 presents the resulting EPPD (step 8).

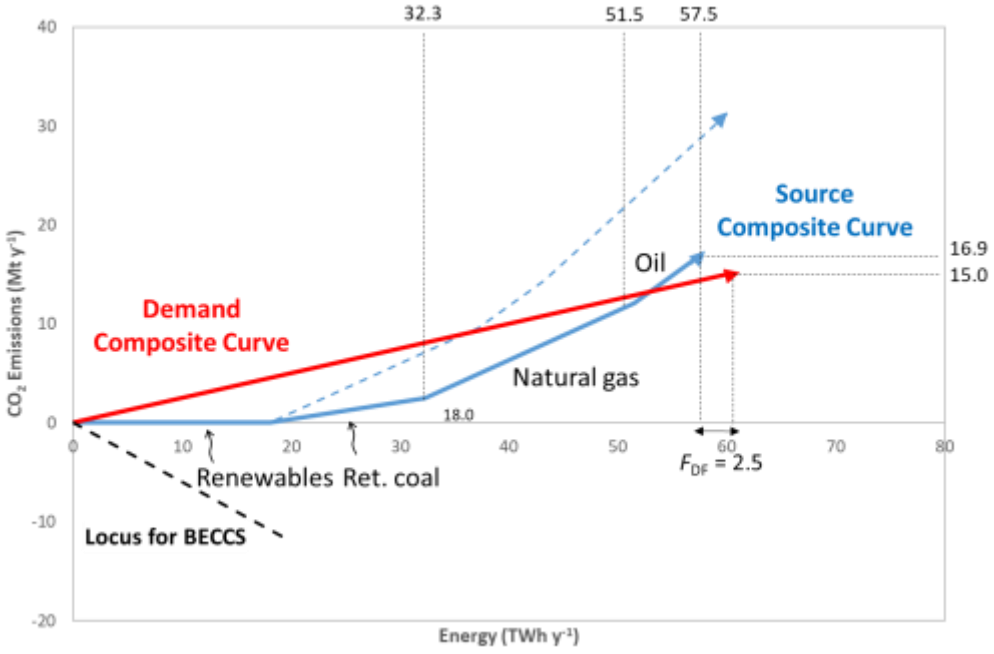


Figure 4-14: Revised EPPD post-CCS deployment for case study (Infeasible)

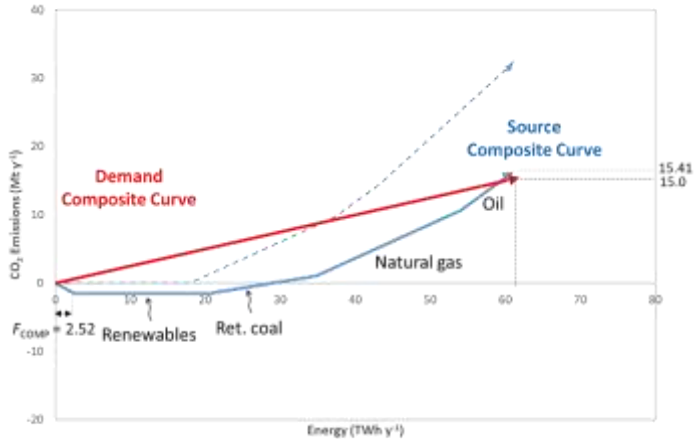
Note that the EPPD in Figure 4-14 is infeasible since the source composite curve is located on the top and to the left of the demand composite curve. The EP-NETs is first examined to see if it is sufficient to be utilised alone. Along the BECCS locus, the source composite curve is slid until it reaches the right end of the demand composite curve, to satisfy the energy demand of the system (see Figure 4-15a; Step (9)). The minimum deployment of BECCS as the compensatory energy (F_{COMP}) is represented by the opening of the leftmost end of the EPPD, equivalent to 2.52 TWh y^{-1} (Step (9)). As observed from Figure 4-15a, the total CO_2 emissions of the source composite curve are higher than the CO_2 emissions limit by 0.41 Mt y^{-1} (= 15.41 – 15 Mt y^{-1}) (Step (10)). This means that EP-NETs alone is insufficient to achieve the CO_2 emissions limit. Therefore, both EP-NETs and EC-NETs must be used to achieve the intended objective.

Two loci corresponding to BECCS and DAC are added to the EPPD, as shown in Figure 4-15b (Step (11)). Figure 4-15c shows 0.41 TWh y^{-1} of BECCS is to be deployed for the energy system. Also, the net CO_2 emissions removal from each NETs may be determined from the vertical distance of

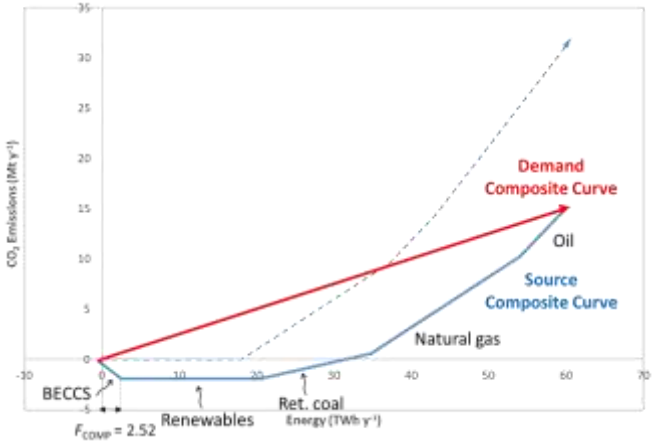
the two loci, i.e., 0.25 (BECCS) and 0.16 Mt y^{-1} (DAC) (see Figure 4-15c). CCS deployment resulted in a lower compensatory energy requirement (to be supplied by BECCS) for CO_2 emissions removal. In comparison with the case without CCS deployment, the energy supply by BECCS decreased by 82% from 16.2 TWh y^{-1} (see Figure 4-11c) to 2.93 TWh y^{-1} (= 2.52 + 0.41 TWh y^{-1}). Once again, it highlights the importance of CCS deployment toward CO_2 emissions reduction, thus reducing the dependency on NETs. Once again, the use of the graphical CEPA tool of EPPD allows the energy planner to set rigorous targets for the minimum deployment of CCS, EP-NETs, and EC-NETs, through the identification of the system bottleneck, i.e., pinch point.

4.5 Chapter Summary

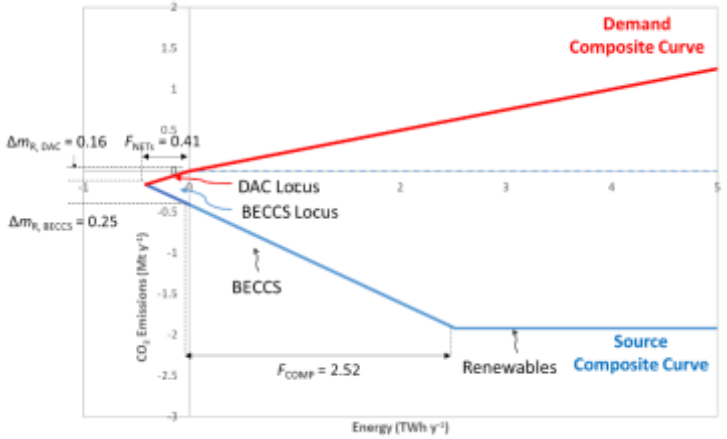
A case study is utilised to demonstrate the graphical targeting technique for the deployment of EC-NETs. When EC-NETs is deployed without CCS, renewable energy sources are utilised as the compensatory energy to fulfil the energy requirement of the EC-NETs system. When CCS is deployed, the consumption of renewable energy sources reduces by 82% from 40.5 to 7.32 TWh y^{-1}. The targeting technique is then demonstrated for cases where EP-NETs and EC-NETs are utilised, with and without CCS deployment. In both cases, EP-NETs are utilised as the compensatory energy source instead of renewable energy sources. When EP-NETs are utilised alongside CCS, the minimum deployment of compensatory energy reduces by 60% from 7.32 to 2.93 TWh y^{-1} due to the CO_2 emissions removal capacity of EP-NETs. The findings from this work highlight the importance of CCS deployment as a CO_2 management tool. The lack of maturity of NETs implies the need to deploy CCS to aid in CDR.



(a)



(b)



(c)

Figure 4-15: EPPD for case study: (a) infeasible EPPD with BECCS as the compensatory energy ; (b) feasible EPPD with BECCS and DAC targeting; (c) zoom-in section for feasible EPPD in (b)

Chapter 5: ALGEBRAIC TARGETING TECHNIQUE FOR THE DEPLOYMENT OF NEGATIVE EMISSIONS TECHNOLOGIES

This chapter presents the results associated with the development of a generic algebraic targeting technique for the deployment of NETs and/or CCS. Although the graphical targeting technique provides transparent views in setting system targets, it is inaccurate for large data sets and involves a cumbersome iterative procedure. The cascade analysis approach proposed by Foo et al. (2008) partially addresses these limitations but is only applicable for cases when renewable energy sources are used during energy planning. In other words, it does not account for cases where CCS is used. A subsequent algebraic targeting technique by Sahu et al. (2014) incorporated both renewable energy sources and CCS during energy planning but is yet to be extended for the deployment of NETs. Given the importance of CDR, a generic algebraic targeting technique is developed in this chapter for the deployment of renewable energy sources, CCS and NETs. This specific class of problems has not been previously solved via any pinch analysis methodology. This efficient algebraic targeting technique eliminates the iterative procedure needed during graphical targeting and can be implemented in commercial spreadsheet software for greater convenience in handling large data sets. The algebraic targeting technique for the deployment of NETs is demonstrated using an example.

5.1 Targeting Technique of Energy-Producing Negative Emissions Technologies without the Deployment of CO_2 Capture and Storage

For this case, it is assumed that only EP-NETs is utilised to satisfy the CO_2 emissions limit (Δm_L) during energy planning, due to reasons such as limited availability of renewable energy sources, the complexity of CO_2 storage (for CSS), high capital expenditure for CCS retrofit, etc. Table 5-1 shows the basic structure of an energy cascade table that is used for the algebraic targeting technique with EP-NETs deployment without CCS.

Table 5-1: Basic structure of an energy cascade table for EP-NETs deployment without CCS

C_k	ΔC_k	$(\sum_j F_{D,j})_k$	$(\sum_i F_{S,i})_k$	M_k	ΔM_k	N_k	$F_{E,k}$	$F_{N,k}$	δ_k	ε_k
									$\delta_0 = 0$	
C_1							$F_{EP\text{-}NET}$	$F_{N,1}$		$\varepsilon_1 = 0$
	ΔC_1								δ_1	
C_2		$(\sum_j F_{D,j})_k$	$(\sum_i F_{S,i})_k$	M_k	ΔM_k	N_k	$F_{E,k}$	$F_{N,2}$		ε_2
	ΔC_2								δ_2	
⋮		⋮	⋮	⋮	⋮	⋮	⋮	⋮		⋮
	⋮								⋮	
⋮		⋮	⋮	⋮	⋮	⋮	⋮	⋮		⋮
	⋮								⋮	
⋮		⋮	⋮	M_{n-2}	ΔM_{n-2}	N_{n-2}	$F_{E,n-2}$	⋮		⋮
	⋮								⋮	
C_{n-1}		$(\sum_j F_{D,j})_{n-1}$	$(\sum_i F_{S,i})_{n-1}$	M_{n-1}	ΔM_{n-1}	N_{n-1}	$F_{E,n-1}$	$F_{N,n-1}$		ε_{n-1}
	ΔC_{n-1}								δ_{n-1}	
C_n										ε_n

The targeting technique for the deployment of EP-NETs (without CCS) is given as follows:

i. The CO_2 intensities (C_k) for all energy demands and sources are arranged in ascending order in Column 1. An arbitrary large value is added at the last level *n* to facilitate calculation steps.

ii. In Column 2, the difference between adjacent levels of CO_2 intensity (ΔC_k) is calculated from Equation 5-1.

$$\Delta C_k = C_{k+1} - C_k \qquad \forall k \qquad \text{Equation 5-1}$$

iii. In Columns 3 and 4, energy demands, and sources are located at their respective intensity level. Note that the EP-NETs with negative CO_2 intensity is usually located at the first level (k = 1).

iv. In Column 5, theoretical energy reduction at level k (M_k) is determined following Equation 5-2. Doing this is meant to determine the amount of CO_2 emissions to be removed from level k with regards to the emissions limit. Note that this calculation step commences from the energy source at level k with the highest CO_2 intensity (i.e., "dirtiest" source) due to its greatest CO_2 emissions contribution.

$$M_k = \frac{\Delta m_{\mathrm{T}} - \Delta m_{\mathrm{L}}}{C_k - C_{\mathrm{COMP}}} \qquad for\ k = n - 1 \qquad \text{Equation 5-2}$$

v. The theoretical energy reduction at level k (M_k) should not exceed its available energy $(\sum_i F_{S,i})_k$. If the value of M_k is greater than that of $(\sum_i F_{S,i})_k$, the difference (ΔM_k) in Column 6 is elevated to level k – 1 with lesser CO_2 intensity, as depicted in Equation 5-3 and Equation 5-4. Equation 5-3 shows that for scenarios where M_k is lesser than $(\sum_i F_{S,i})_k$, the calculation procedure is terminated. In other words, if M_k is lesser than that of $(\sum_i F_{S,i})_k$, no energy reduction from level k – 1 with a lower CO_2 intensity (i.e., cleaner energy source) is required. Meanwhile, Equation 5-4 determines the theoretical energy reduction from level k – 1 with lower CO_2 intensity (i.e., cleaner energy source), if M_k is bigger than that of $(\sum_i F_{S,i})_k$.

$$\Delta M_k = \begin{cases} 0, & M_i \le \left(\sum_i F_{S,i}\right)_k \\ M_k - \left(\sum_i F_{S,i}\right)_k, & M_i > \left(\sum_i F_{S,i}\right)_k \\ for\ k = n-1, n-2, \dots, 2 \end{cases} \qquad \text{Equation 5-3}$$

$$M_{k-1} = \frac{\Delta M_k \times (C_k - C_{\mathrm{COMP}})}{C_{k-1} - C_{\mathrm{COMP}}}\ for\ k = n-1, n-2, \dots, 3 \qquad \text{Equation 5-4}$$

vi. In Column 7, actual energy reduction at level k (N_k) is calculated from Equation 5-5 to ensure that energy reduction at level k does not exceed its available energy $(\sum_i F_{S,i})_k$.

$$N_k = M_k - \Delta M_k \ \ for\ k = n-1, n-2, \dots, 2 \qquad \text{Equation 5-5}$$

vii. In Column 8, net energy available at level k ($F_{E,k}$) is calculated from Equation 5-6, considering the energy deduction at level k.

$$F_{E,i} = F_{S,i} - N_i \ \ for\ i = n-1, n-2, \dots, 2 \qquad \text{Equation 5-6}$$

viii. Subsequently, minimum deployment of EP-NETs as compensatory energy ($F_{EP\text{-}NET}$) is calculated from Equation 5-7, to compensate for reduced energy generation at level k. The calculated $F_{EP\text{-}NET}$ is placed in the top row of Column 8.

$$F_{EP-NET} = \sum_{k=1}^{n} N_k \qquad \text{Equation 5-7}$$

ix. In Column 9, net energy at level k ($F_{N,k}$) is calculated using Equation 5-8.

$$F_{N,k} = F_{E,i} + F_{EP-NET} - \sum_j F_{D,j} \qquad \forall k \qquad \text{Equation 5-8}$$

x. The power cascade is formed in Column 10, where cumulative energy for each interval k (δ_k) is given as the summation of cumulative energy at interval $k-1$ ($\delta_{k\text{-}1}$) with net energy at level k ($F_{N,k}$), as demonstrated in Equation 5-9. For an energy planning

scenario, the last entry of Column 9 should be zero, indicating that the demand constraint is satisfied.

$$\delta_k = \delta_{k-1} + F_{\mathrm{N},k} \qquad \forall k \qquad \text{Equation 5-9}$$

xi. The emission cascade is formed in Column 11, where the cumulative emission load at level *k* (ε_k) is determined. The latter is determined by adding the emission load of the previous level (ε_{k-1}) with the emission load of the interval of interest; the latter is given by the product between cumulative energy and the difference between adjacent levels of CO_2 intensity, as shown in Equation 5-10. Also, all entries in Column 10 should take non-negative values, as indicated in Equation 5-11. The entry of Column 10 which equates to zero indicates the pinch point.

$$\varepsilon_k = \varepsilon_{k-1} + (\delta_{k-1} \times \Delta C_{k-1}) \quad \forall k \qquad \text{Equation 5-10}$$

$$\varepsilon_k \geq 0 \qquad \forall k \qquad \text{Equation 5-11}$$

In the following section, Example 1 is used to depict the algebraic targeting technique for the deployment of EP-NETs without CCS.

5.1.1 Example 1

Example 1 adopts the data presented in Table 3-1, where a mix of renewable energy sources and fossil-based sources satisfy the power demand of 60 TWh y^{-1}, with total CO_2 emissions (Δm_T) of 31.2 Mt y^{-1} (Tan et al., 2009b). For a CO_2 emissions limit (Δm_L) of 15 Mt y^{-1}, removal of 16.2 Mt CO_2 y^{-1} (Δm_R = 31.2 – 15 Mt y^{-1}) is necessary. Initially, CO_2 intensity levels of all energy sources and demands are arranged in ascending order in Column 1 (Step (i)). In this work, BECCS with a CO_2 intensity of -0.6 Mt CO_2 $(TWh)^{-1}$ is the chosen EP-NETs (McGlashan et al., 2012) and placed at the first level of Column 1. The differences between adjacent intensity levels are calculated, while energy demands and sources are located at their respective intensity levels, in Columns 2 – 4, respectively (Steps (ii) and (iii)).

Equation 5-2 (Step (iv)) is first applied to determine the theoretical energy reduction from CO_2-intensive coal sector (M_6) in Column 5, equivalent to 10.1 TWh y^{-1} (= (31.2 – 15)/(1 + 0.6) TWh y^{-1}). Since the value of M_6 is lesser than the available energy provided by the coal sector which is 16.8 TWh y^{-1} (see Column 4), no calculation is performed for ΔM_6 in Column 6. In other words, no energy reduction is necessary for the oil and natural gas sectors. Hence, N_6 (Equation 5-5, Step (vi)) in Column 7 possesses the same value as M_6, i.e., 10.1 TWh y^{-1}. Equation 5-6 (Step (vii)) is then used to determine the net energy available from the sector with the highest CO_2 intensity i.e., coal ($F_{E,6}$) in Column 8, equivalent to 6.7 TWh y^{-1} (= 16.8 – 10.1 TWh y^{-1}). The minimum EP-NETs requirement ($F_{EP\text{-}NET}$) is determined as 10.1 TWh y^{-1} at the top row of Column 8 from Equation 5-7 (Step (viii)). Equation 5-8 (Step (ix)) is then used to calculate net energy at level *k* in Column 9. Lastly, Equation 5-9 (Step (x)) and Equation 5-10 (Step (xi)) are used to determine the power and emission cascades in Columns 10 and 11. The power cascade in Column 10 represents the cumulative energy available at level *k* towards satisfying power demand. The final entry of this column should equal zero, indicating that power demand is fully satisfied. A negative final value indicates that energy sources are insufficient for the demand, while a positive value constitutes excess energy. The emission cascade in Column 11 depicts the cumulative CO_2 emissions load at level *k*. The CO_2 emission is cascaded from level *k* of lower CO_2 intensity to that of higher CO_2 intensity. Like the power cascade, the value at the final row of Column 11 should be zero to satisfy the emissions constraint. Table 5-2 presents the *energy cascade table* for Example 1 involving the deployment of EP-NETs without CCS.

Table 5-2: Energy cascade table for targeting EP-NETs deployment for Example 1

C_k (Mt/TWh)	ΔC_k (Mt/TWh)	$(\sum_j F_{D,j})_k$ (TWh/y)	$(\sum_i F_{S,i})_k$ (TWh/y)	M_k (TWh/y)	ΔM_k (TWh/y)	N_k (TWh/y)	$F_{E,k}$ (TWh/y)	$F_{N,k}$ (TWh/y)	δ_k (TWh/y)	ε_k (Mt/y)
									0	
-0.60							10.1	10.1		0
	0.60						(F_{EP-NET})		10.1	
0			18.0					18.0		6.1
	0.25							(F_{REN})	28.1	
0.25		60						-60.0		13.1
	0.25								-31.9	
0.50			19.2	0	0	0	19.2	19.2		5.1
	0.30							(F_{NG})	-12.7	
0.80			6.0	0	0	0	6.0	6.0		1.3
	0.20							(F_{OIL})	-6.7	
1.00			16.8	10.1	0	10.1	6.7	6.7		0
	9.00					(N_6)	($F_{E,6}$)	(F_{CL})	0	(Pinch)
10.00										0

Table 5-2 shows that the last entries of the power (Column 10) and the emission cascades (Column 11) are both equal to zero. This means that both demand and CO_2 emissions constraints are met. Column 8 of Table 5-2 shows that the energy requirement of the coal sector is reduced by 10.1 TWh y^{-1} to 6.7 TWh y^{-1}. This reduction corresponds to the amount of EP-NETs (F_{EP-NET}) being deployed, i.e., 10.1 TWh y^{-1} (= 16.8 – 6.7 TWh y^{-1}). Table 5-2 also shows the exact amount of fossil that can still be utilised in the planning, i.e., 19.2 TWh y^{-1} of natural gas (F_{NG}), 6.0 TWh y^{-1} of oil (F_{OIL}), and 6.7 TWh y^{-1} of coal (F_{CL}). These results are used to generate the EPPD for EP-NETs deployment (see Figure 3-2b). Note that these results are identical to those obtained from the graphical targeting technique in Chapter 3.1.1.

5.2 Targeting Technique for Deployment of CO_2 Capture and Storage and Renewable Energy Sources

The original graphical targeting technique of CCS deployment by Tan et al. (2009b) had several limitations such as being cumbersome and time-consuming, aside from lacking efficiency in handling large data sets. This work thus presents an alternative algebraic targeting technique as an extension to the previous work by Foo et al. (2008) to determine system targets (i.e., minimum extent of CCS retrofit and minimum compensatory power) for CCS retrofit planning. A renewable energy source is used as compensatory energy during CCS deployment. Table 5-3 shows the basic structure of an *energy cascade table* for the deployment of CCS and renewable energy sources. Note that Columns 5 – 8 are different from those in Table 5-1 (deployment of EP-NETs).

Table 5-3: Basic structure of energy cascade table with deployment of CCS and renewable energy sources

C_k	ΔC_k	$(\sum_j F_{D,j})_k$	$(\sum_i F_{S,i})_k$	$F_{TR,k}$	$\Delta F_{TR,k}$	$F_{AR,k}$	$F_{NetR,k}$	$F_{N,k}$	δ_k	ε_k
									$\delta_0 = 0$	
C_1							F_{COMP}	$F_{N,1}$		$\varepsilon_1 = 0$
	ΔC_1								δ_1	
C_2		$(\sum_j F_{D,j})_k$	$(\sum_i F_{S,i})_k$				$F_{NetR,k}$	$F_{N,2}$		ε_2
	ΔC_2								δ_2	
⋮		⋮	⋮	⋮	⋮	⋮	⋮	⋮		⋮
	⋮								⋮	
⋮		⋮	⋮	⋮	⋮	⋮	⋮	⋮		⋮
	⋮								⋮	
⋮		⋮	⋮	$F_{TR,n-2}$	$\Delta F_{TR,n-2}$	$F_{AR,n-2}$	$F_{NetR,n-2}$	⋮		⋮
	⋮								⋮	
C_{n-1}		$(\sum_j F_{D,j})_{n-1}$	$(\sum_i F_{S,i})_{n-1}$	$F_{TR,n-1}$	$\Delta F_{TR,n-1}$	$F_{AR,n-1}$	$F_{NetR,n-1}$	$F_{N,n-1}$		ε_{n-1}
	ΔC_{n-1}								δ_{n-1}	
C_n										ε_n

The targeting technique for the deployment of CCS and renewable energy during energy planning is as follows. Steps (i) to (iii) follow a similar targeting technique involving the deployment of EP-NETs (see Chapter 5.1). Note that in Step (i) the CO_2 intensities of CCS retrofitted sources at level *k* (Column 1) are to be included; they are calculated using Equation 5-12 (Ooi et al., 2013).

$$C_k = \frac{C_k \times (1 - \mathrm{RR})}{1 - \mathrm{X}} \qquad k \in \text{CCS retrofitted level(s) } k \qquad \text{Equation 5-12}$$

iv. In Column 5, the *theoretical extent of CCS retrofit* at level *k* ($F_{TR,k}$) is determined from Equation 5-13. This calculation step commences from level *k* with the highest CO_2 intensity (*k* = *n* - 1). The power sector with the highest CO_2 intensity contributes the most to total CO_2 emissions (Δm_T).

$$F_{\mathrm{TR},k} = \frac{\Delta m_{\mathrm{T}} - \Delta m_{\mathrm{L}}}{C_k \mathrm{RR} - C_{\mathrm{COMP}} \mathrm{X}} \qquad for\ k = n - 1 \qquad \text{Equation 5-13}$$

where C_{COMP} is the CO_2 intensity of the compensatory energy.

v. The theoretical extent of CCS retrofit at level *k* ($F_{TR,k}$) calculated in Step (iv) should not exceed its available energy $(\sum_i F_{S,i})_k$. If $F_{TR,k}$ is bigger than $(\sum_i F_{S,i})_k$, the difference ($\Delta F_{TR,k}$) in Column 6 is elevated to level *k* - 1 with lower CO_2 intensity (i.e., "cleaner" energy source), as depicted in Equation 5-14 and Equation 5-15. Based on Equation 5-14, if $F_{TR,k}$ is lesser than $(\sum_i F_{S,i})_k$, the calculation procedure is terminated. In other words, cleaner energy source(s) would not be retrofitted with CCS. Equation 5-15 determines the theoretical extent of CCS retrofit on level *k* - 1 with lower CO_2 intensity. CO_2 intensities of these levels are placed at the numerator (*k*) and denominator (*k - 1*) respectively.

$$\Delta F_{\mathrm{TR},k} = \begin{cases} 0, & F_{\mathrm{TR},k} \leq \left(\sum_i F_{S,i}\right)_k \\ F_{\mathrm{TR},k} - \left(\sum_i F_{S,i}\right)_k, & F_{\mathrm{TR},k} > \left(\sum_i F_{S,i}\right)_k \end{cases} \qquad \text{Equation 5-14}$$
$$for\ k = n - 1, n - 2, \ldots, 2$$

$$F_{\mathrm{TR},k-1} = \frac{\Delta F_{\mathrm{TR},k} \times (C_k \mathrm{RR} - C_{\mathrm{COMP}} \mathrm{X})}{C_{k-1} \mathrm{RR} - C_{\mathrm{COMP}} \mathrm{X}} \quad for\ k = n-1, n-2, \ldots, 3 \qquad \text{Equation 5-15}$$

vi. In Column 7, the *actual extent of CCS retrofit* at level *k* ($F_{\mathrm{AR},k}$) is determined using Equation 5-16 to ensure that the extent of CCS retrofit at level *k* is lesser than its available energy $(\sum_i F_{\mathrm{S},i})_k$.

$$F_{\mathrm{AR},k} = F_{\mathrm{TR},k} - \Delta F_{\mathrm{TR},k} \quad for\ i = n-1, n-2, \ldots, 2 \qquad \text{Equation 5-16}$$

vii. In Column 8, the net energy available at level *k* with and without CCS retrofit ($F_{\mathrm{NetR},k}$) is determined from Equation 5-17 and Equation 5-18 respectively.

$$F_{\mathrm{NetR},k} = F_{\mathrm{AR},k}\ (1 - X) \qquad k \in \text{Level } k \text{ with CCS retrofit} \qquad \text{Equation 5-17}$$

$$F_{\mathrm{NetR},k} = \left(\sum_i F_{S,i}\right)_k - F_{\mathrm{AR},k} \qquad k \in \text{Level } k \text{ without CCS retrofit} \qquad \text{Equation 5-18}$$

viii. The original amount of the energy sources is insufficient to meet the demand once the parasitic losses from the CCS retrofit are considered, so additional energy sources are supplied from renewable energy sources. This compensatory energy (F_{COMP}) must be minimised using Equation 5-19 and located at the respective CO_2 intensity level in Column 8.

$$F_{\mathrm{COMP}} = \sum_{k=1}^{n} F_{\mathrm{AR},k}\ \mathrm{X} \qquad \text{Equation 5-19}$$

ix. In Column 9, the net energy for each level k ($F_{N,k}$) is calculated from Equation 5-20.

$$F_{N,k} = F_{COMP} + F_{NetR,k} - \left(\sum_j F_{D,j}\right)_k \qquad \forall k \quad \text{Equation 5-20}$$

x. Power and emission cascades are formed in Columns 10 and 11 respectively, determined using Equation 5-9, Equation 5-10 and Equation 5-11, similar to that in Table 5-1.

In the following section, the algebraic targeting technique with the deployment of CCS and renewable energy sources is presented.

5.2.1 Example 1 (Revisited)

Example 1 from Tan et al. (2009b) is revisited. It is assumed that CCS is used to satisfy the CO_2 emissions limit (Δm_L) of 15 Mt y^{-1}. The *removal ratio* (RR) and *parasitic power loss* (X) of CCS are assumed as 0.85 and 0.15 respectively (Tan et al., 2009b). To compensate for power losses during CCS, renewable energy sources are used. Two scenarios are presented i.e., renewable energy sources with zero (Scenario 1) and non-zero CO_2 intensity (Scenario 2).

For Scenario 1, it is assumed that renewable energy sources with zero CO_2 intensity (C_{COMP} = 0) are used as compensatory energy. CO_2 intensity levels of all energy sources and demands are arranged in ascending order in Column 1 (Step (i)) of Table 5-4. Note that CO_2 intensities of coal, oil and natural gas after CCS retrofit are determined using Equation 5-12 as 0.176, 0.141 and 0.088 Mt TWh^{-1} respectively. Differences between adjacent intensity levels are calculated, while energy demands and sources are located at their respective intensity levels, in Columns 2 – 4, respectively.

Due to its high CO_2 intensity, the theoretical extent of CCS retrofit for the coal sector ($F_{TR,8}$) is determined based on Equation 5-13 (Step(iv)) in Column 5, equating to 19.06 TWh y^{-1} (= (31.2 – 15)/(1 × 0.85) TWh y^{-1}). Note that $F_{TR,8}$ is greater than the available energy from the coal sector, which is 16.8 TWh y^{-1} (see Column 4). The difference between $F_{TR,8}$ and available energy provided by the coal sector ($\Delta F_{TR,8}$) in Column 6 is elevated to the level with lower CO_2 intensity i.e., oil. Based on Equation 5-14 and Equation 5-15 (Step (v)), values of $\Delta F_{TR,8}$ (coal sector) and $F_{TR,7}$ (oil

sector) are determined as 2.26 TWh y^{-1} (= 19.06 – 16.8 TWh y^{-1}) and 2.82 TWh y^{-1} (= (2.26 × 1 × 0.85)/(0.8 × 0.85) TWh y^{-1}), respectively. Since the theoretical extent of CCS retrofit for the oil sector ($F_{TR,7}$) is lower than its available energy (6 TWh y^{-1}, Column 4), no further calculations are necessary.

Actual extent of CCS retrofit ($F_{AR,i}$) for oil and coal sectors are determined from Equation 5-16 (Step (vi)) in Column 7, equating to 2.82 TWh y^{-1} (= 2.82 – 0 TWh y^{-1}) and 16.8 TWh y^{-1} (= 19.06 – 2.26 TWh y^{-1}) respectively. Net energies provided by oil ($F_{Ret,\ OIL}$) and coal ($F_{Ret,\ CL}$) sectors after CCS retrofit are determined using Equation 5-17 (Step (vii)) in Column 8, equating to 2.4 TWh y^{-1} (= 2.82 × (1 – 0.15) TWh y^{-1}) and 14.28 TWh y^{-1} (= 16.8 × (1 – 0.15) TWh y^{-1}) respectively. Note that these values are located at their respective levels of 0.141 Mt TWh^{-1} (oil sector after CCS) and 0.176 Mt TWh^{-1} (coal sector after CCS). Net energies available from natural gas (F_{NG}), oil (F_{OIL}) and coal sectors (F_{CL}) without CCS retrofit are determined from Equation 5-18 (Step (vii)) in Column 8, equating to 19.2 TWh y^{-1} (= 19.2 – 0 TWh y^{-1}), 3.18 TWh y^{-1} (= 6 – 2.82 TWh y^{-1}) and 0 TWh y^{-1} (= 16.8 – 16.8 TWh y^{-1}) respectively. The entire sector of coal power generation is CCS retrofitted. Subsequently, Equation 5-19 (Step (viii)) is used to calculate the minimum deployment of renewable energy sources to be used as compensatory energy (F_{COMP}) for the system at the top row of Column 8 i.e., 2.94 TWh y^{-1} (= (2.82 + 16.8) × 0.15 TWh y^{-1}).

Equation 5-20 (Step (ix)) is used to calculate net energy at level *k* in Column 9. The values in Column 9 represent the energy contribution at level *k* post-CCS deployment. Lastly, Equation 5-9 (Step (x)) and Equation 5-10 (Step (x)) are used to determine the power and emission cascades in Columns 10 and 11 respectively. The results of Scenario 1 are shown in Table 5-4.

Table 5-4: Energy cascade table for Example 1 (Revisited), with renewable energy sources of C_{COMP} = 0 kg CO_2/kWh (Scenario 1)

C_k (Mt/TWh)	ΔC_k (Mt/TWh)	$(\sum_j F_{D,j})_k$ (TWh/y)	$(\sum_i F_{S,i})_k$ (TWh/y)	$F_{TR,k}$ (TWh/y)	$\Delta F_{TR,k}$ (TWh/y)	$F_{AR,k}$ (TWh/y)	$F_{NetR,k}$ (TWh/y)	$F_{N,k}$ (TWh/y)	δ_k (TWh/y)	ε_k (Mt/y)
									0	
0			18.00				2.94	20.94		0
	0.088						(F_{COMP})		20.94	
0.088							0	0		1.85
	0.053								20.94	
0.141							2.40	2.40		2.96
	0.035						($F_{Ret,\ OIL}$)		23.34	
0.176							14.28	14.28		3.78
	0.074						($F_{Ret,\ CL}$)		37.62	
0.250		60						-60.00		6.55
	0.250								-22.38	
0.500			19.20	0	0	0	19.20	19.20		0.95
	0.300						(F_{NG})		-3.18	
0.800			6.00	2.82	0	2.82	3.18	3.18		0
	0.200			($F_{TR,7}$)		($F_{AR,7}$)	(F_{OIL})		0	(Pinch)
1.000			16.80	19.06	2.26	16.80	0	0		0
	9.000			($F_{TR,8}$)	($\Delta F_{TR,8}$)	($F_{AR,8}$)	(F_{CL})		0	
10.000										

Based on Table 5-4, the pinch point occurs at the level corresponding to the oil sector (0.8 Mt CO_2/TWh). Note that the coal sector is located below the pinch point and is thus subjected to 100% CCS retrofit. A total of 2.94 TWh y^{-1} (F_{COMP}) of renewable energy sources are needed as compensatory energy. Results obtained (i.e., minimum compensatory energy and extent of CCS) match previous work (Ooi et al., 2013; Tan et al., 2009b).

In Scenario 2, a renewable energy source that is used as compensatory power for CCS is assumed to have a small CO_2 intensity i.e., C_{COMP} = 0.15 Mt/TWh (Sahu et al., 2014). Although renewable energy sources generation may be regarded as carbon-neutral, its associated processes (e.g.,

manufacture of solar panels, wind turbines, transportation of biomass) generate small but non-trivial life cycle GHG emissions which need to be addressed in the future extensions of this methodology. The targeting technique follows the same as the earlier case, with the energy cascade table for this scenario shown in Table 5-5.

Based on Table 5-5, the deployment of renewable energy sources (as compensatory energy) increased by 3.4% i.e., from 2.94 (Table 5-4) to 3.04 TWh y^{-1}. The increase is due to the rise in the extent of CCS retrofit on the oil sector i.e., from 2.82 to 3.50 TWh y^{-1}. Since a larger amount of renewable energy source is needed as compensatory energy (F_{COMP}), this amount is minimised. Like Table 5-4, the pinch point occurred at the level corresponding to the oil sector. The entire coal sector was again subjected to CCS retrofitting since it is located below the pinch point.

Table 5-5: Energy cascade table for Example 1 (Revisited), with renewable energy sources of C_{COMP} = 0.15 Mt CO2/TWh (Scenario 2)

C_k (Mt/TWh)	ΔC_k (Mt/TWh)	$(\sum_j F_{D,j})_k$ (TWh/y)	$(\sum_i F_{S,i})_k$ (TWh/y)	$F_{TR,k}$ (TWh/y)	$\Delta F_{TR,k}$ (TWh/y)	$F_{AR,k}$ (TWh/y)	$F_{NetR,k}$ (TWh/y)	$F_{N,k}$ (TWh/y)	δ_k (TWh/y)	ε_k (Mt/y)
									0	
0			18.00					18.00		0
	0.088								18.00	
0.088							0	0		1.59
	0.053								18.00	
0.141							2.97	2.97		2.54
	0.009						($F_{Ret,\ OIL}$)		20.97	
0.150							3.04	3.04		2.73
	0.026						(F_{COMP})		24.02	
0.176							14.28	14.28		3.36
	0.074						($F_{Ret,\ CL}$)		38.30	
0.250		60						-60.00		6.18
	0.250								-21.70	
0.500			19.20	0	0	0	19.20	19.20		0.75
	0.300						(F_{NG})		-2.50	
0.800			6.00	3.50	0	3.50	2.50	2.50		0
	0.200						(F_{OIL})		0	(Pinch)
1.000			16.80	19.58	2.78	16.80	0	0		0
	9.000						(F_{CL})		0	
10.000										0

The results obtained from the algebraic targeting technique may be used to construct the CCS Planning Diagram (Tan et al., 2009b), as shown in Figure 5-1 for a scenario with C_{COMP} of 0.15 Mt/TWh. Note that the graphical targeting technique of Tan et al. (2009b) cannot be used for this case. The difference between this algebraic targeting technique in comparison to that of Sahu *et al.* (2014), is that CO_2 emissions from a source of highest CO_2 intensity (i.e., "dirtiest" energy source) are fully removed, before a source of lower CO_2 intensity (i.e., "cleaner" energy source).

The main advantage of this technique is that compensatory energy can be kept to a minimum value. For instance, in the case of Table 5-5 (C_{COMP} = 0.15 Mt/TWh), minimum compensatory energy was determined as 3.04 GWh y^{-1}, as compared to the result of Sahu *et al.* (2014) i.e., 3.81 GWh y^{-1}. The discrepancy is due to the gas power sector being retrofitted with CCS before all CO_2 from the oil sector is removed. The total extent of CCS retrofit in the work of Sahu *et al.* (2014) was reported as 25.4 TWh y^{-1}, in comparison to 20.3 TWh y^{-1} as reported in this work. This result shows that CCS should be retrofitted for a source of the highest CO_2 intensity before it is attempted for that of lower CO_2 intensity.

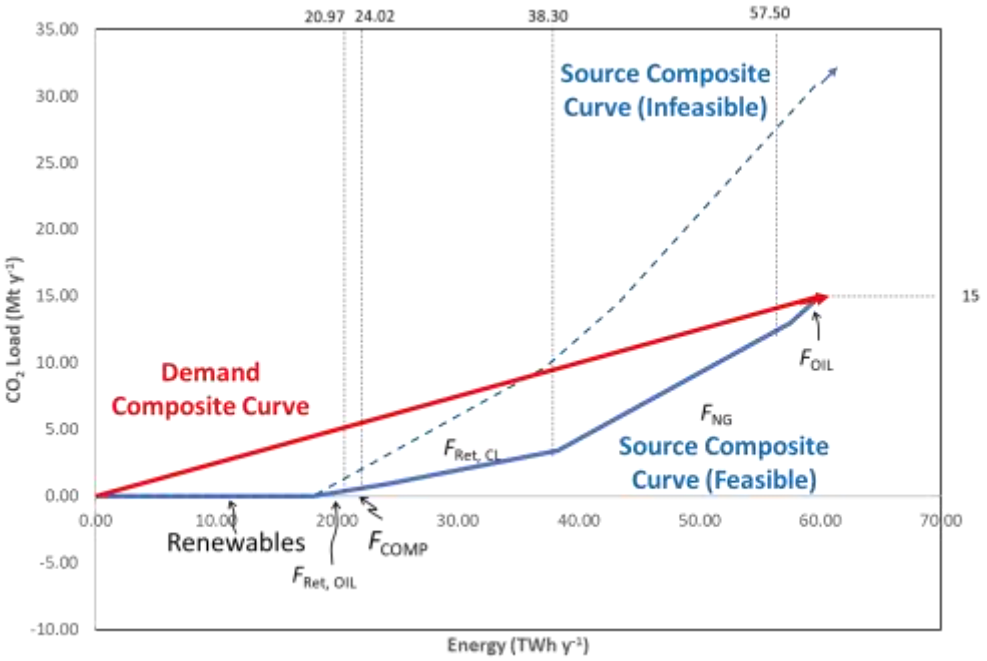


Figure 5-1: Energy planning pinch diagram for the scenario with C_{COMP} of 0.15 Mt/TWh

5.3 Targeting Technique of Energy-Producing Negative Emissions Technologies with the Deployment of CO_2 Capture and Storage

In this section, CCS is deployed during energy planning, while utilising EP-NETs as compensatory energy. In some cases, it is desired to minimise the extent of CCS retrofit, due to reasons such as insufficient storage space for captured CO_2, limited capital expenditure, etc. The targeting technique for this case follows the same as the deployment of CCS and renewable energy

sources, utilising the same energy cascade table as in Table 5-3. Example 1 is revisited to illustrate the algebraic targeting technique.

5.3.1 Example 1 (Revisited)

Example 1 (Tan et al., 2009b) is revisited to illustrate the deployment of CCS with compensatory electricity generation coming from EP-NETs. The removal ratio (*RR*) and the parasitic power losses (*X*) assumptions are the same as before. The sector with the highest CO_2 intensity is the coal sector. Theoretical extent of CCS retrofit for the coal sector ($F_{TR,9}$) is determined based on Equation 5-13 (Step(iv); see last entry of Column 5 in Table 5-6), equating to 17.23 TWh y^{-1} (= (31.2 – 15)/(0.85 – (-0.6 × 0.15)) TWh y^{-1}). Note that $F_{TR,9}$ is greater than available energy from the coal sector, which is 16.8 TWh y^{-1} (see last entry of Column 4). The difference between $F_{TR,9}$ and the available energy provided by the coal sector ($\Delta F_{TR,9}$) in Column 6 is elevated to the level with lower CO_2 intensity (i.e., oil). Based on Equation 5-14 and Equation 5-15 (Step (v)), the values of $\Delta F_{TR,9}$ (coal sector) and $F_{TR,8}$ (oil sector) are calculated as 0.43 TWh y^{-1} (= 17.23 – 16.8 TWh y^{-1}) and 0.53 TWh y^{-1} (= 0.43 × (0.85 – (-0.6 × 0.15)) ÷ ((0.85 × 0.8) – (-0.6 × 0.15)) TWh y^{-1}), respectively. Since the theoretical extent of CCS retrofit for the oil sector ($F_{TR,8}$) is lower than its available energy (6 TWh y^{-1}, second last entry in Column 4), no further calculations are necessary. Following this, the actual extent of CCS retrofit ($F_{AR,k}$) for the oil and coal power sectors are determined from Equation 5-16 (Step (vi)) in Column 7, equalling 0.53 TWh y^{-1} (= 0.53 – 0 TWh y^{-1}) and 16.8 TWh y^{-1} (= 17.23 – 0.43 TWh y^{-1}) respectively. Net energies available from oil ($F_{Ret,\,OIL}$) and coal ($F_{Ret,\,CL}$) sectors after CCS retrofit are calculated from Equation 5-17 (Step (vii)) in Column 8, equalling to 0.45 TWh y^{-1} (= 0.53 × (1 – 0.15) TWh y^{-1}) and 14.28 TWh y^{-1} (= 16.8 × (1 – 0.15) TWh y^{-1}) respectively. Net energies provided by the natural gas (F_{NG}), oil (F_{OIL}) and coal power sectors without CCS retrofit are evaluated from Equation 5-18 (Step (vii)) in Column 8, equating to 19.2 TWh y^{-1} (= 19.2 – 0 TWh y^{-1}), 5.47 TWh y^{-1} (= 6 – 0.53 TWh y^{-1}) and 0 TWh y^{-1} (= 16.8 – 16.8 TWh y^{-1}) respectively. Equation 5-19 (Step (viii)) is used to calculate the minimum EP-NETs requirement to be deployed as make-up energy (F_{COMP}) for the CCS system at the top row of Column 8, i.e., 2.60 TWh y^{-1} (= (0.54 + 16.8) × 0.15 TWh y^{-1}). Equation 5-20 (Step (ix)) is used to calculate the net energy at level *k* in Column 9. Lastly, Equation 5-9 and Equation 5-10 (Step (x))

are used to determine the power and emission cascades in Columns 10 and 11 respectively. Table 5-6 shows the results of the targeting technique.

Table 5-6: Energy cascade table for targeting EP-NETs and CCS deployment for Example 1 (Revisited)

C_k (Mt/TWh)	ΔC_k (Mt/TWh)	$(\sum_j F_{D,j})_k$ (TWh/y)	$(\sum_i F_{S,i})_k$ (TWh/y)	$F_{TR,k}$ (TWh/y)	$\Delta F_{TR,k}$ (TWh/y)	$F_{AR,k}$ (TWh/y)	$F_{NetR,k}$ (TWh/y)	$F_{N,k}$ (TWh/y)	δ_k (TWh/y)	ε_k (Mt/y)
									0	
-0.600							**2.60**	2.60		0
	0.600						(F_{COMP})		2.60	
0			18.0					18.00		1.56
	0.088								20.60	
0.088							0	0		3.38
	0.053								20.60	
0.141							0.45	0.45		4.47
	0.035						($F_{Ret,\ OIL}$)		21.05	
0.176							14.28	14.28		5.21
	0.074						($F_{Ret,\ CL}$)		35.33	
0.250		60						0		7.81
	0.250								-24.67	
0.500			19.2	0	0	0	19.2	19.20		1.64
	0.300						(F_{NG})		-5.47	
0.800			6.0	0.53	0	0.53	5.47	5.47		0
	0.200			($F_{TR,8}$)		($F_{AR,8}$)	(F_{OIL})		0	
1.000			16.8	17.23	0.43	16.80	0	0		0
	9.000			($F_{TR,9}$)	($\Delta F_{TR,9}$)	($F_{AR,9}$)			0	
10.000										0

Based on Table 5-6, power and emission constraints are satisfied by CCS retrofitting 0.53 and 16.8 TWh y^{-1} of the oil and coal sectors respectively. EP-NETs compensatory energy output of 2.6 TWh y^{-1} is needed. By comparing Table 5-2 and Table 5-6, EP-NETs requirement declined by approximately 75% when CCS is deployed. In other words, the deployment of CCS aided in CO_2

emissions removal. The targeted results are then used to plot the Energy Planning Pinch Diagram (see Figure 3-11). Once again, these results match those obtained via the graphical targeting technique (see Chapter 3.2.1). Note however that the latter involves an iterative graphical targeting technique. Apart from being cumbersome, that technique suffers from an inaccuracy problem. With the algebraic targeting technique, these limitations are now overcome.

5.4 Targeting Technique of Energy-Consuming Negative Emissions Technologies with and without the Deployment of CO_2 Capture and Storage

In previous sections, EP-NETs (e.g., BECCS) was deployed during energy planning, where energy was supplied during CO_2 emissions removal. By contrast, this section demonstrates the deployment of EC-NETs (e.g., DAC), where additional energy is to be required for CO_2 emissions removal. In most cases, the additional energy is sourced from renewable energy sources. In a practical situation, it may be necessary to consider different types of NETs during energy planning, as different regions/sectors may have different preferences on the NETs types in achieving their CO_2 emissions removal target. Table 5-7 shows the basic structure of an energy cascade table for the algebraic targeting technique with the deployment of EC-NEs without CCS.

Table 5-7: Basic structure of energy cascade table for deployment of EC-NETs without CCS

C_k	ΔC_k	$(\sum_j F_{D,j})_k$	$(\sum_i F_{S,i})_k$	$F_{E,k}$	$F_{N,k}$	δ_k	ε_k
						$\delta_0 = 0$	
C_1				F_{COMP}	$F_{N,1}$		$\varepsilon_1 = 0$
	ΔC_1					δ_1	
C_2		$(\sum_j F_{D,j})_k$	$(\sum_i F_{S,i})_k$	$F_{E,k}$	$F_{N,2}$		ε_2
	ΔC_2					δ_2	
⋮		$F_{EC\text{-}NET}$	⋮	⋮	⋮		⋮
	⋮					⋮	
⋮		⋮	⋮	⋮	⋮		⋮
	⋮					⋮	
⋮		⋮	⋮	$F_{E,n-2}$	⋮		⋮
	⋮					⋮	
C_{n-1}		$(\sum_j F_{D,j})_{n-1}$	$(\sum_i F_{S,i})_{n-1}$	$F_{E,n-1}$	$F_{N,n-1}$		ε_{n-1}
	ΔC_{n-1}					δ_{n-1}	
C_n							ε_n

The targeting technique for the deployment of EC-NETs without CCS is given as follows. Steps (i) to (iii) follow the same targeting technique involving the deployment of EP-NETs without CCS (see Table 5-1) and hence are omitted here for brevity. Note that for Step (iii), the minimum requirement of EC-NETs ($F_{EC\text{-}NET}$) is calculated from Equation 5-21. Note that EC-NETs has a negative value for its carbon intensity. Hence, it is treated as an energy demand (indicated by its negative intensity) but located at the positive CO_2 intensity level in the energy cascade table.

$$F_{\mathrm{EC-NET}} = \frac{\Delta m_{\mathrm{T}} - \Delta m_{\mathrm{L}}}{C_{\mathrm{EC-NET}} - C_{\mathrm{COMP}}} \qquad \text{Equation 5-21}$$

iv. Compensatory energy is used to fulfil the energy requirement of EC-NETs and is sourced from renewable energy sources. Its minimum requirement (F_{COMP}) is

equivalent to the minimum requirement of EC-NETs ($F_{EC\text{-}NET}$) determined using Equation 5-21. The F_{COMP} is placed at the top row of Column 5 of the energy cascade table (see Table 5-7).

v. In Column 6, the net energy at level k ($F_{N,k}$) is calculated using Equation 5-22.

$$F_{\mathrm{N},k} = \left(\sum_i F_{S,i}\right)_k - \left(\sum_j F_{D,j}\right)_k - F_{\mathrm{EC-NET}} + F_{\mathrm{COMP}} \quad \text{Equation 5-22}$$

vi. The power and emission cascades are formed in Columns 7 and 8 respectively, determined using Equation 5-9, Equation 5-10 and Equation 5-11, similar to that in Table 5-1.

In the following section, the algebraic targeting technique with the deployment of EC-NETs is presented, for scenarios with and without the use of CCS. For the former, the targeting procedure will follow the deployment of CCS and renewable energy (see Chapter 5.2 and Table 5-3). For this case, the minimum requirement of EC-NETs ($F_{EC\text{-}NET}$) is determined using a modified form of Equation 5-21, given as in Equation 5-23. The minimum requirement of compensatory energy (F_{COMP}) is calculated using Equation 5-24 (modified from Equation 5-19); this is meant to cater for the parasitic power losses during CCS, as well as the energy demand of EC-NETs.

$$F_{\mathrm{EC-NET}} = \frac{\mathrm{L_T} - \Delta m_{\mathrm{L}}}{C_{\mathrm{EC-NET}} - C_{\mathrm{COMP}}} \quad \text{Equation 5-23}$$

$$F_{\mathrm{COMP}} = \sum_{k=1}^{n} F_{\mathrm{AR},k}\,\mathrm{X} + F_{\mathrm{EC-NET}} \quad \text{Equation 5-24}$$

where L_T is the total CO_2 emissions after CCS deployment.

5.4.1 Example 1 (Revisited)

Example 1 (Tan et al., 2009b) is revisited to demonstrate the deployment of EC-NETs. Two scenarios are presented. In Scenario 1, EC-NETs is deployed without CCS. In this case, DAC with a CO_2 intensity of -0.4 Mt CO_2 TWh^{-1} is deployed (House et al., 2011). As discussed earlier, it is

treated as an energy demand at the intensity level of 0.4 Mt CO_2 TWh^{-1} (see Table 3-9). Using Equation 5-21, the minimum requirement of EC-NETs ($F_{EC\text{-}NET}$) is calculated as 40.5 TWh y^{-1} (= (31.2-15)/(0.4-0) TWh y^{-1}). Therefore, 40.5 TWh y^{-1} of renewable energy is used as compensatory energy (F_{COMP}) (Step (iv)). Equation 5-22 (Step (v)) is then used to calculate the net energy at level *k* in Column 6. Equation 5-9 and Equation 5-10 (Step(vi)) are used to determine the power and emission cascades in Columns 7 and 8 respectively, with results shown in Table 5-8.

Table 5-8 shows that both energy demand and CO_2 emissions constraints are met (last entries of power (Column 7) and the emission cascades (Column 8) are zero). The increase in NETs deployment is worth mentioning, as compared to EP-NETs. Due to the energy demand of EC-NETs, the minimum requirement of NETs increased by approximately 300%, i.e., from 10.1 TWh/y of EP-NETs (see Table 5-2) to 40.5 TWh/y of EC-NETs. Therefore, it is more worthwhile to deploy EP-NETs for CO_2 emissions removal in comparison to EC-NETs if it is available. Aside from producing energy during CO_2 emissions removal, deployment of EP-NETs does not require further utilisation of renewable energy sources. Note however that in cases where land area is insufficient for the growth of biomass crops, or fluctuations in environmental conditions e.g., the weather leading to an inconsistent supply of biomass crops, EC-NETs would be useful for CO_2 emissions removal. The results in Table 5-8 may be used to generate EPPD for EC-NETs deployment (see Figure 5-2).

Table 5-8: Energy cascade table for EC-NETs deployment without CCS (Scenario 1)

C_k (Mt/TWh)	ΔC_k (Mt/TWh)	$(\sum_j F_{D,j})_k$ (TWh/y)	$(\sum_i F_{S,i})_k$ (TWh/y)	$F_{E,k}$ (TWh/y)	$F_{N,k}$ (TWh/y)	δ_k (TWh/y)	ε_k (Mt/y)
						0	
0			18.0	40.5	58.5		0
	0.25			(F_{COMP})		58.5	
0.25		60			-60.0		14.6
	0.15					-1.5	
0.40		40.5			-40.5		14.4
	0.10	(F_{EC-NET})				-42.0	
0.50			19.2		19.2		10.2
	0.30					-22.8	
0.80			6.0		6.0		3.4
	0.20					-16.8	
1.00			16.8		16.8		0
	9.00						(Pinch)
10.00							0

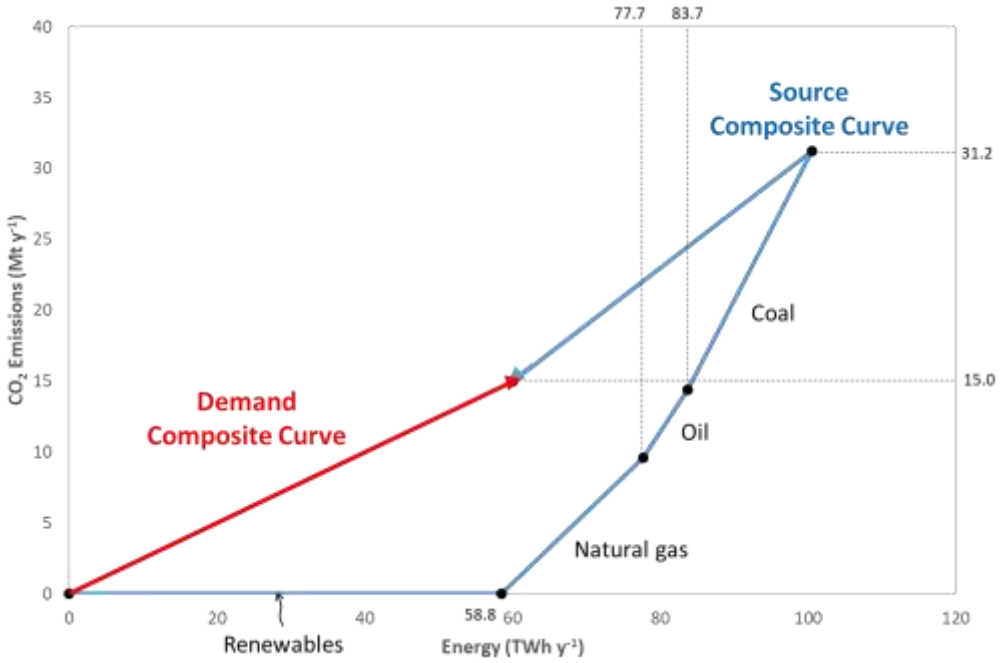


Figure 5-2: EPPD for EC-NETs Deployment without CCS (Scenario 1)

In Scenario 2, the deployment of CCS and EC-NETs is demonstrated. The renewable energy source is used as compensatory power for CCS and is assumed to have a CO_2 intensity of 0.15 Mt/TWh (C_{COMP}) (Sahu et al., 2014). It is also assumed that CCS retrofit will only take place if the entire fossil-based power sector will be fully retrofitted. This can be due to long term planning considerations and/or political reasons that are regional/country-specific. In Chapter 5.2, it had been demonstrated that a total of 16.8 TWh y^{-1} of the coal sector and 3.5 TWh y^{-1} of the oil sector are subjected to CCS retrofit (see Table 5-5). Since the oil sector is not fully retrofitted, it would be excluded from CCS retrofit in this scenario. Therefore, total CO_2 emissions post CCS deployment is calculated as 17.3 Mt y^{-1} i.e., contributed by the individual sectors of coal with CCS (14.28 × 0.176 = 2.5 Mt y^{-1}), natural gas (19.2 × 0.5 = 9.6 Mt y^{-1}), oil (6 × 0.8 = 4.8 Mt y^{-1}) and compensatory energy (16.8 × 0.15 × 0.15 = 0.4 Mt y^{-1}). Hence, to fulfil the CO_2 emissions limit (Δm_L) of 15 Mt y^{-1}, CO_2 emission of 2.3 Mt y^{-1} (= 17.3 - 15 Mt y^{-1}) is removed by EC-NETs. The minimum requirement of EC-NETs ($F_{EC\text{-}NET}$) is calculated from Equation 5-23 as 9.19 TWh y^{-1} (= (17.3 – 15) / (0.4 - 0.15) TWh y^{-1}), which corresponds to a reduction of 77% as compared to that in Scenario 1. The minimum requirement of compensatory energy (F_{COMP}) is calculated from Equation 5-24, equating to 11.71 TWh y^{-1} (= (16.8 × 0.15) + 9.19 TWh y^{-1}), or a reduction of 71%.

The reduction of EC-NETs and compensatory energy are the results of CCS retrofit. The results of Scenario 2 are shown in Table 5-9. The latter shows that the emissions limit of 15 Mt y^{-1} was satisfied by integrating 9.19 TWh y^{-1} of EC-NETs, which is depicted via EPPD in Figure 5-3.

Table 5-9: Energy cascade table for EC-NETs deployment with CCS (Scenario 2)

C_k (Mt/TWh)	ΔC_k (Mt/TWh)	$(\sum_j F_{D,j})_k$ (TWh/y)	$(\sum_i F_{S,i})_k$ (TWh/y)	$F_{TR,k}$ (TWh/y)	$\Delta F_{TR,k}$ (TWh/y)	$F_{AR,k}$ (TWh/y)	$F_{NetR,k}$ (TWh/y)	$F_{N,k}$ (TWh/y)	δ_k (TWh/y)	ε_k (Mt/y)
									0	
0			18.00					18.00		0
	0.088							(F_{REN})	18.00	
0.088							0	0		1.59
	0.053								18.00	
0.141							0	0		2.54
	0.009								18.00	
0.150							11.71	11.71		2.70
	0.026						(F_{COMP})		29.71	
0.176							14.28	14.28		3.49
	0.074						($F_{Ret,\,CL}$)		43.99	
0.250		60						-60.00		6.72
	0.150								-16.01	
0.400		9.19						-9.19		4.32
	0.100	($F_{EC\text{-}NET}$)							-25.20	
0.500			19.20	0	0	0	19.20	19.20		1.80
	0.300						(F_{NG})		-6.00	
0.800			6.00	3.50	0	0	6.00	6.00		0
	0.200						(F_{OIL})		0	(Pinch)
1.000			16.80	19.58	2.78	16.80	0	0		0
	9.000						(F_{CL})		0	
10.000										0

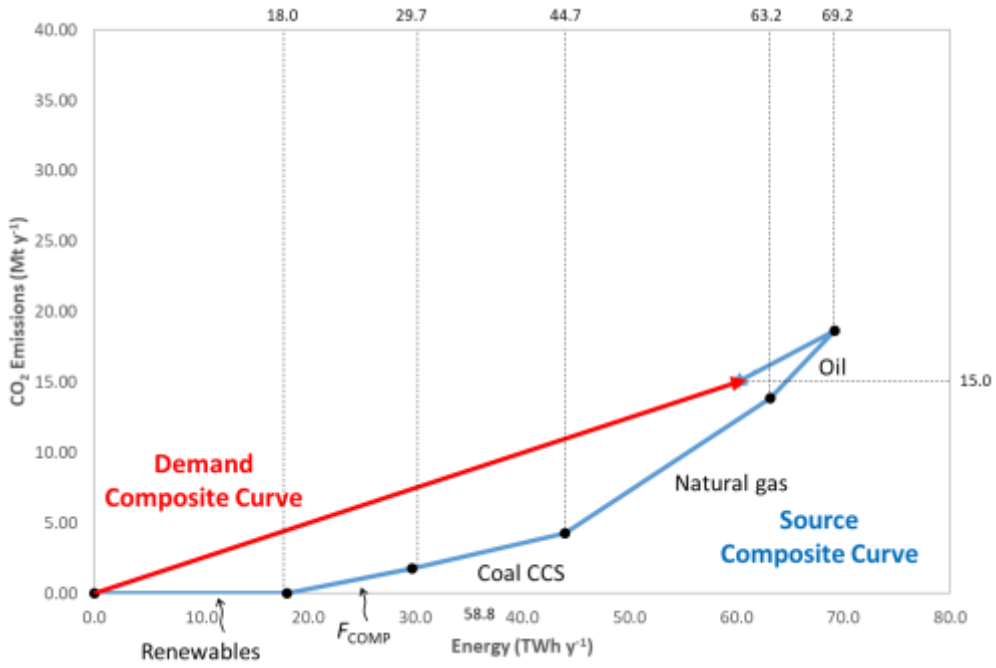


Figure 5-3: EPPD for CCS and EC-NETs Deployment (Scenario 2)

5.5 Chapter Summary

A novel algebraic targeting technique based on CEPA is developed and demonstrated with three CO_2 reduction strategies, i.e., deployment of renewable energy sources, CCS and NETs. This technique is the first Process Integration method that solves this specific class of CO_2 management problems. In the first example, the algebraic targeting technique is employed for an energy planning scenario with the deployment of EP-NETs and renewable energy sources. The remaining two examples incorporate CCS for its energy planning scenario, with the deployment of either renewable energy sources or EP-NETs as compensatory energy. The final example provides an alternative for CO_2 emissions removal by deploying EC-NETs while utilising renewable energy sources as compensatory energy. The algebraic targeting technique developed in this chapter eliminates the iterative procedure employed by the graphical targeting technique, ensuring a more efficient and less time-consuming procedure. Additionally, the algebraic targeting technique is capable of handling large data sets. Nevertheless, the graphical targeting technique can provide a bird's eye view of the entire energy planning problem. As demonstrated in this chapter, solutions obtained from the algebraic targeting technique are often best represented with an EPPD to retain the benefits of the graphical targeting technique.

Chapter 6: MULTIPERIOD ENERGY PLANNING MODEL FOR CO_2-INTENSIVE INDUSTRIES

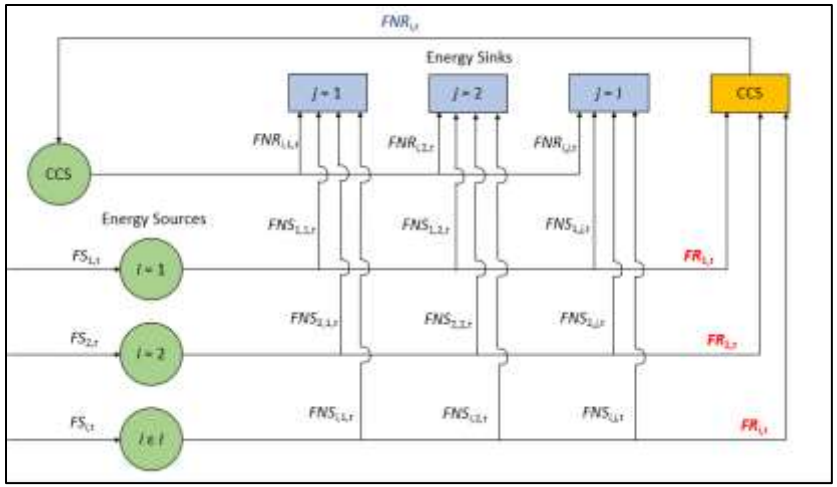
This chapter presents the results associated with the development of a multiperiod energy planning model for CO_2-intensive industries. Until this stage, all energy planning models only considered NETs deployment for the power generation sector. However, note that other industries i.e., cement, petrochemical, refineries etc. also emit large amounts of GHGs which must be mitigated. The lack of a suitable energy planning model for these CO_2-intensive industries is a clear research gap that must be addressed. Most of these industries rely heavily on fossil fuels. High CO_2 emissions from these industries make retrofitting the power generation sector alone insufficient for a region to achieve deep decarbonisation. This work seeks to address the existing research gap by developing a multiperiod energy planning model to determine the optimal deployment of renewable energy sources, CCS and NETs to various industries responsible for emitting large amounts of GHGs i.e., CO_2-intensive industries. A hybrid approach is employed in this work, making the combined use of ATM and *superstructural* models. Before the use of the hybrid approach in this work, the minimum deployment of energy sources to satisfy the demand and CO_2 constraints of all industries is unknown. A superstructure model alone may be used to guarantee the satisfaction of the demand and CO_2 emissions limits of the industries. However, the unknown deployment of energy sources for each industry would introduce non-linearity in the CO_2 intensity calculations. In other words, the flowrate of the energy sources and the CO_2 intensity of the energy sinks are both variables in a problem relying solely on a superstructural model. The presence of both variables would result in a non-linear problem. The hybrid approach in this work ensures linearity, and thus a globally optimum solution if it exists since the satisfaction of the CO_2 constraints takes place via the ATM. The superstructure model is purposed to solely handle the energy demand (no interference of CO_2 emissions) by matching the energy sources to the demand requirement of each industry. Solving the ATM and superstructural model simultaneously ensures that both demand and CO_2 emissions limits for all industries are satisfied in each period. This work also considers CO_2 load transfer between successive periods. At times, aggressive deployment of CCS technology may be preferred at later periods due to lower costs and matured technologies. In this case, the CO_2 emissions limit in earlier periods may be violated,

resulting in a CO_2 debt. Aggressive deployment of mitigation technologies at later periods may result in a CO_2 credit, thus serving as a payback for the CO_2 debts that occurred in earlier periods. The multiperiod energy planning model for CO_2-intensive industries is demonstrated with a case study involving two scenarios i.e., with and without CO_2 load transfer.

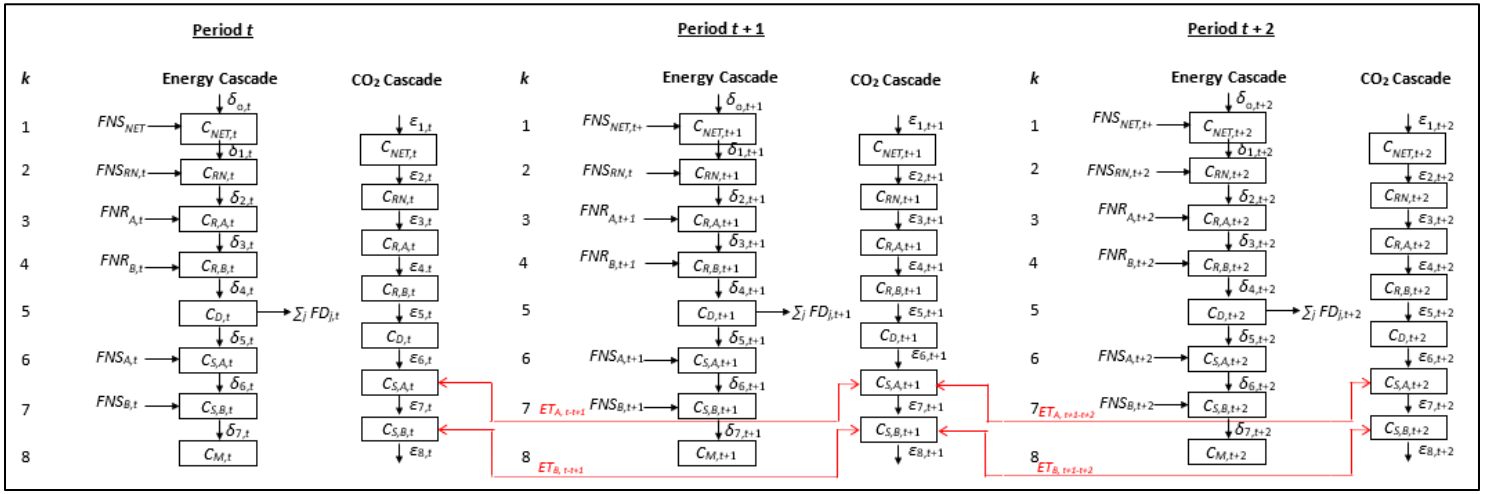
6.1 Methodology of Hybrid Approach in Multiperiod Energy Planning

Multiperiod energy planning models are necessary to handle temporal aspects of carbon management, such as demand variations and progressively stringent emission caps. Models can aid in energy forecast and planning for future investments. To address this need, Ooi et al. (2014) improvised the work by Ooi et al. (2013) to develop a multiperiod energy planning model. This work made use of the ATM to incorporate CCS and renewable energy sources to meet the decreasing CO_2 emissions limits. Later, Lee (2017) developed mixed-integer linear programming (MILP) model to solve a multiperiod energy planning model involving the use of CCS and renewable energy sources. The work by Lee (2017) was further extended to incorporate a multi-footprint energy planning scenario that involves the evaluation of the performances and costs of power generation units with and without the use of CCS (Lee and Lin, 2019).

In this chapter, a multiperiod energy planning model is developed to determine the optimal deployment of energy sources e.g., coal, fuel oil, renewable energy sources, EP-NETs etc. for CO_2-intensive industries e.g., petrochemical, cement, refinery etc. The high GHGs emissions from these industries necessitate the deployment of low carbon sources as part of a mitigation strategy. In this hybrid approach, the ATM and a superstructural model are solved simultaneously to determine the optimal deployment of energy sources. While the superstructural model ensures the demand satisfaction, the ATM satisfies the CO_2 emissions limit in a period to ensure linearity of the problem formulation. Figure 6-1 presents the basic ATM and superstructural model frameworks for multiperiod energy planning.



(a)



(b)

Figure 6-1: Basic frameworks for multiperiod energy planning: (a) Superstructural model and (b) ATM

Based on Figure 6-1a, the superstructural model determines the optimum allocation of energy source *i* in period *t* based on the demand requirement of energy sink *j*. Firstly, the deployment of energy source *i* in period *t*, $FS_{i,t}$ is constrained by its maximum availability, $A_{i,t}$, as demonstrated in Equation 6-1. The latter is dependent on geographical region, costs, weather fluctuations, environmental policies etc. For example, in certain locations with strict CO_2 emissions limits, coal supply may be limited. Elsewhere, weather fluctuations i.e., prolonger draughts may impact agriculture yield, and thus biomass availability.

$$FS_{i,t} \leq A_{i,t} \qquad \forall i \; \forall t \qquad \text{Equation 6-1}$$

Next, the extent of CCS retrofit on energy source *i* in period *t,* $FR_{i,t}$ is determined. The maximum energy that could be subjected to CCS retrofit shall not exceed $FS_{i,t}$, as shown in Equation 6-2. Note that the net energy of energy source *i* without CCS deployment, $FNS_{i,t}$ would be equivalent to $FS_{i,t}$ suppose that CCS deployment is absent.

$$FNS_{i,t} + FR_{i,t} = FS_{i,t} \qquad \forall i \; \forall t \qquad \text{Equation 6-2}$$

Meanwhile, the net energy of energy source *i* after CCS retrofit in period *t*, $FNR_{i,t}$ is lower than the energy subjected to CCS retrofit in period *t*, $FR_{i,t}$ due to the parasitic power losses during CCS deployment, as shown in Equation 6-3.

$$FNR_{i,t} = FR_{i,t} \times \left(1 - X_{i,t}\right) \qquad \forall i \; \forall t \qquad \text{Equation 6-3}$$

where $X_{i,t}$ is the parasitic power loss of energy source *i* in period *t* during CCS deployment.

Since CCS deployment is capital intensive, the extent of CCS retrofit on energy source *i* in period *t*, $FR_{i,t}$ should at least match its deployment in the previous period; demonstrated in Equation 6-4. It would be economically unviable if CCS is only deployed for a single period without continuous implementation. Also, the deployment of renewable energy sources in period *t* should at least match its deployment in the previous period; as shown in Equation 6-5. Similar reasoning as to CCS deployment is applied here.

$$FR_{i,t+1} \geq FR_{i,t} \qquad \forall i; \;\; t = 1,2, \dots, n-1 \qquad \text{Equation 6-4}$$

$$FS_{i,t+1} \geq FS_{i,t} \qquad \forall\, i \in Renewable\ energy;\ t = 1,2,\dots,n-1 \qquad \text{Equation 6-5}$$

Following this, the cumulative deployment of energy source *i* to all energy sinks should match the net energy of energy source *i* with (Equation 6-3) and without CCS retrofit (Equation 6-2), as shown in Equation 6-6 and Equation 6-7 respectively.

$$\sum_j FNR_{i,j,t} = FNR_{i,t} \qquad \forall\, i \in energy\ sources\ with\ CCS\ retrofit;\ \forall t \qquad \text{Equation 6-6}$$

$$\sum_j FNS_{i,j,t} = FNS_{i,t} \qquad \text{Equation 6-7}$$
$$\forall\, i \in energy\ sources\ without\ CCS\ retrofit;\ \forall t$$

where $FNR_{i,j,t}$ and $FNS_{i,j,t}$ is the deployment of energy source *i* with and without CCS retrofit for energy sink *j* in period *t* respectively.

Note that cumulative deployment of renewable energy sources (with and without CCS retrofit) for energy sink *j* in period *t* should at least match its deployment in the previous period; demonstrated in Equation 6-8.

$$FNS_{i,j,t+1} + \frac{FNR_{i,j,t+1}}{1-X} \geq FNS_{i,j,t} + \frac{FNR_{i,j,t}}{1-X} \qquad \text{Equation 6-8}$$
$$\forall\, i \in Renewable\ energy;\ t = 1,2,\dots,n-1$$

Meanwhile, the cumulative deployment of all energy sources with and without CCS retrofit in period *t* should equate to the demand requirement of energy sink *j* in period *t*, $FD_{j,t}$, as demonstrated in Equation 6-9.

$$\sum_i \left(FNS_{i,j,t} + FNR_{i,j,t}\right) = FD_{j,t} \qquad \forall j\ \forall t \qquad \text{Equation 6-9}$$

Equation 6-10 and Equation 6-11 present the binary variables for the deployment of energy source *i* to energy sink *j*. The former involves energy source *i* without CCS deployment, while the latter is for energy source *i* with CCS retrofit. Note that the optimal deployment of energy source *i* for energy sink *j* in period *t* is constrained by the availability of energy source *i*.

$$FNS_{i,j,t} \leq A_{i,t} \times B_{i,j,t} \qquad \forall i\ \forall j\ \forall t \qquad \text{Equation 6-10}$$

$$FNR_{i,j,t} \leq A_{i,t} \times C_{i,j,t} \qquad \forall i \; \forall j \; \forall t \qquad \text{Equation 6-11}$$

where $C_{i,j,t}$ and $B_{i,j,t}$ and are binary variables for the deployment of energy source *i* with and without CCS retrofit to energy sink *j* in period *t* respectively.

Subsequently, the net energy available from energy source *i* with and without CCS retrofit is fed to the ATM. In other words, the net energy available from energy source *i* with and without CCS retrofit is placed at the respective CO_2 intensity level at the ATM. This forms the linkage between the superstructural model and the ATM to ensure that both models are solved simultaneously. As shown in Figure 6-1b, the ATM consists of two cascades i.e., energy and CO_2 cascades represent the flow of energy and CO_2 emissions for energy sources which are arranged according to an increasing order of CO_2 intensities respectively. The red arrows at the bottom of Figure 6-1b represent the CO_2 load transfer between successive periods. For example, the CO_2 load may be transferred from the first to the second period and vice versa. Note that the CO_2 load transfer is to take place for energy sources with high CO_2 intensities e.g., coal, fuel oil etc. This is done to mitigate the CO_2 emissions that originate from these heavy CO_2 emitting energy sources. The transfer of CO_2 load may allow a greater mitigation strategy to be employed in later periods to compensate for the less aggressive mitigation approach during earlier periods. Meanwhile, a large, arbitrary value of CO_2 emission intensity, C_M is added at the bottommost level to facilitate the ATM calculations.

Next, observe that levels *k* = 3 and *k* = 4 (see Figure 6-1b) consist of energy source *i* retrofitted with CCS. Due to the CO_2 load removal by CCS technology, the CO_2 intensity of CCS retrofitted energy source *i* is much lower; calculated from Equation 6-12.

$$C_{R,i,t} = \frac{C_{S,i,t} \times \left(1 - RR_{i,t}\right)}{\left(1 - X_{i,t}\right)} \qquad \forall i \; \forall t \qquad \text{Equation 6-12}$$

where $C_{R,i,t}$ and $C_{S,i,t}$ are the CO_2 intensities of energy source *i* with and without CCS retrofit respectively, while $RR_{i,t}$ represent the removal ratio of energy source *i* period *t* during CCS deployment.

The power cascade is then calculated via Equation 6-13. Note that the power cascade considers all energy sources and demands to ensure that the total demand of period *t* is satisfied. Also, the net energy flow in the power cascade may either take a positive or a negative value. The former represents surplus energy indicating a greater energy availability in comparison to the demand requirement for level *k*. Meanwhile, a negative energy flow implies an energy deficit where the demand requirement is greater than the energy available at level *k*. Note that the net energy flow of the power cascade in the final CO_2 intensity level i.e., *k* = *m* must be zero, as shown in Equation 6-14. A zero value implies that the energy demand of period *t* is satisfied.

$$\delta_{k,t} = \delta_{k-1,t} + \left(\sum_i \left(FNR_{i,t} + FNS_{i,t}\right) - \sum_j FD_{j,t}\right)_k \qquad \forall k\ \forall t \qquad \text{Equation 6-13}$$

$$\delta_{k,t} = 0 \qquad k = m; \forall t \qquad \text{Equation 6-14}$$

The emission cascade is calculated similarly to the power cascade except that the former considers the CO_2 load transfer between successive periods, as shown in Equation 6-15. Pre-matured technologies (CCS and NETs) may result in they are being unsuitable for deployment in earlier periods. Consequently, the CO_2 emissions limit may be violated. However, in later periods, those technologies are expected to undergo improvements in terms of efficiencies, costs, ease of deployment etc. Therefore, mitigation actions may be deployed aggressively in later periods. CO_2 load transfer would allow the CO_2 emissions to be significantly below the emissions limit (CO_2 credit) in later periods to compensate for the CO_2 debt in earlier periods. Due to the accumulative nature of the CO_2 emissions going down the CO_2 intensity levels, the emission cascade values may only be positive, as demonstrated in Equation 6-16. Negative values imply that the CO_2 emissions are elevated upwards, and thus infeasible. Also, note that the CO_2 emissions at the first cascade level (*k* = 1) would be zero due to the absence of any CO_2 emissions before the first CO_2 intensity level.

$$\varepsilon_{k,t} = \varepsilon_{k-1,\mathrm{t}} + \delta_{k-1,\mathrm{t}}\left(C_{k,t} - C_{k-1,\mathrm{t}}\right) + ET_{i,t-1\to t} - ET_{i,t\to t+1} \qquad \forall k\ \forall t \qquad \text{Equation 6-15}$$

$$\varepsilon_{k,t} \geq 0 \qquad \forall k\ \forall t \qquad \text{Equation 6-16}$$

where $ET_{i,t\to t+1}$ represents the CO_2 load transfer of energy source *i* between successive periods.

Based on Equation 6-17, the objective function of the hybrid approach is set to minimise the cumulative deployment of renewable energy sources for all periods, subject to the constraints in Equation 6-1 until Equation 6-16. The minimization of the deployment of renewable energy sources is consistent with the present efforts taken by countries for climate change mitigation. Although CCS technologies are effective in CO_2 emissions removal, there has not been an extensive deployment of CCS globally. Most CCS plants are still in the development phase as mentioned in Section 1.1. The linearity of the problem formulation enables the achievement of a global optimum solution if it exists.

$$Minimise \sum_{t} FS_{i,t} \qquad \forall\, i \in Renewable\ energy \qquad \text{Equation 6-17}$$

Since both continuous and binary variables exist in this work, the problem formulation is classified as a MILP model. Note that if a superstructural model is solely used in this work, the problem formulation would be classified as a mixed-integer non-linear programming (MINLP) model. The unknown flowrates of the energy sources would introduce non-linearity in the CO_2 intensity calculation (Equation 6-15) for each industry. An MINLP model may generate a locally optimum solution which is undesirable. This is now avoidable using the hybrid approach developed in this chapter. The problem formulation for the hybrid approach in this work is set up in Python, by using an open-source modelling language, Pyomo. Since the formulation is a MILP model, the optimisation problem is solved to global optimality by using the CPLEX solver from GAMS. By using an Intel Core i5 consisting of four cores, eight logical processors and a CPU of 1.6 GHz, the optimisation problem is solved in a negligible time of five seconds. The Python formulation for the multiperiod energy planning model is available on the Github page; accessible via https://github.com/mchlshort/DECO2.

The next section presents the application of the hybrid approach for a case study to demonstrate the multiperiod energy planning for CO_2-intensive industries. A case study consisting of two scenarios i.e., with and without CO_2 load transfer is evaluated based on the proposed methodology.

6.2 Case Study

Malaysia is a CO_2-intensive nation whose rapid development and industrialisation put it on the cusp of developed country status. As of year 2019, Malaysia generated close to 176 TWh of electricity (Energy Commission, 2021). Approximately half of the generated electricity was consumed in the industrial sector alone (Energy Commission, 2021). This shows that there is an urgent need to address the GHGs emissions that originate from the industrial sector. Despite the COVID-19 pandemic decreasing the total electricity demand in year 2020, it did little to dampen the electricity generation growth in year 2021. Electricity generation is projected to further rise with an annual growth of 0.9% and 1.7% for years 2021-2030 and years 2030-2039 respectively. Beyond year 2039, the electricity generation growth should revert to its usual 2% annual growth, as observed before the pandemic (Energy Commission, 2020). As part of its commitment to the Paris Agreement, Malaysia aims to become a carbon-neutral nation by year 2050 (Salim, 2021). Additionally, it was further mentioned that carbon pricing and a carbon tax would be implemented to aid in achieving the nation's net-zero emissions target (Salim, 2021). Therefore, this work provides important groundwork for CCEP to be conducted for CO_2-intensive industries in Malaysia.

This case study evaluates five industries, i.e., refinery, petrochemical, oleochemical, cement and power generation, for the mitigation of their GHGs emissions. As shown in Table 6-1, each industry is made up of several plants, each with a specified demand. For the power generation industry, its energy demand is currently contributed equally by coal and natural gas, with CO_2 intensities of 1 and 0.5 kt/GWh respectively. Meanwhile, for the remaining industries, their thermal energy demands are contributed equally by fuel oil and natural gas, where the former has a CO_2 intensity of 0.8 kt/GWh. The total CO_2 emissions from each industrial sector are calculated for period t and given in the last column of Table 6-1. It is assumed that energy planning is to be performed for three periods, with each spanning a time interval of five years.

Table 6-1: Industrial plant data for (a) Period 1, (b) Period 2 and (c) Period 3

(a)

Period *t*	Industry	Plants	Demand / GWh y^{-1}	Total Demand / GWh y^{-1}	CO_2 emissions / kt y^{-1}
Period 1	Power Generation	PG1	200	1,000	750.00
		PG2	300		
		PG3	275		
		PG4	225		
	Refinery	R1	150	600	390.00
		R2	130		
		R3	180		
		R4	140		
	Oleochemical	O1	40	200	130.00
		O2	45		
		O3	50		
		O4	35		
		O5	30		
	Petrochemical	PC1	40	250	162.50
		PC2	50		
		PC3	60		
		PC4	55		
		PC5	45		
	Cement	C1	30	90	58.50
		C2	40		
		C3	20		
	GRAND TOTAL			**2,140**	**1,491.00**
	CO_2 EMISSIONS LIMIT = 1,000 kt y^{-1}				

Table 6-1: Industrial plant data for (a) Period 1, (b) Period 2 and (c) Period 3 (continued)

(b)

Period *t*	Industry	Plants	Demand / GWh y^{-1}	Total Demand / GWh y^{-1}	CO_2 load / kt y^{-1}
Period 2	Power Generation	PG1	221	1,104	828.06
		PG2	331		
		PG3	304		
		PG4	248		
	Refinery	R1	166	662	430.59
		R2	144		
		R3	199		
		R4	155		
	Oleochemical	O1	44	221	143.53
		O2	50		
		O3	55		
		O4	39		
		O5	33		
	Petrochemical	P1	44	276	179.41
		P2	55		
		P3	66		
		P4	61		
		P5	50		
	Cement	C1	33	99	64.59
		C2	44		
		C3	22		
	GRAND TOTAL			**2,363**	**1,646.00**
	CO_2 EMISSIONS LIMIT = 850 kt y^{-1}				

Table 6-1: Industrial plant data for (a) Period 1, (b) Period 2 and (c) Period 3 (continued)

(c)

Period *t*	Industry	Plants	Demand / GWh y^{-1}	Total Demand / GWh y^{-1}	CO_2 load / kt y^{-1}
Period 3	Power Generation	PG1	244	1,219	914.25
		PG2	366		
		PG3	335		
		PG4	274		
	Refinery	R1	183	731	475.41
		R2	158		
		R3	219		
		R4	171		
	Oleochemical	O1	49	244	158.47
		O2	55		
		O3	61		
		O4	43		
		O5	37		
	Petrochemical	P1	49	305	198.09
		P2	61		
		P3	73		
		P4	67		
		P5	55		
	Cement	C1	37	110	71.31
		C2	49		
		C3	24		
	GRAND TOTAL			**2,609**	**1,818.00**
	CO_2 EMISSIONS LIMIT = 700 kt y^{-1}				

Based on the data in Table 6-1, multiperiod energy planning is performed for all power generation (PG), refineries (R), oleochemical (O), petrochemical (PC), and cement (C) plants. Between successive periods, the demand for each plant is assumed to have an annual growth of 2%, similar to the rising trend of Malaysia's electricity generation sector (Energy Commission, 2020). Note that the demand increase is accompanied by the rise of the total CO_2 emissions from 1,491 kt y^{-1} in Period 1 to 1,818 kt y^{-1} in Period 3. The CO_2 emission limits of Periods 1, 2 and 3 are assumed as 1,000, 850 and 700 kt y^{-1} respectively. In other words, CO_2 emissions reductions of 491, 796 and 1,118 kt y^{-1} are necessary for Periods 1, 2 and 3 respectively. The CO_2 emissions removal may take place with the deployment of CCS technology, renewable energy sources and NETs. The hybrid approach in this work would determine the optimum deployment of mitigation technologies in period *t*. Table 6-2 presents the availability of energy sources in period *t*.

Table 6-2: Availability and CO_2 intensities of energy sources

<table>
<tr><th rowspan="2">Energy Sources</th><th colspan="3">Availability / GWh y^{-1}</th><th rowspan="2">CO_2 Intensity / kt $(GWh)^{-1}$</th></tr>
<tr><th>Period 1</th><th>Period 2</th><th>Period 3</th></tr>
<tr><td>Biomass CCS</td><td colspan="3" rowspan="4">-</td><td>-0.600</td></tr>
<tr><td>Biogas CCS</td><td>-0.300</td></tr>
<tr><td>Natural Gas CCS</td><td>0.059</td></tr>
<tr><td>Fuel Oil CCS</td><td>0.094</td></tr>
<tr><td>Biomass</td><td>100</td><td>600</td><td>1,100</td><td>0.100</td></tr>
<tr><td>Coal CCS</td><td colspan="3">-</td><td>0.118</td></tr>
<tr><td>Biogas</td><td>100</td><td>600</td><td>1,100</td><td>0.200</td></tr>
<tr><td>Natural Gas</td><td colspan="3">5,000</td><td>0.500</td></tr>
<tr><td>Fuel Oil</td><td rowspan="2">500</td><td rowspan="2">250</td><td rowspan="2">0</td><td>0.800</td></tr>
<tr><td>Coal</td><td>1.000</td></tr>
</table>

Based on Table 6-2, despite an unlimited supply of natural gas, note that the availability of coal and fuel oil decreases from 500 GWh y^{-1} in Period 1 to eventually being phased out in Period 3. Since both coal and fuel oil have high CO_2 intensities i.e., 1 and 0.8 kt GWh^{-1} respectively, it is expected to be gradually phased out, aligning with goals set by the Malaysian government to be a carbon-neutral nation by year 2050 (Salim, 2021). Next, note that the availabilities of biomass and biogas are set to increase from 100 GWh y^{-1} in Period 1 to 1,100 GWh y^{-1} in Period 3. Once again, the rise in the availability of renewable energy sources aligns with Malaysia's power generation plan which targets 31% installed renewable energy capacity by year 2025 (MIDA, 2021). This target rises to 40% by year 2035 (MIDA, 2021). Between successive periods, it is assumed that a greater amount of agriculture waste would be available as biomass or biogas. Note that the CO_2 intensities of biomass and biogas are much lower at 0.1 and 0.2 kt GWh^{-1} respectively. Meanwhile, the CO_2 intensities of fossil-based energy sources retrofitted with CCS are calculated from Equation 6-12. It is assumed that the removal ratio and parasitic power losses of the CCS system are 0.90 and 0.15 respectively (Tan et al., 2009b). Once again, note that the lower CO_2 intensities of CCS retrofitted fossil-based energy sources are due to the CO_2 emissions removal during CCS deployment. Also, the CO_2 intensities of both biomass and biogas with CCS retrofit are negative, implying a net negative carbon cycle. In other words, upon CCS deployment, the CO_2 emissions from the combustion of biomass and biogas are lower than the CO_2 that was previously absorbed from the atmosphere. Both biomass and biogas with CCS retrofit are categorised as NETs, specifically EP-NETs due to their energy generation capacity and CO_2 emissions removal (negative CO_2 intensity). Despite an abundant supply of fossil-based energy sources, complete reliance on those energy sources would result in the total CO_2 emissions exceeding the CO_2 emissions limit. Therefore, the deployment of CCS technology, NETs and renewable energy sources is pivotal in meeting the CO_2 emissions limits. This case study considers two scenarios i.e., with and without CO_2 load transfer. The next section presents the scenario without CO_2 load transfer.

6.3 Scenario 1 (without CO_2 load transfer)

Scenario 1 is investigated based on the data presented in Table 6-1 and Table 6-2. The absence of CO_2 load transfer means that the CO_2 emissions limit for each period must be satisfied, i.e., no

CO_2 debt or credit for any period. Also, the lack of maturity for CCS technologies translates to the absence of CCS deployment in the first two periods (Fajardy, 2021). Realistically, CCS technology is far from fully developed and ready for commercial deployment. Therefore, CCS deployment for all energy sources is only permitted in the final period i.e., Period 3, as demonstrated in Equation 6-18.

$$FR_{i,t} = 0 \qquad \forall i\ ;\ \ t = 1\ and\ 2 \qquad \text{Equation 6-18}$$

Next, the usage of coal is only restricted to the power generation industry, as depicted in Equation 6-19 and Equation 6-20. The reasoning behind these constraints is the lack of utilisation of coal in other industries i.e., petrochemical, cement etc.

$$FNS_{i,j,t} = 0 \qquad i\ \in Coal\ without\ CCS\ retrofit;\ j \notin Power\ Generation;\ \forall t \qquad \text{Equation 6-19}$$

$$FNR_{i,j,t} = 0 \qquad i\ \in Coal\ with\ CCS\ retrofit;\ j \notin Power\ Generation;\ \forall t \qquad \text{Equation 6-20}$$

Similarly, the usage of biomass and biogas is restricted solely to the power generation and oleochemical industries due to the similar reason mentioned for the usage of coal; depicted by Equation 6-21 and Equation 6-22. Palm oil wastes are examples of biomass. The oleochemical industry may utilise these palm oil wastes as biomass to satisfy its energy demand. However, such a situation is not present in refineries, petrochemical, and cement industries.

$$FNS_{i,j,t} = 0 \qquad i\ \in Biomass\ and\ Biogas\ without\ CCS\ retrofit;\ j \notin Power\ Generation\ and\ Oleochemical;\ \forall t \qquad \text{Equation 6-21}$$

$$FNR_{i,j,t} = 0 \qquad i\ \in Biomass\ and\ Biogas\ with\ CCS\ retrofit;\ j \notin Power\ Generation\ and\ Oleochemical;\ \forall t \qquad \text{Equation 6-22}$$

Since Scenario 1 does not involve CO_2 load transfer between successive periods, both Equation 6-23 and Equation 6-24 which set the load transfer to zero must be satisfied.

$$ET_{i,t-1\rightarrow t} = 0 \qquad \forall t \qquad \text{Equation 6-23}$$

$$ET_{i,t\rightarrow t+1} = 0 \qquad \forall t \qquad \text{Equation 6-24}$$

Note that Equation 6-18 - Equation 6-22 are applied for the superstructural model as it is responsible for the demand satisfaction of the industries. Meanwhile, Equation 6-23 and Equation 6-24 are applied for ATM since it satisfies the CO_2 emissions constraints. The hybrid approach in this work minimises the objective function (total deployment of biomass and biogas) in Equation 6-17 subject to the constraints in Equation 6-1 - Equation 6-16 and Equation 6-18 - Equation 6-24. Figure 6-2 and Table 6-3 present the results for Scenario 1.

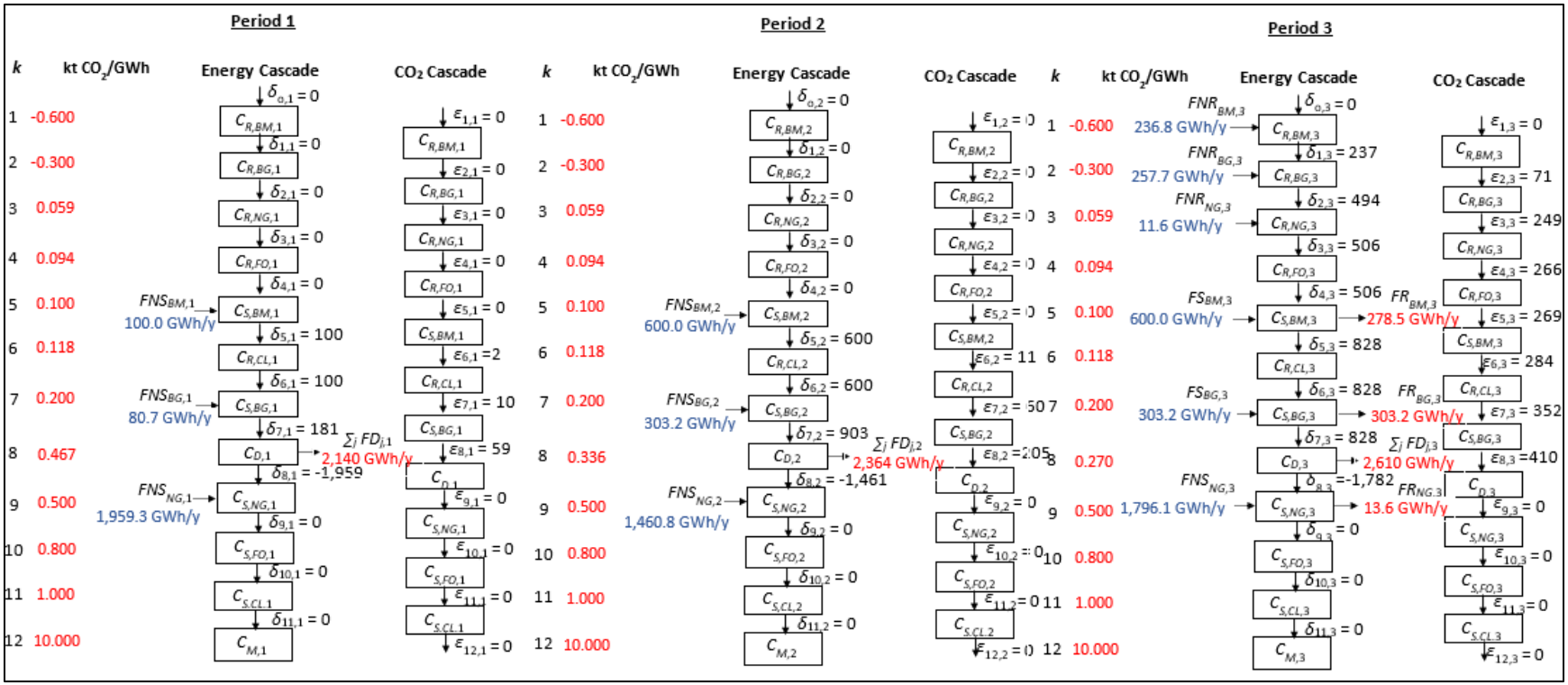


Figure 6-2: ATM results for Scenario 1

Table 6-3: Optimal allocation of energy sources for Scenario 1

Period	Energy		Energy Sinks / GWh y^{-1}																			
		PG 1	**PG 2**	**PG 3**	**PG 4**	**R1**	**R2**	**R3**	**R4**	**O1**	**O2**	**O3**	**O4**	**O5**	**PC1**	**PC2**	**PC3**	**PC4**	**PC5**	**C1**	**C2**	**C3**
1	**Demand**	**200**	**300**	**275**	**225**	**150**	**130**	**180**	**140**	**40**	**45**	**50**	**35**	**30**	**40**	**50**	**60**	**55**	**45**	**30**	**40**	**20**
	Biomass	70	-	-	-	-	-	-	-	-	-	-	-	30	-	-	-	-	-	-	-	-
	Biogas	-	-	-	81	-	-	-	-	-	-	-	-	-	-	-	-	-	-	-	-	-
	Natural Gas	130	300	275	144	150	130	180	140	40	45	50	35	-	40	50	60	55	45	30	40	20
2	**Demand**	**221**	**331**	**304**	**248**	**166**	**144**	**199**	**155**	**44**	**50**	**55**	**39**	**33**	**44**	**55**	**66**	**61**	**50**	**33**	**44**	**22**
	Biomass	202	178	-	-	-	-	-	-	44	50	55	39	33	-	-	-	-	-	-	-	-
	Biogas	-	55	-	248	-	-	-	-	-	-	-	-	-	-	-	-	-	-	-	-	-
	Natural Gas	20	98	304	0	166	144	199	155	0	0	0	0	0	44	55	66	61	50	33	44	22
3	**Demand**	**244**	**366**	**335**	**274**	**183**	**158**	**219**	**171**	**49**	**55**	**61**	**43**	**37**	**49**	**61**	**73**	**67**	**55**	**37**	**49**	**24**
	Biomass CCS	171	-	-	-	-	-	-	-	37	-	-	-	28	-	-	-	-	-	-	-	-
	Biogas CCS	-	47	-	211	-	-	-	-	-	-	-	-	-	-	-	-	-	-	-	-	-
	Natural Gas CCS	-	-	-	-	-	-	-	-	12	-	-	-	-	-	-	-	-	-	-	-	-
	Biomass	-	178	-	-	-	-	-	-	-	50	55	39	-	-	-	-	-	-	-	-	-
	Natural Gas	73	142	335	63	183	158	219	171	-	5	6	4	9	49	61	73	67	55	37	49	24

Based on Figure 6-2 and Table 6-3, the total deployment of renewable energy sources e.g., biomass and biogas are minimised at 1,987.1 GWh y^{-1} (see Figure 6-2) to satisfy the energy demand and CO_2 emission constraints for all periods. In Period 1, natural gas, biomass, and biogas are utilised to satisfy the energy demand of 2,140 GWh y^{-1} and the CO_2 emissions limit of 1,000 kt y^{-1}. Note that both biomass and biogas are considered low-carbon energy sources. Biomass is utilised completely subject to their availability of 100 GWh y^{-1} in Period 1 (see Table 6-2). Fuel oil and coal are not deployed in Period 1 due to their high CO_2 intensities. Moving on to Period 2, greater availability of biomass and biogas i.e., 600 GWh y^{-1} means that lesser fossil-based energy sources are now required to satisfy the energy demand of 2,364 GWh y^{-1}. The deployment of natural gas decreased by 499 GWh y^{-1}, from 1,959 GWh y^{-1} in Period 1 to 1,460 GWh y^{-1} in Period 2. While biomass is utilised completely, 303 GWh y^{-1} of biogas, comprising approximately 51% of its net availability is deployed. In Period 3, both biomass and biogas are deployed at the same amount as in Period 2, but this time all plants that use biogas are subjected to CCS retrofit for CO_2 emissions removal. Meanwhile, approximately 46% of biomass resources utilised by the plants (278.5 GWh y^{-1}) is subjected to CCS retrofit. The removal of CO_2 emissions from both biomass and biogas during CCS results in a negative CO_2 intensity. Doing this converts the biomass and biogas as EP-NETs, which allows Period 3 to meet the stringent CO_2 emissions limit of 700 kt y^{-1}. However, the parasitic power losses during CCS mean that more natural gas is deployed in Period 3. It is observed that the deployment of natural gas in Period 3 increased by 335.3 GWh y^{-1} to 1,796 GWh y^{-1}, where only 13.6 GWh y^{-1} is subjected to CCS retrofit. Overall, the target deployment of energy sources obtained from the hybrid approach satisfies the energy demand of each industrial plant, as well as the CO_2 emission limits for all periods. Figure 6-3 presents the energy mix and CO_2 emissions from the power generation industry (other sectors are omitted for brevity).

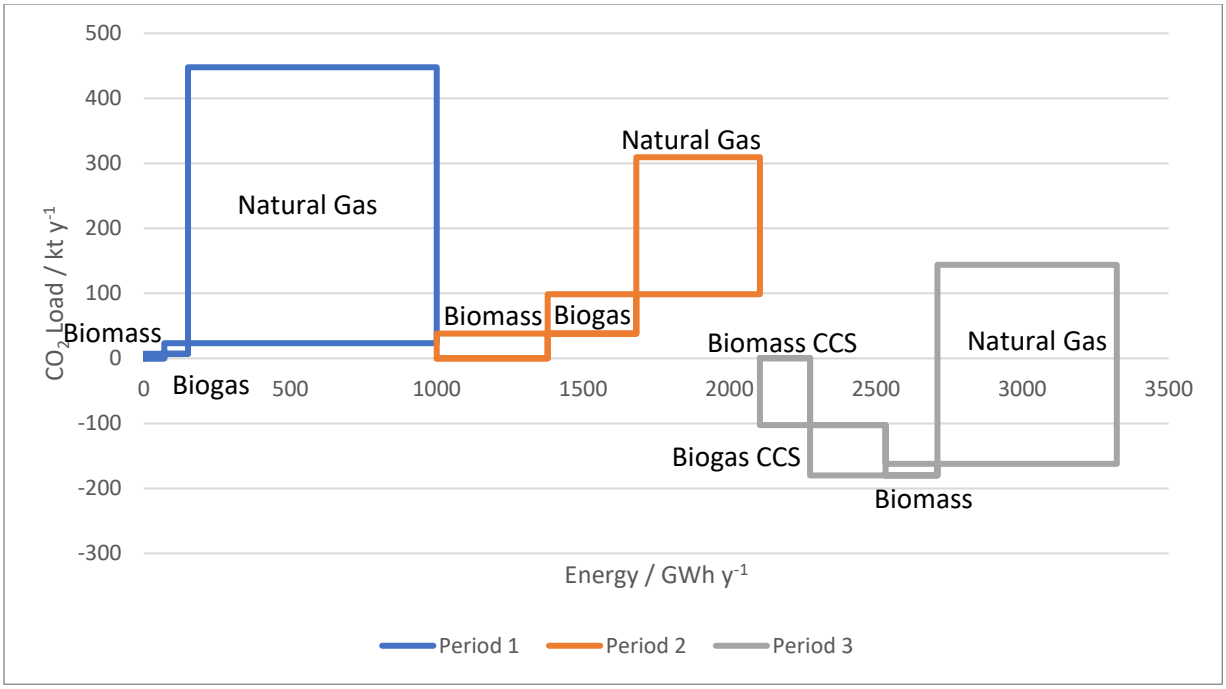


Figure 6-3: Energy mix and CO_2 load contribution from the power generation industry (PG1-PG4) for Scenario 1

Based on Figure 6-3, it may be observed that the total CO_2 emissions from the power generation industry declined gradually across the periods. Period 1 saw the greatest deployment of natural gas, thus contributing to its highest CO_2 emissions. Moving to Period 2, the greater deployment of 'cleaner' fuels e.g., biomass and biogas in Period 2 reduced the total CO_2 emissions in comparison to Period 1. In Period 3, CCS deployment further removed the CO_2 emissions, thus decreasing the total CO_2 emissions. The result demonstrates that the deployment of renewable energy sources, CCS and NETs are all required to meet the CO_2 emission limits.

6.4 Scenario 2 (With CO_2 Load Transfer)

In Scenario 2, CO_2 load transfer is permitted between successive periods. The CO_2 emissions limit for a period may be violated (CO_2 debt) provided that the CO_2 emissions limit at the end of the planning horizon (i.e., Period 3) is satisfied. Typically, the CO_2 emissions at the latest periods would be lower than the emissions limit (CO_2 credit) to compensate for the CO_2 debt at earlier periods. The objective function in Equation 6-17 is minimised subject to the constraints in Equation 6-1 - Equation 6-16 and Equation 6-18 - Equation 6-22. Figure 6-4 and Table 6-4 present the results for Scenario 2.

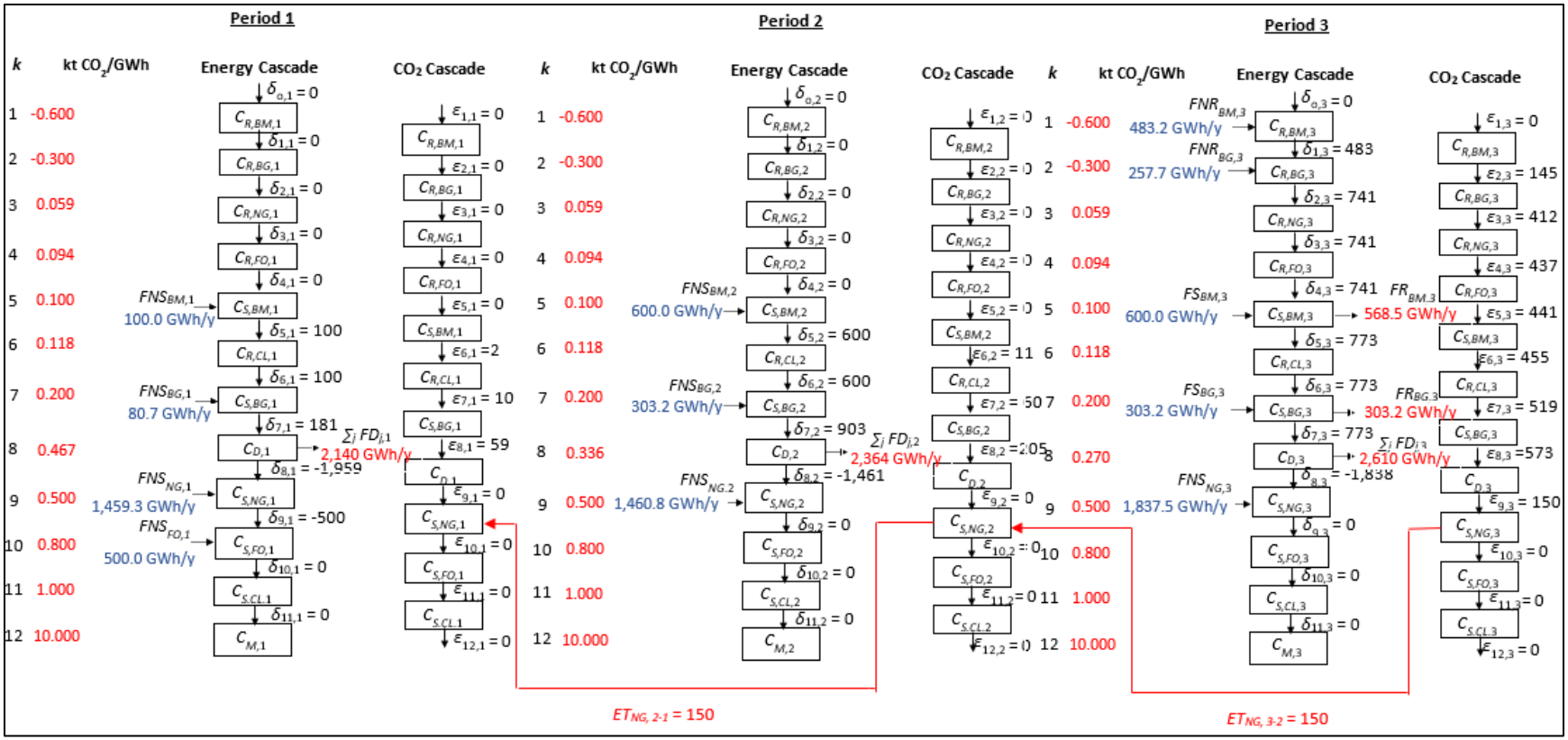


Figure 6-4: ATM results for Scenario 2

Table 6-4: Optimal allocation of energy sources for Scenario 2

Period	Energy		Energy Sinks / GWh y^{-1}																		
		PG1	PG2	PG3	PG4	R1	R2	R3	R4	O1	O2	O3	O4	O5	PC1	PC2	PC3	PC4	PC5	C1	C2	C3
1	**Demand**	**200**	**300**	**275**	**225**	**150**	**130**	**180**	**140**	**40**	**45**	**50**	**35**	**30**	**40**	**50**	**60**	**55**	**45**	**30**	**40**	**20**
	Biomass	70	-	-	-	-	-	-	-	-	-	-	-	30	-	-	-	-	-	-	-	-
	Biogas	-	-	81	-	-	-	-	-	-	-	-	-	-	-	-	-	-	-	-	-	-
	Natural Gas	130	300	49	-	150	130	180	140	40	-	-	-	-	40	50	60	55	45	30	40	20
	Fuel Oil	-	-	145	225	-	-	-	-	-	45	50	35	-	-	-	-	-	-	-	-	-
2	**Demand**	**221**	**331**	**304**	**248**	**166**	**144**	**199**	**155**	**44**	**50**	**55**	**39**	**33**	**44**	**55**	**66**	**61**	**50**	**33**	**44**	**22**
	Biomass	221	-	-	171	-	-	-	-	32	50	55	39	33	-	-	-	-	-	-	-	-
	Biogas	-	223	81	-	-	-	-	-	-	-	-	-	-	-	-	-	-	-	-	-	-
	Natural Gas	-	109	223	78	166	144	199	155	13	-	-	-	-	44	55	66	61	50	33	44	22
3	**Demand**	**244**	**366**	**335**	**274**	**183**	**158**	**219**	**171**	**49**	**55**	**61**	**43**	**37**	**49**	**61**	**73**	**67**	**55**	**37**	**49**	**24**
	Biomass CCS	188	-	-	145	-	-	-	-	-	43	47	33	28	-	-	-	-	-	-	-	-
	Biogas CCS	-	189	69	-	-	-	-	-	-	-	-	-	-	-	-	-	-	-	-	-	-
	Biomass	-	-	-	-	-	-	-	-	32	-	-	-	-	-	-	-	-	-	-	-	-
	Natural Gas	56	177	266	129	183	158	219	171	18	13	14	10	9	49	61	73	67	55	37	49	24

Based on Figure 6-4 and Table 6-4, the total deployment of renewable energy sources e.g., biomass and biogas are minimised at 1,987.1 GWh y^{-1} (see Figure 6-4), similar to Scenario 1. The results of Period 1 are like those in Scenario 1, with the exception that lesser natural gas is deployed. The demand deficit is thus compensated with the deployment of 500 GWh y^{-1} fuel oil. Note that all fuel oil is deployed in Period 1. As fuel oil has high CO_2 intensity, the CO_2 emissions limit in Period 1 is violated, with a CO_2 debt of 150 kt y^{-1}. As for Period 2, the results are identical to those in Scenario 1, where the deployment of biomass, biogas, and natural gas is observed. The CO_2 emissions limit in Period 2 is satisfied with no CO_2 debt or credit. Since the CO_2 emissions limit is violated in Period 1, greater aggressive mitigation strategies are expected in Period 3, to compensate for the CO_2 debt. Consequently, close to 95% of biomass sources deployed by plants are now retrofitted with CCS, resulting in a CO_2 credit of 150 kt y^{-1}. This CO_2 credit will compensate for the CO_2 debt in Period 1 (see Figure 6-5). Note that CCS deployment results in higher parasitic power loss in Period 3 versus Scenario 1. Therefore, the deployment of natural gas increased by 376.7 GWh y^{-1} to 1,837.5 GWh y^{-1}. Note that the deployment of natural gas in Period 3 of Scenario 2 is 41.5 GWh y^{-1} higher in comparison to Scenario 1.

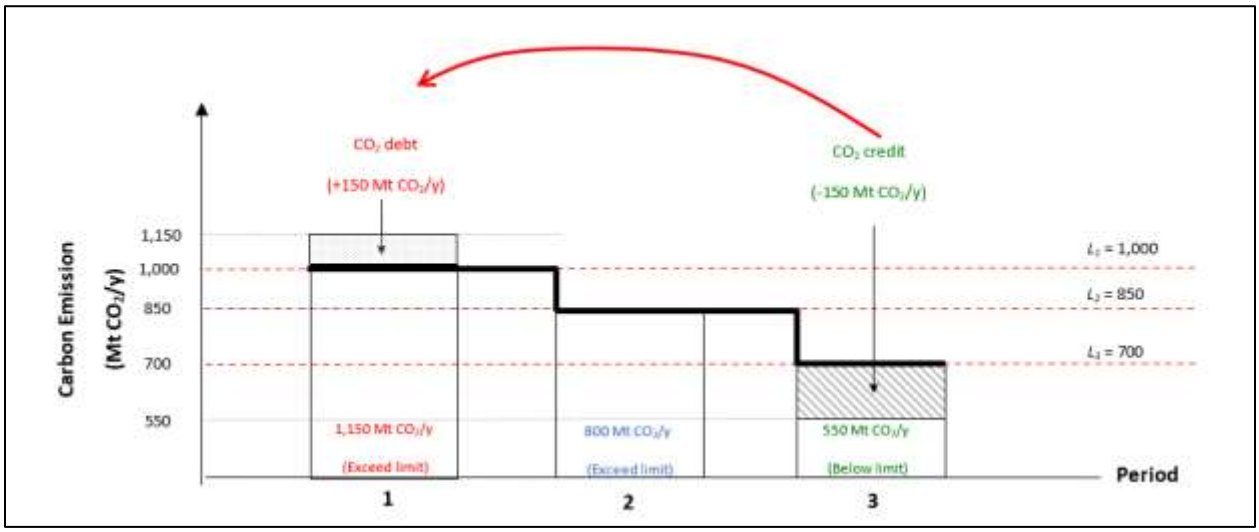


Figure 6-5: CO_2 load transfer for Scenario 2

Overall, the target deployment of energy sources obtained from the hybrid approach satisfies the energy demand of each industrial plant, as well as the CO_2 emission limits at the end of the

last period, as observed in Figure 6-5. Figure 6-6 presents the energy mix and CO_2 emissions contribution from the oleochemical industry (other sectors are omitted for brevity).

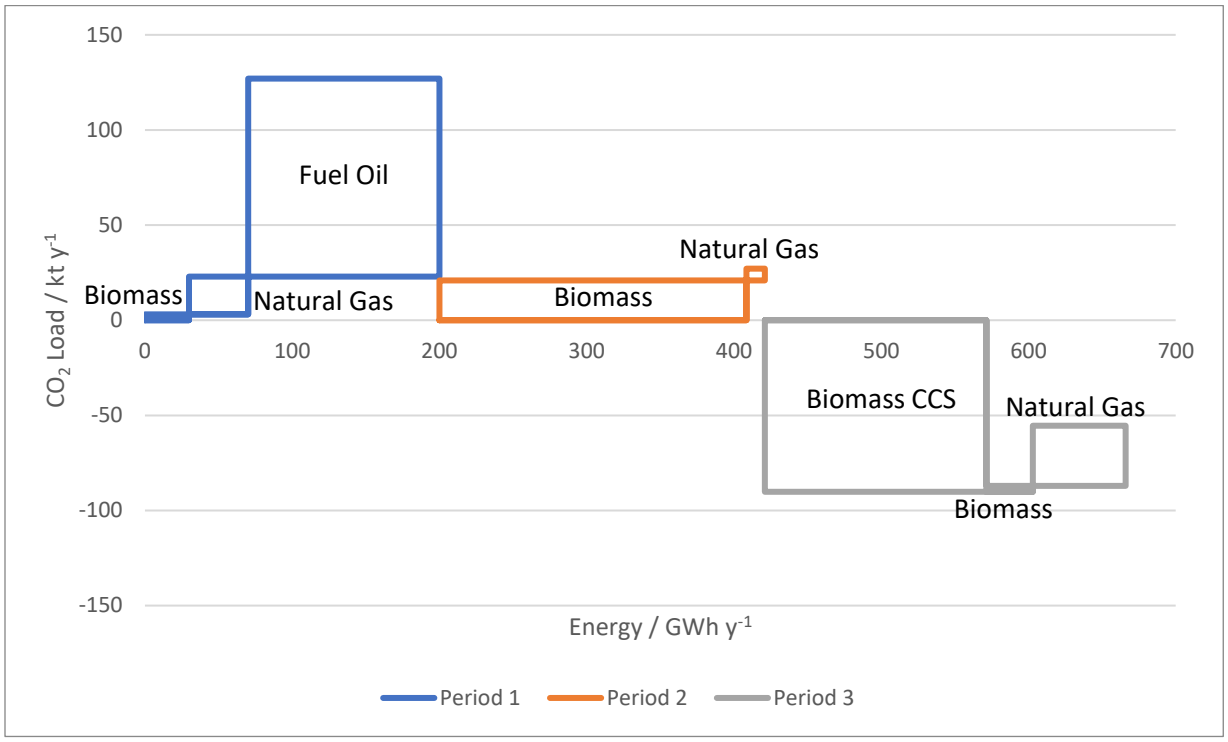


Figure 6-6: Energy mix and CO_2 load contribution from the oleochemical industry (O1 – O5) for Scenario 2

Based on Figure 6-6, it is evident that for the oleochemical industry, the CO_2 emissions contribution from fossil-based sources (i.e., natural gas and fuel oil) from Period 1 is significantly higher than that of renewable energy sources (i.e., biomass and biogas). Therefore, the total CO_2 emissions are highest in Period 1, as compared to other periods. Moving on to Period 2, the deployment of a 'cleaner' energy source i.e., biomass reduces the CO_2 emissions. In Period 3, the deployment of CCS on plants that utilise biomass sources results in a net negative CO_2 intensity, despite the deployment of natural gas. The results in Figure 6-6 demonstrate the importance of deploying renewable energy sources, CCS and NETs in mitigating CO_2 emissions and achieving net-zero emissions.

6.5 Chapter Summary

A multiperiod energy planning model was developed for the mitigation of emissions originating from CO_2-intensive industries. A hybrid model is proposed in this work, combining the use of ATM and superstructural models to determine the optimal deployment of energy sources to respective industrial plants. The satisfaction of the demand and CO_2 emissions constraints took place via the superstructural model and ATM respectively. Two scenarios of a case study, i.e., with and without CO_2 load transfer, were considered. The results of the two scenarios indicated the need for the deployment of low-carbon energy sources (biomass and biogas) for the mitigation of CO_2 emissions. In addition, once CCS technology matures, it would be a favoured source of decarbonisation technology. Its use would complement the existing mitigation strategy by renewable energy sources. Also, for the scenario involving CO_2 load transfer, aggressive mitigation strategies may be employed in later periods to offset the higher emissions in earlier periods.

Chapter 7: CONCLUSIONS AND FUTURE WORK

7.1 Conclusion

In this research, a modelling framework to aid in the planning of the deployment of NETs considering the effects on both system carbon and energy balance. A novel graphical targeting technique is initially developed for the deployment of EP-NETs during energy planning. This research was based on the CEPA technique which guarantees an optimal solution for high-level energy planning. The graphical targeting technique provides intuitive insights into the minimum EP-NETs requirement and the optimum CCS retrofit allocation for each energy source. Next, a new extension of CEPA methodology is developed for energy planning considering the deployment of EC-NETs systems. The minimum deployment of EC-NETs is determined with the aid of EPPD and pinch point; the latter is viewed as the bottleneck of the energy planning system. If a lower amount of EC-NETs is deployed (in comparison to the target obtained from CEPA), the CO_2 emissions limit of a region would be violated. The case study results demonstrate that despite the CO_2 emissions removal capacity of EC-NETs, additional compensatory energy in the form of either EP-NETs or renewable energy sources is required due to the energy demand of EC-NETs. Therefore, the minimum deployment of EC-NETs is much higher in comparison to cases that rely solely on EP-NETs for CO_2 emissions removal. The graphical targeting technique had limitations such as the inability to deal with large sets of data as well as its cumbersome and time-consuming technique. Therefore, a novel algebraic targeting technique based on CEPA is developed and demonstrated with three CO_2 reduction strategies i.e., deployment of renewable energy sources, CCS and NETs. This technique is the first process integration method that solves this specific class of CO_2 management problems. The results of the algebraic targeting technique are like those obtained from the graphical targeting technique. This is followed by the development of a multiperiod energy planning model which involved a hybrid approach consisting of the ATM and superstructural model. This work demonstrated the criticality of mitigating emissions in CO_2 intensive industries aside from the power generation sector. Once again, the importance of CCS and NETs deployment is highlighted in later periods to achieve the necessary climate change targets.

On a grand scale, the findings from this research highlight the importance of CCS and NETs deployment as a CO_2 management tool. Presently, NETs lack the technology maturity for a full-scale commercial deployment. In other words, limiting global warming to within 1.5 °C above pre-industrial levels would not succeed if all mitigation strategies were to rely solely on NETs. Therefore, this research highlights the contribution of CCS to aid in CDR. CCS deployment allows the deployment of other mitigation strategies i.e., renewable energy sources and NETs to be reduced. However, this research also proves that the sole deployment of CCS is not sufficient to meet climate change targets. As emphasised by IPCC (2022), limiting global warming to safe and manageable levels would require an aggressive deployment of renewable energy sources to ensure that the use of CCS and/or NETs would have a beneficial impact. Recent trends such as cheaper solar PV and wind energy have demonstrated that the right direction had been employed to mitigate climate change impacts. However, such actions must be compounded and accelerated in the upcoming decades to stand any realistic chance of managing climate change impacts. On that note, this research provides the tools for countries and/or industries to incorporate NETs during energy planning. The developed targeting techniques provide good insights into which CO_2 emissions removal is achieved by utilising EC-NETs, EP-NETs, renewable energy sources and/or CCS. The methodology developed here based on CEPA can be used to rationalise decisions on future decarbonisation initiatives. Aside from setting targets for NETs deployment, the pinch-based approach is particularly beneficial in setting an initial direction for decarbonisation initiatives, as observed in this research. Renewable energy sources, CCS and NETS may act as climate stabilisation wedges to contribute to the global decarbonisation efforts. Nevertheless, the present low technology maturity of NETs may force the incorporation of more than one type of NETs during energy planning scenarios; deployment of NETs will also need to be considered along with complementary carbon management strategies. This kind of micro-level planning may be done with ATM or a superstructural model, as demonstrated in Chapter 6.

7.2 Future Work

One shortcoming of this research is the lack of assessment of the cost constraint posed by the deployment of NETs as a tool for CDR. The deployment of EC-NETs would involve the use of either renewable energy sources or EP-NETs as compensatory energy. However, note that the

availabilities of renewable energy sources and EP-NETs are dependent on the geographical region, weather etc. Therefore, there are different costs associated with the deployment of compensatory energy which need to be investigated. On the other hand, recent land competition between agriculture and biomass crops had hampered the development of BECCS as a tool for CDR. Specifically, different types of biomasses would have varying CO_2 intensities and costs. Consequently, a more in-depth economic viability must be performed before assessing the suitability of deploying EP-NETs and EC-NETs during energy planning.

On the other hand, land and water footprints should be considered during the deployment of various NETs. As mentioned previously, various biomass crops would have different land and water footprints. The appropriate choice of biomass should be made depending on the type of biomass that minimises the overall footprint. Further research should pay attention to these various footprints, instead of solely minimising the carbon footprint. Last but not least, epistemic uncertainties in the cost and performance of future NETs should be addressed (Bandyopadhyay, 2020). Dynamic models to address progressive decarbonisation targets should also be developed.

Appendix A

The research work regarding the extended graphical targeting technique for the deployment of EP-NETs and/or CCS during CCEP (Chapter 3) was published in the Industrial and Engineering Chemistry Research journal. Meanwhile, the research work regarding the novel algebraic targeting technique for the deployment of renewable energy sources, CCS and NETs (Chapter 5) was published in a special conference issue with the ENERGY journal. Most recently, the graphical targeting technique for the deployment of EC-NETs during CCEP (Chapter 4) was published in the Renewable and Sustainable Energy Reviews journal. The details of the peer-reviewed journal publication are as follows:

1. Nair, P. N. S. B., Tan, R. R. and Foo, D. C. Y. (2020) 'Extended Graphical Approach for the Deployment of Negative Emission Technologies', *Industrial and Engineering Chemistry Research*, 59(42), pp. 18977–18990. doi: 10.1021/acs.iecr.0c03817. **(Chapter 3)**

2. Nair, P. N. S. B., Tan, R. R. and Foo, D. C. Y. (2021) 'A Generic Algebraic Targeting Approach for Integration of Renewable Energy Sources, CO2 Capture and Storage and Negative Emission Technologies in Carbon-Constrained Energy Planning', *Energy*, 235, p. 121280. doi: 10.1016/j.energy.2021.121280. **(Chapter 5)**

3. Nair, P. N. S. B., Tan, R. R. and Foo, D. C. Y. (2022) 'Extended graphical approach for the implementation of energy-consuming negative emission technologies', *Renewable and Sustainable Energy Reviews*, 158, p. 112082. doi: 10.1016/J.RSER.2022.112082. **(Chapter 4)**

4. Jia, X. *et al.* (2022) 'Regional carbon drawdown with enhanced weathering of non-hazardous industrial wastes', *Resources, Conservation and Recycling*, 176(July 2021), p. 105910. doi: 10.1016/j.resconrec.2021.105910.

Additionally, this research had been/will be presented at several conferences such as Process Systems Engineering (PSE) Asia 2020, the 14th Symposium of Process Systems Engineering (PSE Kyoto 2021), the 4th Sustainable Process Integration Laboratory (SPIL) Scientific Conference etc. Meanwhile, the details regarding the published conference papers are as follows:

1. Nair, P. N. S. B., Tan R. R. and Foo, D. C. Y., (2020). Negative Emissions Technologies for Carbon-constrained Energy Planning (CCEP), PSE Asia 2020, Taipei

2. Nair, P. N. S. B., Tan R. R. and Foo, D. C. Y., (2020). Targeting for the Deployment of Negative Emission Technologies for Multi-period Carbon-Constrained Energy Planning (CCEP). SPIL Conference

3. Nair, P. N. S. B., Foo, D. C. Y., Tan R. R. and Short, M., (2021). Targeting for the Deployment of Negative Emission Technologies in Multiperiod Energy Planning Problems. PRES'21 Conference

4. Nair, P. N. S. B., Foo, D. C. Y., Tan R. R., Short, M., Kikuchi, Y., Cossutta, M., Tan, J., (2021) Decision Support Software for Optimal Decarbonisation Policymaking for Carbon-Constrained Growth in Developing Countries – A Malaysian Case Study. AIChE Annual Meeting

5. Nair, P. N. S. B., Tan R. R. and Foo, D. C. Y., Short, M., (2021). Targeting for the Deployment of Negative Emission Technologies for Multiperiod Carbon-Constrained Energy Planning (CCEP). PSE 2021, Kyoto (to be presented)

Appendix B

The mathematical formulation for the graphical targeting technique in Chapter 3 is as follows:

Subscripts:

i index for energy source i

EP-NET Energy-producing NETs

EC-NET Energy-consuming NETs

L Limit

D Demand

Parameters:

$F_{S,i}$ Energy from source i

$F_{R,i}$ Minimum extent of CCS retrofit on source i

$F_{NS,i}$ Net energy from source i without CCS retrofit

$F_{NR,i}$ Net energy from source i with CCS retrofit

$C_{S,i}$ Carbon intensity of source i

$C_{R,i}$ Carbon intensity of source i with CCS retrofit

$C_{EP\text{-}NET}$ Carbon intensity of EP-NETs

$C_{EC\text{-}NET}$ Carbon intensity of EC-NETs

Δm_L CO_2 emission limit

F_D Total demand

Decision Variables

$F_{EP\text{-}NET}$ Minimum deployment of EP-NETs

$F_{EC\text{-}NET}$ Minimum deployment of EC-NETs

F_{NET} Total deployment of NETs

Objective Function

$$\text{Min } F_{\text{NET}} \qquad \text{Equation B-1}$$

Constraint 1 (Energy constraint)

$$F_{\text{EP-NET}} + \sum_i \left(F_{\text{S},i} + F_{\text{NR},i} + F_{\text{NS},i}\right) = F_{\text{D}} + F_{EC-NET} \qquad \text{Equation B-2}$$

Constraint 2 (CO_2 constraint)

$$F_{\text{EP-NET}} C_{\text{EP-NET}} + F_{\text{EC-NET}} C_{\text{EC-NET}} + \sum_i \left(F_{\text{S},i} C_{\text{S},i} + F_{\text{NR},i} C_{\text{R},i} + F_{\text{NS},i} C_{\text{S},i}\right) = \Delta m_{\text{L}} \qquad \text{Equation B-3}$$

Constraint 3 (NETs constraint)

$$F_{\text{EP-NET}} + F_{\text{EC-NET}} = F_{\text{NET}} \qquad \text{Equation B-4}$$

Constraint 4 (inequality constraint)

$$F_{\text{S},i}, F_{\text{R},i}, F_{\text{NS},i}, F_{\text{NR},i}, F_{\text{EP-NET},}, F_{\text{EC-NET},} \geq 0 \qquad \forall i \qquad \text{Equation B-5}$$

$$F_{\text{R},i} \leq F_{\text{S},i} \qquad \forall i \qquad \text{Equation B-6}$$

The above formulation is a linear program (LP) that can be solved to achieve a global solution. The LINGO formulation is presented as follows:

```
SETS:
```

```
SOURCES /1..4/: C, CR, FS, FR, FNR, FNS;

ENDSETS

DATA:

FS = 18   19.2 6    16.8;

C =  0    0.5  0.8  1;

CEPNET = -0.6;

CECNET = -0.4;

DEMAND = 60;

LIMIT = 15;

X = 0.15;

RR = 0.85;

ENDDATA

MIN = FNET;

@FOR(SOURCES(I): CR(I) = C(I) * (1 - RR) / (1 - X));

@FOR(SOURCES(I): FNS(I) = FS(I) - FR(I));

@FOR(SOURCES(I): FNR(I) = FR(I) * (1 - X));

FR(1) = 0;

@SUM(SOURCES(I): FNS(I) + FNR(I)) + FEPNET = DEMAND + FECNET;

@SUM(SOURCES(I): (FNS(I)*C(I)) + (FNR(I)*CR(I))) + (FEPNET*CEPNET)
+ (FECNET*CECNET)  = LIMIT;

@FOR(SOURCES(I): FR(I) <= F(I));

FEPNET + FECNET = FNET;

END
```

Appendix C

The mathematical formulation for the multiperiod energy planning model in Chapter 6 is as follows:

```
import pyomo.environ as pyo

from pyomo.opt import SolverFactory

import pandas as pd

import os

cwd = os.getcwd()

model = pyo.ConcreteModel()

file_name = r'Multiperiod_Case_1_Scenario_2.xlsx'


model.availability = pd.read_excel(file_name, sheet_name = 'SOURCES', index_col = 0, header = 2).to_dict()

model.CI = pd.read_excel(file_name, sheet_name = 'INTENSITY', index_col = 0, header = 2).to_dict()

model.D = pd.read_excel(file_name, sheet_name = 'DEMAND', index_col = 0, header = 2).to_dict()

model.SK = pd.read_excel(file_name, sheet_name = 'SINK', index_col = 0, header = 2).to_dict()

model.CO2 = pd.read_excel(file_name, sheet_name = 'CO2', index_col = 0, header = 2).to_dict()

model.CO2_CCS = pd.read_excel(file_name, sheet_name = 'CO2_CCS', index_col = 0, header = 2).to_dict()


numperiods = 4

periods = list(range(1,numperiods,1))

level = list(range(1,13,1))

X = 0.15
```

```
def hybrid_energy_planning(model,i,k):
    #model.K = model.CI.keys()
    model.S = model.availability.keys()
    model.T = model.SK.keys()

#LIST OF VARIABLES
    #This variable determines the deployment of energy source s in period i
    model.energy_source = pyo.Var(i, model.S, domain = pyo.NonNegativeReals)

    #This variable determines the deployment of energy source s without CCS retrofit in period i
    model.FS_source = pyo.Var(i, model.S, domain = pyo.NonNegativeReals)
    #model.energy_cascade.pprint()

    #This variable determines the extent of CCS retrofit on energy source s in period i
    model.FR_source = pyo.Var(i, model.S, domain = pyo.NonNegativeReals)
    #model.energy_cascade.pprint()

    #This variable determines the net energy available from energy source s after CCS deployment in period
i
    model.FNR_source = pyo.Var(i, model.S, domain = pyo.NonNegativeReals)
    #model.energy_cascade.pprint()

    #This variable determines the deployment of energy source s without CCS retrofit in industry t in period
i
```

```
model.FS_plant = pyo.Var(i, model.S, model.T, domain = pyo.NonNegativeReals)

#model.energy_cascade.pprint()


#This variable determines the deployment of energy source s with CCS retrofit in industry t in period i

model.FNR_plant = pyo.Var(i, model.S, model.T, domain = pyo.NonNegativeReals)

#model.energy_cascade.pprint()


#This variable determines the total deployment of energy source s on industry t in period i

model.energy_plant = pyo.Var(i, model.S, model.T, domain = pyo.NonNegativeReals)

#model.energy_cascade.pprint()


#This variable determines the minimum deployment of renewable energy sources in period i

model.energy_ren = pyo.Var(i, domain = pyo.NonNegativeReals)


#This variable determines the total deployment of renewable energy sources in all periods

model.energy_ren_total = pyo.Var(domain = pyo.NonNegativeReals)


#This variable determines the net energy at level k for period i

model.FNET = pyo.Var(i, k, domain = pyo.Reals)


#This variable determines energy cascade at level k for period i

model.energy_cascade = pyo.Var(i, k, domain = pyo.Reals)

#model.energy_cascade.pprint()
```

```
#This variable determines emissions cascade at level k for period i
model.emission_cascade = pyo.Var(i, k, domain = pyo.NonNegativeReals)
#model.emission_cascade.pprint()

#This variable determines the total CO2 load for period i
model.CO2_load = pyo.Var(i, domain = pyo.NonNegativeReals)

#This variable determines the CO2 load transfer between periods 1 and 2
model.NG_12 = pyo.Var(domain = pyo.NonNegativeReals)
model.NG_21 = pyo.Var(domain = pyo.NonNegativeReals)
model.FO_12 = pyo.Var(domain = pyo.NonNegativeReals)
model.FO_21 = pyo.Var(domain = pyo.NonNegativeReals)
model.CL_12 = pyo.Var(domain = pyo.NonNegativeReals)
model.CL_21 = pyo.Var(domain = pyo.NonNegativeReals)

#This variable determines the CO2 load transfer between periods 2 and 3
model.NG_23 = pyo.Var(domain = pyo.NonNegativeReals)
model.NG_32 = pyo.Var(domain = pyo.NonNegativeReals)
model.FO_23 = pyo.Var(domain = pyo.NonNegativeReals)
model.FO_32 = pyo.Var(domain = pyo.NonNegativeReals)
model.CL_23 = pyo.Var(domain = pyo.NonNegativeReals)
model.CL_32 = pyo.Var(domain = pyo.NonNegativeReals)
```

```
#OBJECTIVE FUNCTION
model.obj = pyo.Objective(expr = model.energy_ren_total, sense = pyo.minimize)

#CONSTRAINTS
#The deployment of energy source s in period i should not exceed its availability
def energy_source(model, i, s):
    return model.energy_source[i,s] <= model.availability[s][i]
model.Cons_1 = pyo.Constraint(i, model.S, rule = energy_source)

#The cumulative deployment of energy source s with and without CCS retrofit should equal to the deployment of energy source s in period i
def total_source(model, i, s):
    return model.FS_source[i,s] + model.FR_source[i,s] == model.energy_source[i,s]
model.Cons_2 = pyo.Constraint(i, model.S, rule = total_source)

#The net energy available from energy source s after CCS retrofit in period i is reduced due to the parisitic power losses
def CCS_net_energy(model, i, s):
    return model.FNR_source[i,s] == model.FR_source[i,s] * (1 - X)
model.Cons_3 = pyo.Constraint(i, model.S, rule = CCS_net_energy)

#No CCS deployment takes place in periods 1 and 2
def CCS_constraint_1(model, i, s):
    if i == 1 or i == 2:
```

```
        return model.FR_source[i,s] == 0
    else:
        return pyo.Constraint.Skip
model.Cons_4 = pyo.Constraint(i, model.S, rule = CCS_constraint_1)
```

#The deployment of energy source s without CCS retrofit in industry t should equal to its target deployment in period i

```
def plant_without_CCS(model, i, s):
    return model.FS_source[i,s] == sum(model.FS_plant[i,s,t] for t in model.T)
model.Cons_5 = pyo.Constraint(i, model.S, rule = plant_without_CCS)
```

#The deployment of energy source s with CCS retrofit in industry t should equal to its target deployment in period i

```
def plant_with_CCS(model, i, s):
    return model.FNR_source[i,s] == sum(model.FNR_plant[i,s,t] for t in model.T)
model.Cons_6 = pyo.Constraint(i, model.S, rule = plant_with_CCS)
```

#The cumulative deployment of all energy sources (with and without CCS) should match the demand of industry t in period i

```
def plant_demand(model, i, t):
    return model.SK[t][i] == sum(model.FNR_plant[i,s,t] + model.FS_plant[i,s,t] for s in model.S)
model.Cons_7 = pyo.Constraint(i, model.T, rule = plant_demand)
```

#This constraint determines the deployment of energy source s for industry t in period i

```
def plant_energy(model, i, s, t):
    return model.energy_plant[i,s,t] == (model.FNR_plant[i,s,t]/(1 - X)) + model.FS_plant[i,s,t]
model.Cons_8 = pyo.Constraint(i, model.S, model.T, rule = plant_energy)

#The deployment of biomass in period i should at least match its deployment in the previous period
def biomass_constraint(model, i):
    if i == numperiods - 1:
        return pyo.Constraint.Skip
    else:
        return model.energy_source[i+1,'Biomass'] >= model.energy_source[i,'Biomass']
model.Cons_9 = pyo.Constraint(i, rule = biomass_constraint)

#The deployment of biogas in period i should at least match its deployment in the previous period
def biogas_constraint(model, i):
    if i == numperiods - 1:
        return pyo.Constraint.Skip
    else:
        return model.energy_source[i+1,'Biogas'] >= model.energy_source[i,'Biogas']
model.Cons_10 = pyo.Constraint(i, rule = biogas_constraint)

#The deployment of fuel oil should at least match coal in period i
def energy_constraint_1(model,i):
    return model.energy_source[i,'Fuel_Oil'] >= model.energy_source[i,'Coal']
```

```
model.Cons_11 = pyo.Constraint(i, rule = energy_constraint_1)


#The deployment of natural gas should at least match fuel oil in period i
def energy_constraint_2(model,i):
    return model.energy_source[i,'NG'] >= model.energy_source[i,'Fuel_Oil']
model.Cons_12 = pyo.Constraint(i, rule = energy_constraint_2)


#The deployment of biomass for industry t in period i should at least match its deployment in the previous period
def biomass_plant(model, i, t):
    if i == numperiods - 1:
        return pyo.Constraint.Skip
    else:
        return model.energy_plant[i+1,'Biomass',t] >= model.energy_plant[i,'Biomass',t]
model.Cons_27 = pyo.Constraint(i, model.T, rule = biomass_plant)


#The deployment of biomass for industry t in period i should at least match its deployment in the previous period
def biogas_plant(model, i, t):
    if i == numperiods - 1:
        return pyo.Constraint.Skip
    else:
        return model.energy_plant[i+1,'Biogas',t] >= model.energy_plant[i,'Biogas',t]
model.Cons_28 = pyo.Constraint(i, model.T, rule = biogas_plant)
```

```
#This constraint ensures that biomass is not deployed for all refineries, petrochemical and cement industries (without CCS)
def fix_BM_wo_CCS(model, i, t):
    if t == 'R1' or t == 'R2' or t == 'R3' or t == 'R4':
        return model.FS_plant[i,'Biomass',t] == 0
    elif t == 'PC1' or t == 'PC2' or t == 'PC3' or t == 'PC4' or t == 'PC5':
        return model.FS_plant[i,'Biomass',t] == 0
    elif t == 'C1' or t == 'C2' or t == 'C3':
        return model.FS_plant[i,'Biomass',t] == 0
    else:
        return pyo.Constraint.Skip
model.Cons_13 = pyo.Constraint(i, model.T, rule = fix_BM_wo_CCS)

#This constraint ensures that biogas is not deployed for all refineries, petrochemical and cement industries(without CCS)
def fix_BG_wo_CCS(model, i, t):
    if t == 'R1' or t == 'R2' or t == 'R3' or t == 'R4':
        return model.FS_plant[i,'Biogas',t] == 0
    elif t == 'PC1' or t == 'PC2' or t == 'PC3' or t == 'PC4' or t == 'PC5':
        return model.FS_plant[i,'Biogas',t] == 0
    elif t == 'C1' or t == 'C2' or t == 'C3':
        return model.FS_plant[i,'Biogas',t] == 0
    else:
```

```
        return pyo.Constraint.Skip
    model.Cons_14 = pyo.Constraint(i, model.T, rule = fix_BG_wo_CCS)
```

#This constraint ensures that coal is not deployed for all refineries, petrochemical, oleochemical and cement industries (without CCS)

```
    def fix_CL_wo_CCS(model, i, t):
        if t == 'R1' or t == 'R2' or t == 'R3' or t == 'R4':
            return model.FS_plant[i,'Coal',t] == 0
        elif t == 'O1' or t == 'O2' or t == 'O3' or t == 'O4' or t == 'O5':
            return model.FS_plant[i,'Coal',t] == 0
        elif t == 'PC1' or t == 'PC2' or t == 'PC3' or t == 'PC4' or t == 'PC5':
            return model.FS_plant[i,'Coal',t] == 0
        elif t == 'C1' or t == 'C2' or t == 'C3':
            return model.FS_plant[i,'Coal',t] == 0
        else:
            return pyo.Constraint.Skip
    model.Cons_15 = pyo.Constraint(i, model.T, rule = fix_CL_wo_CCS)
```

#This constraint ensures that biomass is not deployed for all refineries, petrochemical and cement industries (with CCS)

```
    def fix_BM_w_CCS(model, i, t):
        if t == 'R1' or t == 'R2' or t == 'R3' or t == 'R4':
            return model.FNR_plant[i,'Biomass',t] == 0
        elif t == 'PC1' or t == 'PC2' or t == 'PC3' or t == 'PC4' or t == 'PC5':
```

```
        return model.FNR_plant[i,'Biomass',t] == 0
    elif t == 'C1' or t == 'C2' or t == 'C3':
        return model.FNR_plant[i,'Biomass',t] == 0
    else:
        return pyo.Constraint.Skip
model.Cons_16 = pyo.Constraint(i, model.T, rule = fix_BM_w_CCS)
```

#This constraint ensures that biogas is not deployed for all refineries, petrochemical and cement industries(with CCS)

```
def fix_BG_w_CCS(model, i, t):
    if t == 'R1' or t == 'R2' or t == 'R3' or t == 'R4':
        return model.FNR_plant[i,'Biogas',t] == 0
    elif t == 'PC1' or t == 'PC2' or t == 'PC3' or t == 'PC4' or t == 'PC5':
        return model.FNR_plant[i,'Biogas',t] == 0
    elif t == 'C1' or t == 'C2' or t == 'C3':
        return model.FNR_plant[i,'Biogas',t] == 0
    else:
        return pyo.Constraint.Skip

model.Cons_17 = pyo.Constraint(i, model.T, rule = fix_BG_w_CCS)
```

#This constraint ensures that coal is not deployed for all refineries, petrochemical, oleochemical and cement industries (with CCS)

```
def fix_CL_w_CCS(model, i, t):
```

```
        if t == 'R1' or t == 'R2' or t == 'R3' or t == 'R4':
            return model.FNR_plant[i,'Coal',t] == 0
        elif t == 'O1' or t == 'O2' or t == 'O3' or t == 'O4' or t == 'O5':
            return model.FNR_plant[i,'Coal',t] == 0
        elif t == 'PC1' or t == 'PC2' or t == 'PC3' or t == 'PC4' or t == 'PC5':
            return model.FNR_plant[i,'Coal',t] == 0
        elif t == 'C1' or t == 'C2' or t == 'C3':
            return model.FNR_plant[i,'Coal',t] == 0
        else:
            return pyo.Constraint.Skip
    model.Cons_18 = pyo.Constraint(i, model.T, rule = fix_CL_w_CCS)

    #This constraint determine the deployment of renewable energy sources in period i
    def renewable(model, i):
        return model.energy_ren[i] == model.energy_source[i,'Biomass'] + model.energy_source[i,'Biogas']
    model.Cons_19 = pyo.Constraint(i, rule = renewable)

    #This constraint determine the cumulative deployment of renewable energy sources for all periods
    def renewable_total(model):
        return model.energy_ren_total == sum(model.energy_source[i,'Biomass'] +
model.energy_source[i,'Biogas'] for i in periods)
    model.Cons_20 = pyo.Constraint(rule = renewable_total)
```

```
#This constraint determines the energy cascade for the ATM
def NET_ENERGY(model, i, k):
    if k == 8:
        return model.FNET[i,k] == model.D['Demand'][i]
    elif k == 1:
        return model.FNET[i,k] == model.FNR_source[i,'Biomass']
    elif k == 2:
        return model.FNET[i,k] == model.FNR_source[i,'Biogas']
    elif k == 3:
        return model.FNET[i,k] == model.FNR_source[i,'NG']
    elif k == 4:
        return model.FNET[i,k] == model.FNR_source[i,'Fuel_Oil']
    elif k == 6:
        return model.FNET[i,k] == model.FNR_source[i,'Coal']
    elif k == 5:
        return model.FNET[i,k] == model.FS_source[i,'Biomass']
    elif k == 7:
        return model.FNET[i,k] == model.FS_source[i,'Biogas']
    elif k == 9:
        return model.FNET[i,k] == model.FS_source[i,'NG']
    elif k == 10:
        return model.FNET[i,k] == model.FS_source[i,'Fuel_Oil']
```

```
    elif k == 11:
        return model.FNET[i,k] == model.FS_source[i,'Coal']
    else:
        return model.FNET[i,k] == 0
model.Cons_21 = pyo.Constraint(i, k, rule = NET_ENERGY)

#This constraint determines the energy cascade for the ATM
def EG_CASCADE(model, i, k):
    #print(i,k,model.energy_cascade[i,k])
    if k == 1:
        return model.energy_cascade[i,k] == model.FNET[i,k]
    else:
        return model.energy_cascade[i,k] == model.energy_cascade[i,k-1] + model.FNET[i,k]
model.Cons_22 = pyo.Constraint(i, k, rule = EG_CASCADE)

#This constraint determines the emissions cascade for the ATM
def EM_CASCADE(model, i, k):
    #print(i,k,model.emission_cascade[i,k])
    if k == 1:
        return model.emission_cascade[i,k] == 0
    elif k == 10 and i == 1:
        return model.emission_cascade[i,k] == model.emission_cascade[i,k-1] +
(model.energy_cascade[i,k-1] * (model.CI[k][i] - model.CI[k-1][i])) - model.NG_12 + model.NG_21
```

```
    elif k == 11 and i == 1:
        return model.emission_cascade[i,k] == model.emission_cascade[i,k-1] + (model.energy_cascade[i,k-1] * (model.CI[k][i] - model.CI[k-1][i])) - model.FO_12 + model.FO_21
    elif k == 12 and i == 1:
        return model.emission_cascade[i,k] == model.emission_cascade[i,k-1] + (model.energy_cascade[i,k-1] * (model.CI[k][i] - model.CI[k-1][i])) - model.CL_12 + model.CL_21
    elif k == 10 and i == 2:
        return model.emission_cascade[i,k] == model.emission_cascade[i,k-1] + (model.energy_cascade[i,k-1] * (model.CI[k][i] - model.CI[k-1][i])) - model.NG_21 - model.NG_23 + model.NG_12 + model.NG_32
    elif k == 11 and i == 2:
        return model.emission_cascade[i,k] == model.emission_cascade[i,k-1] + (model.energy_cascade[i,k-1] * (model.CI[k][i] - model.CI[k-1][i])) - model.FO_21 - model.FO_23 + model.FO_12 + model.FO_32
    elif k == 12 and i == 2:
        return model.emission_cascade[i,k] == model.emission_cascade[i,k-1] + (model.energy_cascade[i,k-1] * (model.CI[k][i] - model.CI[k-1][i])) - model.CL_21 - model.CL_23 + model.CL_12 + model.CL_32
    elif k == 10 and i == 3:
        return model.emission_cascade[i,k] == model.emission_cascade[i,k-1] + (model.energy_cascade[i,k-1] * (model.CI[k][i] - model.CI[k-1][i])) - model.NG_32 + model.NG_23
    elif k == 11 and i == 3:
        return model.emission_cascade[i,k] == model.emission_cascade[i,k-1] + (model.energy_cascade[i,k-1] * (model.CI[k][i] - model.CI[k-1][i])) - model.FO_32 + model.FO_23
    elif k == 12 and i == 3:
```

```
        return model.emission_cascade[i,k] == model.emission_cascade[i,k-1] + (model.energy_cascade[i,k-1] * (model.CI[k][i] - model.CI[k-1][i])) - model.CL_32 + model.CL_23
    else:
        return model.emission_cascade[i,k] == model.emission_cascade[i,k-1] + (model.energy_cascade[i,k-1] * (model.CI[k][i] - model.CI[k-1][i]))
model.Cons_23 = pyo.Constraint(i, k, rule = EM_CASCADE)

#This constraint sets the final value of the energy cascade to be 0 so that the demand is satisfied
def EG_CASCADE_CONS(model, i, k):
    if k == 12:
        return model.energy_cascade[i,k] == 0
    else:
        return pyo.Constraint.Skip
model.Cons_24 = pyo.Constraint(i, k, rule = EG_CASCADE_CONS)

    #This constraint sets the final value of the emissions cascade to be 0 so that the CO2 constraint is satisfied
def EM_CASCADE_CONS(model, i, k):
    if k == 12:
        return model.emission_cascade[i,k] == 0
    else:
        return pyo.Constraint.Skip
model.Cons_25 = pyo.Constraint(i, k, rule = EM_CASCADE_CONS)
```

```
    #This variable determine the total CO2 load contribution from all energy sources

    def CO2_load(model, i, s):

        return model.CO2_load[i] == sum((model.FS_source[i,s] * model.CO2[s][i]) + (model.FNR_source[i,s]
* model.CO2_CCS[s][i]) for s in model.S)

    model.Cons_26 = pyo.Constraint(i, model.S, rule = CO2_load)


    opt = SolverFactory('gams')

    results = opt.solve(model, solver = 'cplex')

    print(results)

    return model
```

REFERENCES

Al-Mohannadi, D.M., Alnouri, S.Y., Bishnu, S.K., Linke, P., 2016. Multi-period carbon integration. J. Clean. Prod. 136, 150–158. https://doi.org/10.1016/J.JCLEPRO.2016.03.027

Al-Mohannadi, D.M., Linke, P., 2016. On the systematic carbon integration of industrial parks for climate footprint reduction. J. Clean. Prod. 112, 4053–4064. https://doi.org/10.1016/J.JCLEPRO.2015.05.094

Alcalde, J., Smith, P., Haszeldine, R.S., Bond, C.E., 2018. The potential for implementation of Negative Emission Technologies in Scotland. Int. J. Greenh. Gas Control 76, 85–91. https://doi.org/10.1016/J.IJGGC.2018.06.021

Andiappan, V., Foo, D.C.Y., Tan, R.R., 2019. Process-to-Policy (P2Pol): using carbon emission pinch analysis (CEPA) tools for policy-making in the energy sector. Clean Technol. Environ. Policy 2019 217 21, 1383–1388. https://doi.org/10.1007/S10098-019-01721-0

Atkins, M.J., Morrison, A.S., Walmsley, M.R.W., 2010. Carbon Emissions Pinch Analysis (CEPA) for emissions reduction in the New Zealand electricity sector. Appl. Energy 87, 982–987. https://doi.org/10.1016/j.apenergy.2009.09.002

Bach, L.T., Gill, S.J., Rickaby, R.E.M., Gore, S., Renforth, P., 2019. CO2 Removal With Enhanced Weathering and Ocean Alkalinity Enhancement: Potential Risks and Co-benefits for Marine Pelagic Ecosystems. Front. Clim. 1. https://doi.org/10.3389/FCLIM.2019.00007

Baležentis, T., Štreimikienė, D., Melnikienė, R., Zeng, S., 2019. Prospects of green growth in the electricity sector in Baltic States: Pinch analysis based on ecological footprint. Resour. Conserv. Recycl. 142, 37–48. https://doi.org/10.1016/j.resconrec.2018.11.013

Bandyopadhyay, S., 2020. Interval Pinch Analysis for Resource Conservation Networks with Epistemic Uncertainties. Ind. Eng. Chem. Res. 59, 13669–13681. https://doi.org/10.1021/ACS.IECR.0C02811

Bandyopadhyay, S., Sahu, G.C., Foo, D.C.Y., Tan, R.R., 2010. Segregated targeting for multiple resource networks using decomposition algorithm. AIChE J. 56, 1235–1248. https://doi.org/10.1002/aic.12050

Bednar, J., Obersteiner, M., Baklanov, A., Thomson, M., Wagner, F., Geden, O., Allen, M., Hall, J.W., 2021. Operationalizing the net-negative carbon economy. Nature 596, 377–383. https://doi.org/10.1038/s41586-021-03723-9

Behrens, P., Rodrigues, J.F.D., Brás, T., Silva, C., 2016. Environmental, economic, and social impacts of feed-in tariffs: A Portuguese perspective 2000–2010. Appl. Energy 173, 309–319. https://doi.org/10.1016/J.APENERGY.2016.04.044

Cossutta, M., Foo, D.C.Y., Tan, R.R., 2021. Carbon emission spinch analysis (CEPA) for planning the decarbonization of the UK power sector. Sustain. Prod. Consum. 25, 259–270. https://doi.org/10.1016/j.spc.2020.08.013

Creutzig, F., Breyer, C., Hilaire, J., Minx, J., Peters, G.P., Socolow, R., 2019. The mutual dependence of negative emission technologies and energy systems. Energy Environ. Sci. 12, 1805–1817. https://doi.org/10.1039/c8ee03682a

Crilly, D., Zhelev, T., 2010. Further emissions and energy targeting: An application of CO2 emissions pinch analysis to the Irish electricity generation sector. Clean Technol. Environ. Policy 12, 177–189.

https://doi.org/10.1007/s10098-009-0245-0

Crilly, D., Zhelev, T., 2008. Emissions targeting and planning: An application of CO2 emissions pinch analysis (CEPA) to the Irish electricity generation sector. Energy 33, 1498–1507. https://doi.org/10.1016/j.energy.2008.05.015

El-Halwagi, M.M., 2012. Sustainable Design Through Process Integration, Sustainable Design Through Process Integration. Elsevier Inc. https://doi.org/10.1016/C2009-0-20226-1

El-Halwagi, M.M., Manousiouthakis, V., 1989. Synthesis of mass exchange networks. AIChE J. 35, 1233–1244. https://doi.org/10.1002/aic.690350802

Energy Commission, 2021. Malaysia Energy Statistics Handbook 2020.

Energy Commission, 2020. Report on Peninsular Malaysia Generation Development Plan 2020 (2021-2039).

Fajardy, M., 2021. CCUS in Power [WWW Document]. IEA. URL https://www.iea.org/reports/ccus-in-power (accessed 8.25.21).

Fischetti, M., 2021. There's Still Time to Fix Climate--About 11 Years - Scientific American [WWW Document]. Sci. Am. URL https://www.scientificamerican.com/article/theres-still-time-to-fix-climate-about-11-years/?fbclid=IwAR21cZO_ub075eZERVl3I7PizqhtM3YhZOkrLiTzKuDiZVv1peHuOEwkvFY (accessed 11.1.21).

Foo, D.C.Y., 2012. Process Integration for Resource Conservation. CRC Press. https://doi.org/10.1201/b12079

Foo, D.C.Y., Tan, R.R., 2020. Process Integration Approaches to Planning Carbon Management Networks, Process Integration Approaches to Planning Carbon Management Networks. CRC Press, Boca Raton, Florida. https://doi.org/10.1201/9781351170888

Foo, D.C.Y., Tan, R.R., 2016. A review on process integration techniques for carbon emissions and environmental footprint problems. Process Saf. Environ. Prot. 103, 291–307. https://doi.org/10.1016/j.psep.2015.11.007

Foo, D.C.Y., Tan, R.R., Ng, D.K.S., 2008. Carbon and footprint-constrained energy planning using cascade analysis technique. Energy 33, 1480–1488. https://doi.org/10.1016/j.energy.2008.03.003

Galán-Martín, Á., Vázquez, D., Cobo, S., Mac Dowell, N., Caballero, J.A., Guillén-Gosálbez, G., 2021. Delaying carbon dioxide removal in the European Union puts climate targets at risk. Nat. Commun. 12, 1–12. https://doi.org/10.1038/s41467-021-26680-3

Gibbins, J., Chalmers, H., 2008. Carbon capture and storage. Energy Policy 36, 4317–4322. https://doi.org/10.1016/J.ENPOL.2008.09.058

Hohmann, E.C., 1971. Optimum Networks for Heat Exchange. University of Southern California.

House, K.Z., Baclig, A.C., Ranjan, M., Van Nierop, E.A., Wilcox, J., Herzog, H.J., 2011. Economic and energetic analysis of capturing CO2from ambient air. Proc. Natl. Acad. Sci. U. S. A. 108, 20428–20433. https://doi.org/10.1073/pnas.1012253108

IEA, 2021a. World Energy Outlook 2021 [WWW Document]. World Energy Outlook. URL

https://www.iea.org/reports/world-energy-outlook-2021 (accessed 1.20.22).

IEA, 2021b. Direct Air Capture [WWW Document]. IEA. URL https://www.iea.org/reports/direct-air-capture (accessed 1.21.22).

IEA, 2019. Electricity generation by fuel and scenario, 2018-2040 [WWW Document]. World Energy Outlook. URL https://www.iea.org/data-and-statistics/charts/electricity-generation-by-fuel-and-scenario-2018-2040 (accessed 1.20.22).

IPCC, 2022. Synthesis Report [WWW Document]. Synth. Rep. Sixth Assess. Rep. URL https://www.ipcc.ch/ar6-syr/ (accessed 12.7.21).

IPCC, 2021. The Physical Science Basis [WWW Document]. AR6 Clim. Chang. 2021. URL https://www.ipcc.ch/report/sixth-assessment-report-working-group-i/ (accessed 11.1.21).

IPCC, 2019a. Summary for Policymakers [WWW Document]. Clim. Chang. L. URL https://www.ipcc.ch/srccl/chapter/summary-for-policymakers/ (accessed 1.20.22).

IPCC, 2019b. Summary for Policymakers [WWW Document]. Ocean Cryosph. a Chang. Clim. URL https://www.ipcc.ch/srocc/chapter/summary-for-policymakers/ (accessed 1.20.22).

IPCC, 2018. Summary for Policymakers [WWW Document]. Glob. Warm. 1.5°C. URL https://www.ipcc.ch/sr15/chapter/spm/ (accessed 1.20.22).

Klemeš, J.J., Varbanov, P.S., Walmsley, T.G., Jia, X., 2018. New directions in the implementation of Pinch Methodology (PM). Renew. Sustain. Energy Rev. 98, 439–468. https://doi.org/10.1016/J.RSER.2018.09.030

Lee, J.-Y., 2017. A multi-period optimisation model for planning carbon sequestration retrofits in the electricity sector. Appl. Energy 198, 12–20. https://doi.org/10.1016/J.APENERGY.2017.04.032

Lee, J.Y., Lin, H.F., 2019. Multi-Footprint Constrained Energy Sector Planning. Energies 12, 2329. https://doi.org/10.3390/EN12122329

Lee, S.C., Ng, D.K.S., Foo, D.C.Y., Tan, R.R., 2009. Extended pinch targeting techniques for carbon-constrained energy sector planning. Appl. Energy 86, 60–67. https://doi.org/10.1016/j.apenergy.2008.04.002

Levvy, B.S., Patz, J.A., 2015. Climate Change, Human Rights, and Social Justice. Ann. Glob. Heal. 81, 310–322. https://doi.org/10.1016/J.AOGH.2015.08.008

Liang, L., Lu, Q., 2015. Optimization of China's energy structure based on carbon pinch analysis. Resour. Sci. 291–298.

Lim, X.Y., Foo, D.C.Y., Tan, R.R., 2018. Pinch analysis for the planning of power generation sector in the United Arab Emirates: A climate-energy-water nexus study. J. Clean. Prod. 180, 11–19. https://doi.org/10.1016/J.JCLEPRO.2018.01.158

Linnhoff, B., Dhole, V.R., 1993. Targeting for CO2 emissions for Total Sites. Chem. Eng. Technol. 16, 252–259. https://doi.org/10.1002/CEAT.270160407

Linnhoff, B., Flower, J.R., 1978. Synthesis of Heat Exchanger Networks. AIChE J. 24, 633–642.

Linnhoff, B., Townsend, D.W., Boland, D., Hewitt, G.F., Thomas, B.E.A., Guy, A.R., Marshall, R.H., 1982. A User Guide on Process Integration for the Efficient Use of Energy. Institution of Chemical Engineers,

Rugby, the United Kingdom.

Lopez, N.S.A., Foo, D.C.Y., Tan, R.R., 2021. Optimizing regional electricity trading with Carbon Emissions Pinch Analysis. Energy 237, 121544. https://doi.org/10.1016/J.ENERGY.2021.121544

Ludin, N.A., Mustafa, N.I., Hanafiah, M.M., Ibrahim, M.A., Asri Mat Teridi, M., Sepeai, S., Zaharim, A., Sopian, K., 2018. Prospects of life cycle assessment of renewable energy from solar photovoltaic technologies: A review. Renew. Sustain. Energy Rev. 96, 11–28. https://doi.org/10.1016/J.RSER.2018.07.048

McGlashan, N., Shah, N., Caldecott, B., Workman, M., 2012. High-level techno-economic assessment of negative emissions technologies. Process Saf. Environ. Prot. 90, 501–510. https://doi.org/10.1016/j.psep.2012.10.004

McLaren, D., 2012. A comparative global assessment of potential negative emissions technologies. Process Saf. Environ. Prot. 90, 489–500. https://doi.org/10.1016/j.psep.2012.10.005

MIDA, 2021. Malaysia aims 31% RE capacity by 2025 [WWW Document]. Malaysian Invest. Dev. Auth. URL https://www.mida.gov.my/mida-news/malaysia-aims-31-re-capacity-by-2025/ (accessed 2.27.22).

Mohd Idris, M.N., Hashim, H., 2021. Integrating palm oil biomass waste utilization in coal-fired power plants for meeting near-term emission targets. J. Environ. Manage. 296, 113118. https://doi.org/10.1016/J.JENVMAN.2021.113118

Ooi, R.E.H., Foo, D.C.Y., Tan, R.R., 2014. Targeting for carbon sequestration retrofit planning in the power generation sector for multi-period problems. Appl. Energy 113, 477–487. https://doi.org/10.1016/j.apenergy.2013.07.047

Ooi, R.E.H., Foo, D.C.Y., Tan, R.R., Ng, D.K.S., Smith, R., 2013. Carbon constrained energy planning (CCEP) for sustainable power generation sector with automated targeting model. Ind. Eng. Chem. Res. 52, 9889–9896. https://doi.org/10.1021/ie4005018

Paice, E., 2022. By 2050, a quarter of the world's people will be African – this will shape our future [WWW Document]. Guard. URL https://www.theguardian.com/global-development/2022/jan/20/by-2050-a-quarter-of-the-worlds-people-will-be-african-this-will-shape-our-future (accessed 2.2.22).

Pękala, Ł.M., Tan, R.R., Foo, D.C.Y., Jezowski, J.M., 2010. Optimal energy planning models with carbon footprint constraints. Appl. Energy 87, 1903–1910. https://doi.org/10.1016/j.apenergy.2009.12.012

Priya, G.S.K., Bandyopadhyay, S., 2013. Emission constrained power system plannin.A pinch analysis based study of Indian electricity sector. Clean Technol. Environ. Policy 15, 771–782. https://doi.org/10.1007/s10098-012-0541-y

Project Drawdown, 2020. The Drawdown Review.

Ramli, A.F., Muis, Z.A., Ho, W.S., Idris, A.M., Mohtar, A., 2019. Carbon Emission Pinch Analysis: an application to the transportation sector in Iskandar Malaysia for 2025. Clean Technol. Environ. Policy 21, 1899–1911. https://doi.org/10.1007/s10098-018-1579-2

Ramsook, D., Boodlal, D., Maharaj, R., 2022. Multi-period Carbon Emission Pinch Analysis (CEPA) for reducing emissions in the Trinidad and Tobago power generation sector. Carbon Manag. 1–14. https://doi.org/10.1080/17583004.2022.2038273

Sahu, G.C., Bandyopadhyay, S., Foo, D.C.Y., Ng, D.K.S., Tan, R.R., 2014. Targeting for optimal grid-wide

deployment of carbon capture and storage (CCS) technology. Process Saf. Environ. Prot. 92, 835–848. https://doi.org/10.1016/j.psep.2013.05.003

Salim, S., 2021. 12MP: Malaysia committed to becoming carbon-neutral nation by 2050, says PM | The Edge Markets [WWW Document]. Edge Mark. URL https://www.theedgemarkets.com/article/12mp-malaysia-committed-becoming-carbonneutral-nation-2050-says-pm (accessed 12.20.21).

Salman, B., Nomanbhay, S., Foo, D.C.Y., 2019. Carbon emissions pinch analysis (CEPA) for energy sector planning in Nigeria. Clean Technol. Environ. Policy 21, 93–108. https://doi.org/10.1007/s10098-018-1620-5

Shenoy, U. V., 2010. Targeting and design of energy allocation networks for carbon emission reduction. Chem. Eng. Sci. 65, 6155–6168. https://doi.org/10.1016/j.ces.2010.08.040

Smith, P., Davis, S.J., Creutzig, F., Fuss, S., Minx, J., Gabrielle, B., Kato, E., Jackson, R.B., Cowie, A., Kriegler, E., Van Vuuren, D.P., Rogelj, J., Ciais, P., Milne, J., Canadell, J.G., McCollum, D., Peters, G., Andrew, R., Krey, V., Shrestha, G., Friedlingstein, P., Gasser, T., Grübler, A., Heidug, W.K., Jonas, M., Jones, C.D., Kraxner, F., Littleton, E., Lowe, J., Moreira, J.R., Nakicenovic, N., Obersteiner, M., Patwardhan, A., Rogner, M., Rubin, E., Sharifi, A., Torvanger, A., Yamagata, Y., Edmonds, J., Yongsung, C., 2016a. Biophysical and economic limits to negative CO2 emissions. Nat. Clim. Chang. https://doi.org/10.1038/nclimate2870

Smith, P., Haszeldine, R.S., Smith, S.M., 2016b. Preliminary assessment of the potential for, and limitations to, terrestrial negative emission technologies in the UK. Environ. Sci. Process. Impacts 18, 1400–1405. https://doi.org/10.1039/c6em00386a

Smith, R., 2016. Chemical Process Design and Integration, 2nd ed. Wiley, Somerset.

Stram, B.N., 2016. Key challenges to expanding renewable energy. Energy Policy 96, 728–734. https://doi.org/10.1016/J.ENPOL.2016.05.034

Su, W., Ye, Y., Zhang, C., Baležentis, T., Štreimikienė, D., 2020. Sustainable energy development in the major power-generating countries of the European Union: The Pinch Analysis. J. Clean. Prod. 256, 120696. https://doi.org/10.1016/j.jclepro.2020.120696

Tan, R.R., 2016. A multi-period source–sink mixed integer linear programming model for biochar-based carbon sequestration systems. Sustain. Prod. Consum. 8, 57–63. https://doi.org/10.1016/J.SPC.2016.08.001

Tan, R.R., Aviso, K.B., 2019. A linear program for optimizing enhanced weathering networks. Results Eng. 3, 100028. https://doi.org/10.1016/J.RINENG.2019.100028

Tan, R.R., Aviso, K.B., Bandyopadhyay, S., Ng, D.K.S., 2013. Optimal source–sink matching in carbon capture and storage systems with time, injection rate, and capacity constraints. Environ. Prog. Sustain. Energy 32, 411–416. https://doi.org/10.1002/EP.11630

Tan, R.R., Aviso, K.B., Foo, D.C.Y., 2018. Carbon emissions pinch analysis of economic systems. J. Clean. Prod. 182, 863–871. https://doi.org/10.1016/J.JCLEPRO.2018.02.082

Tan, R.R., Aviso, K.B., Foo, D.C.Y., 2017. P-graph and Monte Carlo simulation approach to planning carbon management networks. Comput. Chem. Eng. 106, 872–882. https://doi.org/10.1016/J.COMPCHEMENG.2017.01.047

Tan, R.R., Foo, D.C.Y., 2017. Carbon Emissions Pinch Analysis for Sustainable Energy Planning, in: Encyclopedia of Sustainable Technologies. Elsevier, pp. 231–237. https://doi.org/10.1016/B978-0-12-409548-9.10148-4

Tan, R.R., Foo, D.C.Y., 2013. Pinch Analysis for Sustainable Energy Planning Using Diverse Quality Measures, in: Handbook of Process Integration (PI): Minimisation of Energy and Water Use, Waste and Emissions. Elsevier Inc., pp. 505–523. https://doi.org/10.1533/9780857097255.4.505

Tan, R.R., Foo, D.C.Y., 2007. Pinch analysis approach to carbon-constrained energy sector planning. Energy 32, 1422–1429. https://doi.org/10.1016/j.energy.2006.09.018

Tan, R.R., Foo, D.C.Y., Aviso, K.B., Ng, D.K.S., 2009a. The use of graphical pinch analysis for visualizing water footprint constraints in biofuel production. Appl. Energy 86, 605–609. https://doi.org/10.1016/J.APENERGY.2008.10.004

Tan, R.R., Ng, D.K.S., Foo, D.C.Y., 2009b. Pinch analysis approach to carbon-constrained planning for sustainable power generation. J. Clean. Prod. 17, 940–944. https://doi.org/10.1016/j.jclepro.2009.02.007

Thengane, S.K., Tan, R.R., Foo, D.C.Y., Bandyopadhyay, S., 2019. A Pinch-Based Approach for Targeting Carbon Capture, Utilization, and Storage Systems. Ind. Eng. Chem. Res. 58, 3188–3198. https://doi.org/10.1021/ACS.IECR.8B06156

Tjan, W., Tan, R.R., Foo, D.C.Y., 2010. A graphical representation of carbon footprint reduction for chemical processes. J. Clean. Prod. 18, 848–856. https://doi.org/10.1016/J.JCLEPRO.2009.12.002

Umeda, T., Itoh, J., Shiroko, K., 1978. Heat Exchange System Synthesis. Chem. Eng. Prog. 70–76.

United Nations Climate Change, 2021a. COP26 The Glasgow Climate Pact. Glasglow.

United Nations Climate Change, 2021b. COP26 keeps 1.5C alive and finalises Paris Agreement [WWW Document]. UN Clim. Chang. Conf. UK 2021. URL https://ukcop26.org/cop26-keeps-1-5c-alive-and-finalises-paris-agreement/ (accessed 4.14.22).

United Nations Environment Programme, 2019. Emissions Gap Report. Nairobi.

United States Environmental Protection Agency, 2021. Importance of Methane [WWW Document]. Glob. Methane Initiat. URL https://www.epa.gov/gmi/importance-methane (accessed 12.8.21).

Walmsley, M.R.W., Walmsley, T.G., Atkins, M.J., 2015a. Achieving 33% renewable electricity generation by 2020 in California. Energy 92, 260–269. https://doi.org/10.1016/j.energy.2015.05.087

Walmsley, M.R.W., Walmsley, T.G., Atkins, M.J., Kamp, P.J.J., Neale, J.R., 2014. Minimising carbon emissions and energy expended for electricity generation in New Zealand through to 2050. Appl. Energy 135, 656–665. https://doi.org/10.1016/J.APENERGY.2014.04.048

Walmsley, M.R.W., Walmsley, T.G., Atkins, M.J., Kamp, P.J.J., Neale, J.R., Chand, A., 2015b. Carbon Emissions Pinch Analysis for emissions reductions in the New Zealand transport sector through to 2050. Energy 92, 569–576. https://doi.org/10.1016/J.ENERGY.2015.04.069

World Meteorological Organization, 2020. Carbon dioxide levels continue at record levels, despite COVID-19 lockdown [WWW Document]. Press Releases. URL https://public.wmo.int/en/media/press-release/carbon-dioxide-levels-continue-record-levels-despite-covid-19-lockdown (accessed 1.20.22).

Yap, J.Y., Tan, J., Foo, D.C.Y., Tan, R.R., Papadokonstantakis, S., Badr, S., 2020. A graphical method for carbon dioxide emissions reduction in multi–product plants. Process Saf. Environ. Prot. 133, 51–63. https://doi.org/10.1016/J.PSEP.2019.10.028